

**Advanced Flexible Wing Technology Assessment  
for the New Strategic Airlifter**

by  
Jerry M. Wohletz

B.S Aerospace Engineering  
University of Kansas, 1994

Submitted to the Department of Aeronautics and Astronautics in partial  
fulfillment of the requirements for the degree of

Master of Engineering

at the

MASSACHUSETTS INSTITUTE OF TECHNOLOGY

June 1997

© Jerry M Wohletz 1997. All Rights Reserved.

The author hereby grants to MIT permission to reproduce and to distribute publicly  
paper and electronic copies of this thesis document in whole or in part.

Author .....  
.....  
Department of Aeronautics and Astronautics  
May 31, 1996

Certified by .....  
.....  
Charles Boppe  
Senior Lecturer, Department of Aeronautics and Astronautics  
Thesis Supervisor

Certified by .....  
.....  
Mark Drela  
Associate Professor of Aeronautics and Astronautics  
Thesis Supervisor

Accepted by .....  
.....  
Jaime Peraire  
Chairman, Departmental Graduate Committee

MASSACHUSETTS INSTITUTE OF TECHNOLOGY

AERO

JUN 19 1997



# Advanced Flexible Wing Technology Assessment for the New Strategic Airlifter

by  
Jerry M. Wohletz

Submitted to the Department of Aeronautics and Astronautics on May 23, 1997, in partial fulfillment of the requirements for the degree of Master of Engineering

## Abstract

An Advanced Flexible Wing (AFW) technology assessment as applied to the New Strategic Airlifter (NSA) is reported in this thesis. The seed for this project originated from an assessment study performed on a generic strike fighter where significant potential weight savings were identified. The AFW concept — also known as Active Aeroelastic Wing (AAW) — is composed of several elements that serve to make aeroelastic deformations an asset rather than a limitation on the wing's design. The focus of this assessment study is to determine if the *roll control* element of the AFW concept can be used for the NSA, and what is the potential wing structural weight savings that can be achieved by using the technology. The *load alleviation*, *drag reduction*, and *flutter suppression* elements of AFW are not explored nor are the effects of reducing the torsional stiffness on the flutter characteristics. The thesis objectives were completed. Based on a maximum allowable aileron deflection of  $25^\circ$ , the *roll control* aspect of AFW does not offer potential wing structural weight savings if a traditional inboard aileron configuration is used as the primary roll control device at high dynamic pressures. However, the concept does offer a potential wing structural weight reduction of approximately 8% if an outboard aileron configuration is used as the primary roll control device at high dynamic pressures. Furthermore, the aileron control configurations do not reverse within the flight envelope. Sensitivity analysis revealed that reducing torsional stiffness results in a reduction in aerodynamic spanwise efficiency. However, the spanwise efficiency can be recovered with the addition of washin angle at the tip. Finally, requirements analysis raised physical design questions relating to cost, structural weight, aerodynamic efficiency, reliability, maintainability, and supportability. The assessment recommendation is that further analysis is required to assess the other potential benefits of AFW such as load alleviation, drag reduction, and flutter suppression for the NSA.

Thesis Supervisor: Charles Boppe  
Title: Senior Lecturer, Department of Aeronautics and Astronautics

Thesis Supervisor: Mark Drela  
Title: Associate Professor of Aeronautics and Astronautics





# Acknowledgments

I would like to thank all of those people who made this thesis possible. First and foremost, I would like to thank my fiancée, Tina Park, and my family for all of the support they provided me throughout this project. Additionally, I would like to thank my office mates and teammate Shawn Hanegan for being there when it counts. Thanks guys!

I would also like to thank the faculty for their support and advice. Special thanks goes out to Charlie Boppe, Professor Mark Drela, and Visiting Professor Terry Weisshaar from Purdue University. Their contribution to this project was above and beyond the call of duty. I would also like to thank my research advisor Professor James Paduano for being patient and understanding. Last but not least, I would like to thank Professor Mark Ewing at the University of Kansas for his insightful advice.

In addition to the faculty support, I would like to express my appreciation to our industry contacts. I would like to thank my employer McDonnell Douglas Aerospace. Specifically I would like to thank Darin Groll for fighting for my educational leave of absence, and Rudy Yurkovich for providing assistance and computer resources. Additionally, I would like to thank Lockheed Martin who sponsored the project, provided the baseline configuration, provided their computer tools, and most importantly, they provided direction. Thank you Mark Norris. In addition to Lockheed, Wright-Patterson Airforce Base personnel had a vital role in the success of this project. Special thanks goes out to Ray Kolonay for those late evening conversations.



# Table of Contents

<b>Abstract.....</b>	<b>3</b>
<b>Acknowledgments .....</b>	<b>5</b>
<b>Table of Contents.....</b>	<b>7</b>
<b>List of Figures .....</b>	<b>9</b>
<b>List of Tables .....</b>	<b>11</b>
<b>Chapter 1 Introduction.....</b>	<b>13</b>
1.1 Background Work .....	14
1.2 NSA Assessment Study Objectives.....	15
1.3 Thesis Overview.....	19
<b>Chapter 2 Requirements Analysis .....</b>	<b>21</b>
2.1 Requirements Hierarchy .....	21
2.2 Explicit Customer Needs.....	23
2.3 Implicit Customer Needs.....	25
2.5 Requirements QFD Build.....	30
2.6 Conclusions .....	33
<b>Chapter 3 Baseline Configuration and Mission.....</b>	<b>35</b>
3.1 NSA Baseline Configuration.....	35
3.2 Wing Structural Layout .....	38
3.3 Wing Material Selection.....	45
3.4 Baseline Missions and Design Point Selection .....	46
3.5 V-n Diagram for Selected Design Point.....	47
3.6 Roll Performance for Selected Design Point.....	50
3.6 Conclusions .....	51
<b>Chapter 4 NSA Wing Design and Sensitivity Analysis.....</b>	<b>55</b>
4.1 NSA Wing Design Process Overview .....	55
4.2 NSA Wing Design.....	57
4.2.1 ASTROS Structural Modeling .....	57
4.2.2 Aerodynamic Modeling.....	61
4.2.3 Multidisciplinary Optimization .....	63
4.2.4 NSA Design Results.....	68

4.3 NSA Sensitivity Analysis .....	81
4.4 Conclusions .....	87
<b>Chapter 5 Conclusions and Recommendations.....</b>	<b>89</b>
5.1 Conclusions .....	89
5.2 Recommendations .....	93
5.3 Contribution .....	94
<b>References.....</b>	<b>95</b>
<b>Appendix A Operational Requirements Document .....</b>	<b>99</b>
<b>Appendix B DOC Assessment Study for Narrow-Body Commercial Transport .</b>	<b>105</b>

# List of Figures

Figure 1.1 Aeroelastic Effects on Steady State Roll Rate .....	17
Figure 1.2 Allowable Aileron Deflection Versus Required Wing Structural Weight for Desired Roll Performance.....	18
Figure 2.1 Requirements Hierarchy Build Example .....	24
Figure 2.2 Typical DOC Breakdown for Narrow-Body Transports.....	27
Figure 2.3 DOC Relationship Matrix.....	29
Figure 2.4 NSA Requirements QFD .....	32
Figure 3.1 NSA LGA180D Configuration Three-View .....	36
Figure 3.2 Typical Transport Wing Layout.....	39
Figure 3.3 Supercritical Airfoil Ordinates.....	42
Figure 3.4 Selected Wing Structural Arrangement for the NSA.....	44
Figure 3.5 NSA Baseline Operation Mission.....	46
Figure 3.5 V-n Diagram for Initial Operational Cruise Point .....	49
Figure 4.1 NSA Wing Design Process .....	55
Figure 4.2 ASTROS Design Model Schematic.....	59
Figure 4.4 Maximum Allowable Aileron Deflection Versus Required Wing Structural Weight for Level I Roll Performance.....	70
Figure 4.5 Aileron Effectiveness Ratio Required Versus Required Wing Structural Weight for Level I Roll Performance .....	71
Figure 4.6 Aileron Effectiveness Ratio Required for Level I Roll Performance Versus Maximum Allowable Aileron Deflection .....	72
Figure 4.7 Maximum Allowable Aileron Deflection Versus Potential Wing Structural Weight Reduction .....	74
Figure 4.8 NSA Minimum Weight Wing Structural Deflections for the Outboard Aileron Configuration at $M=0.69$ , $N_z=2.5$ g's.....	75
Figure 4.9 NSA Wing Minimum Weight Structural Deflections for the Outboard Aileron Configuration at $M=1.07$ , $N_z=2.5$ g's.....	76

Figure 4.10 NSA Wing Minimum Weight Structural Deflections for the Outboard Aileron Configuration at $M=0.86$ , $N_z=-1.0$ g's.....	77
Figure 4.11 NSA Wing Minimum Weight Structural Deflections for the Outboard Aileron Configuration at $M=0.50$ , $N_z=-1.0$ g's.....	78
Figure 4.12 NSA Wing Minimum Weight Structural Deflections for the Outboard Aileron Configuration at $M=0.82$ , $N_z=1.0$ g's.....	79
Figure 4.13 ASWING Model Schematic .....	82
Figure 4.14 Control Effectiveness Versus Equivalent Airspeed.....	83
Figure 4.15 Span Efficiency Versus Percentage Change in Torsional Stiffness for $M=0.82$ , $h=32,000$ ft, and $1.0$ g's.....	84
Figure 4.16 Span Efficiency Versus Washin Angle for $M=0.82$ , $H=32,000$ ft, and $1.0$ g's. ....	85

## List of Tables

Table 2.1 Subset of Explicit Customer Needs.....	23
Table 2.2 DOC Relationship Matrix Results .....	28
Table 2.3 Explicit and Implicit Customer Needs .....	30
Table 2.3 Explicit and Implicit Customer Needs .....	33
Table 3.1 Aluminum Material Properties used in NSA Wing Design .....	45
Table 3.2 V-n Diagram Parameters for Initial Cruise Point.....	47
Table 3.3 Design Points for Initial Operational Cruise Condition .....	50





# Chapter 1 Introduction

Cost of aerospace products is one of the most critical issues that face the aerospace engineering industry. For aircraft, the cost is proportional to the gross take-off weight; thus, cost reduction can be achieved by weight reduction. Throughout the history of aviation, there has been significant advances made in the reduction of the aircraft weight that include the use of aluminum and composite materials. Another proposed approach to reducing the aircraft weight is the Advanced Flexible Wing (AFW) concept, and this is the focus of this thesis.

The AFW concept — also known as Active Aeroelastic Wing (AAW)— is composed of several elements that serve to make aeroelastic deformations an asset rather than a limitation on the wing's design. These elements include the use of wing deformation for roll control, load alleviation, and drag reduction. All of these elements involve controlling the spanwise lift distribution through wing warping, which is a concept as old as powered flight itself. The Wright brothers took advantage of the flexible nature of their wings to roll their aircraft through mechanical wing warping.

Traditionally, aircraft wings are designed for bending and torsional stiffness considerations; however, the idea of AFW is to design the wing only for bending stiffness. The bending stiffness impacts mainly static and dynamic stability. Wing divergence and flutter denote static and dynamic instability respectively. The torsional stiffness impacts mainly performance and dynamic stability. Performance here means whether or not the elastic wing can produce adequate roll. Currently, transport and fighter wings are designed such that the wing will not fail for the expected design loads and that the wing will have inherent performance that is adequate for the desired mission. Thus, the concept of AFW is to design transport or fighter wing such that the wing will not fail for the expected design load, but the wing's passive performance will be inadequate for the desired mission. As a result, an active approach will then have to be employed to obtain the desired performance.

By designing the wing's structure for bending stiffness only, there exists an opportunity for a reduction in wing's structural weight. However, this can only be realized if the torsional stiffness is a design driver. If the design of the wing is governed by bending strength only — resulting aeroelastic twist effects are negligible — then the potential weight savings from the AFW concept will be minimal. On the other hand, if the design of the wing is governed by bending and torsional strength so that the resulting aeroelastic twist effect is significant, the AFW concept may provide potential weight savings.

## 1.1 Background Work

The background work on AFW has been primarily focused on military fighter applications. In the mid 1980s, Rockwell International Corporation pioneered and advanced the AFW concept. In 1991, a number of wind tunnel tests at NASA Langley were performed to demonstrate the AFW concept, and an entire section of the AIAA Journal of Aircraft was devoted to the discussion of the results [Ref 1.1-1.10]. “The key program accomplishments included single- and multiple-mode flutter suppression, load alleviation, and load control during rapid roll maneuvers, and multi-input/multi-output multiple-function active controls test above the open-loop flutter boundary” [Ref 1.1].

In 1994, Lockheed Martin and Rockwell teamed to perform a joint AFW assessment study on a generic strike fighter. Their investigation was focused on the potential weight savings that might be realized by using AFW for a baseline aircraft which was a single engine, single seat, conventional takeoff and landing generic strike fighter [Ref 1.11]. Two wings were investigated, one conventional and one AFW, and both of them shared commonality of planform, thickness to chord ratio, and control surface layout. The results of their assessment study offered a potential gross takeoff weight reduction of 7.1%, and potential empty weight savings of 8.7%. In addition to weight, the following potential benefits were identified:

- Control Surface Reversal Compensation
- Flutter Suppression

- Load Alleviation
- Multipoint Twist Optimization
- Elastic Mode Control

The recommendations were that a higher fidelity analysis is required in order to further substantiate the potential savings, and design integration issues and consequences need to be evaluated.

In 1997, McDonnell Douglas Aerospace, Rockwell International Corporation, NASA, and the USAF teamed to perform a joint AAW flight test program [Ref. 1.12-1.13]. The aircraft selected for the flight test program is the F/A-18 Hornet. Currently, the operational F/A-18 uses aeroelastic wing warping for roll control in the transonic speed range, which is accomplished by deflecting the leading edge flaps. This is believed to be the first modern use of this technology in a production aircraft. The first flight of the AAW F/A-18 is expected in the year 2000.

## 1.2 NSA Assessment Study Objectives

*The focus of this assessment study is to determine if the roll control element of the AFW concept can be used for the New Strategic Airlifter NSA, and what is the potential wing structural weight savings that can be achieved by using the technology.* More specifically, the present objectives are to:

1. Identify the minimum weight design with no torsional constraints for roll performance,
2. Identify the region of aileron control: non-reversed or reversed,
3. Identify the potential weight savings based on the maximum allowable aileron deflections, and
4. Identify the sensitivities of torsional stiffness on reversal speed, span efficiency, and maximum strain.

Other aspects of AFW including the load alleviation, drag reduction, and flutter suppression and the effects of reducing the torsional stiffness on the flutter characteristics are not addressed in this study but merit attention in future investigations.

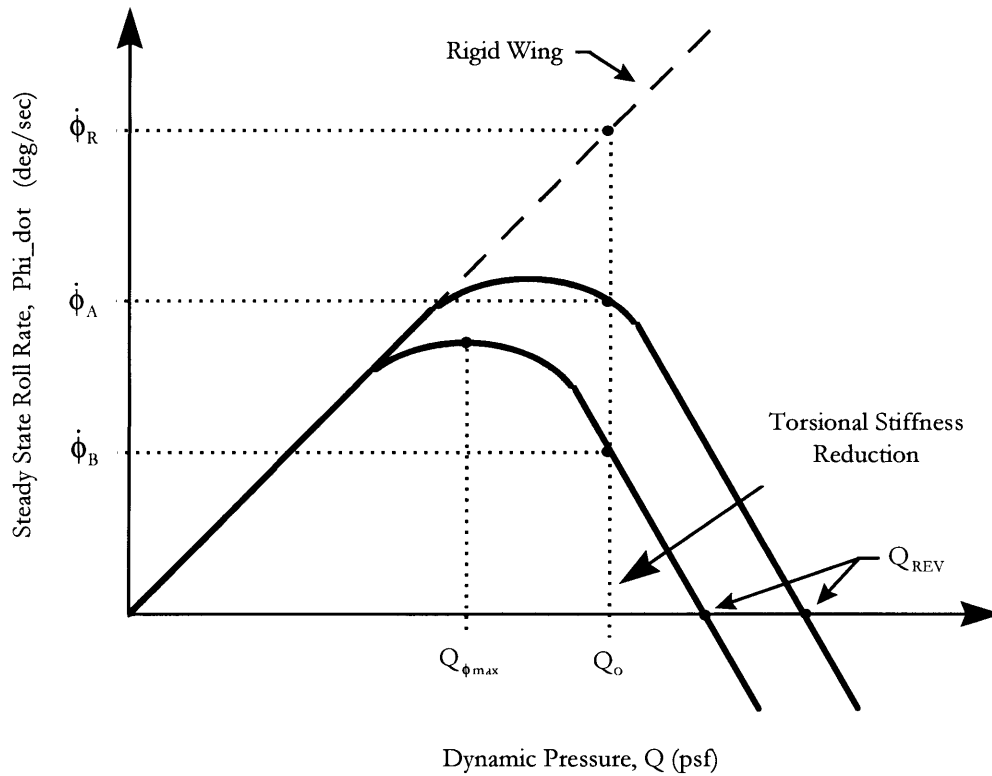
For this study, the Lockheed Martin Aeronautical System Company generously provided a baseline AFW configuration — the NSA which is a proposed replacement for the aging C-141 fleet. The NSA concept is a medium size military cargo plane proposed to perform both military and commercial missions. Military roles include deployment, tanker and airdrop. Commercial missions include overnight delivery and intermodal. The military deployment mission is used for this assessment study.

To further expand the concept of aeroelasticity and its relationship to the objectives, two illustrations will be used. The first illustration will demonstrate the effects of speed on roll control. Figure 1.1 illustrates the steady state roll rate for a given aileron deflection as a function of speed and torsional stiffness. For a rigid wing, the roll rate is perfectly proportional to the true airspeed. For a flexible wing, this is true only at small low dynamic pressures. However, as the dynamic pressure increases, the steady state roll rate of the flexible wing becomes progressively smaller than that of the rigid wing. At a  $Q_{\dot{\phi}_{\max}}$ , the maximum attainable roll rate for a given aileron deflection is achieved. Above that dynamic pressure, the roll rate decreases and eventually becomes zero at the reversal dynamic pressure,  $Q_{\text{rev}}$ . Above the reversal dynamic pressure, a positive aileron deflection produces a negative steady state roll rate.

Reduction of the torsional stiffness reduces the reversal dynamic pressure, the maximum attainable steady state roll rate, and the speed at the maximum roll rate. The figure also characterizes the Aileron Effectiveness Ratio (AER) which is the ratio between the flexible and rigid steady state roll rates:

$$\text{AER}_A = \frac{\dot{\phi}_A}{\dot{\phi}_R}$$

Thus, for a given Mach number, a reduction in the torsional stiffness results in a reduction in the AER. It is worth noting that the AER is sometimes referred to as the aileron flex to rigid ratio.

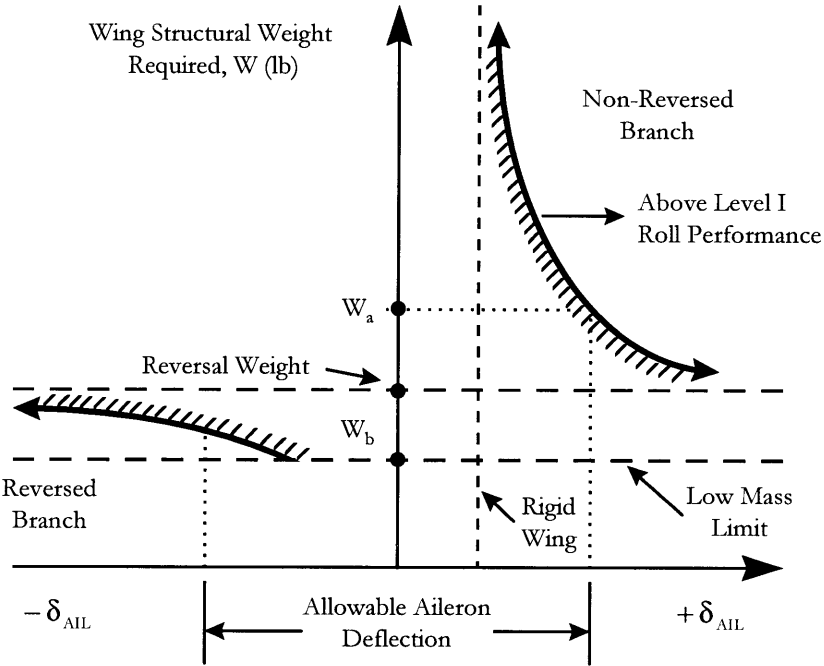


**Figure 1.1 Aeroelastic Effects on Steady State Roll Rate**

This figure illustrates the aeroelastic effects for variations in airspeed; what follows is a look at the aeroelastic effects for variations in wing structural weight. Figure 1.2 illustrates the constant speed aileron deflection required for the desired roll performance versus the wing structural weight. Note, the required wing structural weight is composed of the structural weight required for bending constraints and the structural weight required for torsional constraints. Additionally, structural weight variations are directly proportional to variations in torsional constraints if the bending stiffness constraints are held constant. The infinite structural weight corresponds to rigid body torsional constraints, and the low mass limit corresponds to zero torsional constraints. Thus, this representation illustrates the variations in structural weight due to the variations in torsional constraints with the bending constraints held constant.

For a rigid wing, which has infinite weight, there exists a lower bound on the aileron deflection required to satisfy the desired roll performance. As the structural weight decreases, the required aileron deflection increases, and becomes infinite at the reversal weight. Below the reversal weight,

the required aileron deflection increases from negative infinity. As the structural weight decreases further, it approaches the minimum mass limit which represents a wing that is designed for bending considerations only.



**Figure 1.2 Allowable Aileron Deflection Versus Required Wing Structural Weight for Desired Roll Performance**

Figure 1.2 allows for the determination of the wing structural weight required for a desired roll performance, if the maximum aileron deflection is given. This maximum allowable aileron deflection is the deflection before the aileron tears off the wing. For a traditional wing design, the wing weight would remain in the non-reversed branch of this figure and this corresponds a wing structural weight  $W_a$ . However, if the AFW concept is employed, the wing will be allowed to reverse and the resultant weight would be  $W_b$ . Thus, the potential weight saving due to the AFW concept is:

$$\Delta W_{\text{WING}} = W_a - W_b$$

## 1.3 Thesis Overview

Chapter 2.0 details the requirements analysis that was performed on the NSA. It includes a discussion of the Operational Requirements Document (ORD) that was provided by Lockheed. The chapter also contains a discussion of the requirement hierarchy and the resultant extraction of customer needs. A discussion of implicit customer needs is presented. A quality function deployment analysis is performed on the combined explicit and implicit customer needs. The quality functional deployment generates a prioritized list of technical requirements to satisfy the customer needs identified in the ORD.

Chapter 3.0 defines the technical requirements for the NSA wing design. The chapter details the NSA configuration provided by Lockheed. Then, a wing structural layout followed by materials selection is identified. The baseline mission is identified and a single point in the flight envelope is selected for this evaluation. For this flight point, a V-n diagram is constructed, and six resultant design points are identified. Finally, the roll performance for the flight point is discussed.

Chapter 4.0 contains the NSA wing design and sensitivity analysis. The first section in this chapter outlines the design process methodology used for the wing design. Following this section, the synthesis of the wing is discussed. Finally, sensitivity analysis is performed.

Chapter 5.0 contains the conclusions, recommendations, and contributions of this AFW assessment study, and Chapter 6.0 contains the References.





## Chapter 2 Requirements Analysis

The purpose of the requirements analysis is to translate customer's words into technical requirements that are used for the physical design process. The requirements analysis for this project is based on the Operational Requirements Document (ORD) for the New Strategic Airlifter (NSA). The ORD is contained in Appendix A. The NSA was selected by Lockheed as the baseline configuration for which to perform the AFW assessment study. A detailed description of the NSA is contained in Chapter 3. The key concept of the requirement analysis that relates to the AFW assessments is that an initial requirement analysis must be performed on the entire aircraft. Results of this global requirement analysis are technical requirements which the design must demonstrate to satisfy the customer's needs. From these global technical requirements, specific technical requirements for the wing and that of AFW technology are identified.

This chapter details the extraction of derived technical requirements for the AFW wing from the ORD. The requirements analysis procedures consisted of sequential steps which are structured to ensure that the derived technical requirements are in concert with the customer's words. The first step of the analysis is to construct a requirements hierarchy. The second step is to extract explicit customer requirements from the requirements hierarchy. The third step is to generate implicit customer needs. The final step is to compile the explicit and implicit customer needs and perform a Quality Function Deployment (QFD). Results of the QFD are derived technical requirements which ideally satisfy the customer's needs specified in the ORD.

### 2.1 Requirements Hierarchy

A requirements hierarchy was constructed based on the ORD. The procedures used in constructing the requirements hierarchy are as follows:

1. separate customer needs into mission scenarios;
2. extract operational requirement functions; and
3. categorize operational requirement functions into requirement types.

The NSA has both military and commercial missions. For the military role, the ORD specifies a deployment, airdrop, and a tanker mission. The commercial scenarios consist of an overnight and an intermodal mission. Operational requirement functions are defined as operational actions or activities needed to solve the customers needs. [Ref. 2.1] Requirement types are defined as follows:

- **Performance** requirement types are flexible requirements that measure how well the function performs.
- **Reliability** requirement types are flexible requirements that measure how well a function performs over time.
- **Maintainability** requirement types are flexible requirements that measure how well the system can be fixed if failure occurs.
- **Extensibility** requirement types are flexible requirement the measure the ability of the design to adapt to new changes or requirements.
- **Constraints** requirement types are non-flexible requirements that place limits on the design.

Note, constraints affect the design trades between the flexible requirements.

An example of the how the customer’s words were dissected into the a requirements hierarchy format is detailed below:

Customers Words: “Design Life of 40,000 flight hours with a maintenance man-hours per flight hour of 20.0”

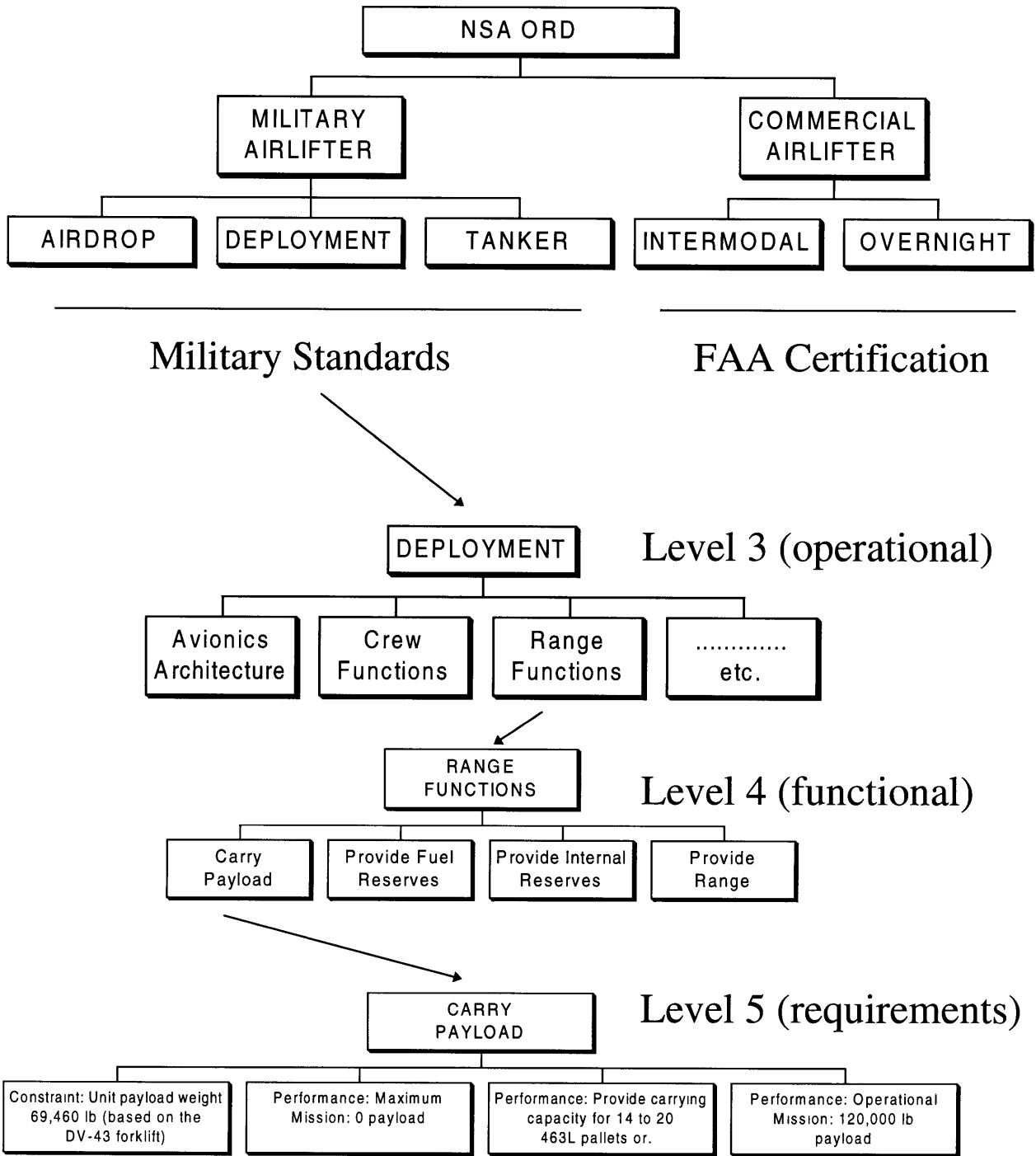
Requirement Function:	Provide Reliability/Maintainability
Requirement Types:	
Reliability Requirement:	<i>Design Life of 40,000 Flight Hours</i>
Maintainability Requirement:	<i>Maintenance Man-Hour per Flight Hour of 20.0</i>

Through this analysis, a requirement hierarchy was constructed. An example of the requirements hierarchy is illustrated in Figure 2.1.

## 2.2 Explicit Customer Needs

The explicit customer needs were extracted from the requirements hierarchy. The basis for selection of the explicit customer needs was dependent on the emphasis placed on the requirement in the ORD. Due to the immense size of the requirements hierarchy and the resultant explicit customer needs, a subset of the explicit customer needs was selected for this analysis — the subset reflects the primary design drivers for the NSA. Furthermore, the subset of explicit customer needs was prioritized, and appropriate weighting terms are illustrated in Table 2.1:

Priority Weighting	Explicit Customer Needs
10	Large Payload Capacity
10	Long Range
10	Reliability, Maintainability, and Supportability
7	Advanced Flight Management System
7	Survivability
4	High Speed
4	High Altitude



**Figure 2.1 Requirements Hierarchy Build Example**

## 2.3 Implicit Customer Needs

The NSA's ORD obtained from Lockheed was primarily focused on performance requirements. As a result, the explicit customer needs identified in the previous section are only performance related. Basing the requirements analysis entirely on performance related requirements would most certainly result in unacceptable derived technical requirements. Today, cost is a critical requirement — sometimes a constraint — in any military procurement program, and is also a primary factor in a commercial program. Thus, cost considerations must be included in the requirements analysis. This was accomplished through implicit customer needs.

To incorporate cost considerations into the requirements analysis, the concept of cost has to be quantified in terms of customer needs. Traditionally, cost is quantified in terms of Life Cycle Cost, LCC. The LCC includes the following divisions: [Ref. 2.2]

- Research, Development, Test, and Evaluation Cost
  - *Cost associated with conceptual, preliminary, and detailed design*
- Acquisition Cost
  - *Cost associated with manufacturing and profit*
- Operating Cost
  - *Cost associated with operating the airplane which includes Indirect Operation Cost and Direct Operating Cost*
- Disposal Cost
  - *Cost associated with the disposal of an aircraft.*

Based on data presented in Reference 2.2, the Operating Cost typically ranges from 50-75% of the LCC, and the Acquisition Cost ranges from 25-50% of the LCC. Thus, the Operating Cost is the primary contributor to the LCC. However, due to budgetary constraints, military procurement often weighs the Acquisition Cost equally to or above that of the Operating Cost.

The Operating Cost is typically subcategorized into Indirect Operating Cost (IOC) and Direct Operating Cost (DOC). IOC division includes all cost that is associated with passengers, ground operations at the gate, promotions, sales, entertainment, and general administration. Traditionally, it is assumed that the airplane designer has little influence on this category of cost. DOC division includes cost associated with flight hours, and is highly influenced by the designer.

At this point, the cost considerations have been quantified in terms of LCC, and the Operating Cost has been determined to be the primary contributor to LCC. Furthermore, the Operating Cost has to be quantified as Indirect Operating Cost and Direct Operating Cost from which it is assumed that the designer only affects the Direct Operating Cost. Thus, the cost consideration will be expressed in terms of Direct Operating Cost.

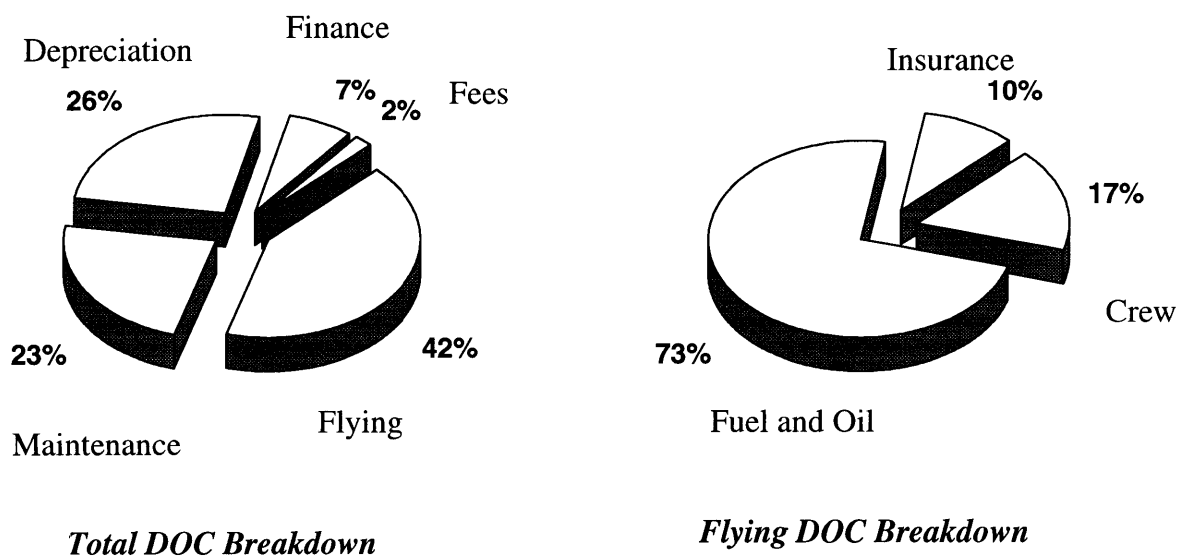
The objective now is to translate the DOC into tangible implicit customer needs. Due to the lack of actual DOC data, empirical estimates of DOC were used. [Ref. 2.2] The empirical estimates for DOC are subcategorized as follows

- Flying Cost
- Maintenance Cost
- Depreciation Cost
- Miscellaneous Cost

The Flying DOC estimate is further subcategorized to include crew, fuel and oil, and insurance costs.

In order to use the empirical DOC estimates, an airplane preliminary design database is required. However, a military cargo configuration database was not available. Therefore, a preliminary design database was obtained from previous work by the author which included a DOC study of narrow-body aircraft. [Ref. 2.3] A reproduction of the DOC study has been duplicated in Appendix B. It is assumed that the general trends of DOC for a narrow-body commercial transport are representative of the DOC for military cargo planes. This assumption is a necessity due to the lack of better information.

The DOC estimates were performed on three different narrow-body aircraft: MD-90-50, B737-300, and A320-200. Furthermore, DOC estimates were computed for the following ranges: 1000 NM, 1500 NM, 2000 NM, and 3000 NM missions were applicable. The key assumptions used for these calculations are referred to Appendix C. Based on the DOC estimates for the cited aircraft and missions, an average is computed. The results of which are illustrated in Figure 2.2.



**Figure 2.2 Typical DOC Breakdown for Narrow-Body Transports**

The next step in determining the implicit customer needs is to select the important empirical parameters that affect the distributions presented in Figure 2.2. This is accomplished by using a relationship matrix to prioritize the parameters which influence the empirical estimates of the DOC. The relationship matrix is illustrated in Figure 2.3. The subcategorization of the DOC is included in the left column of the figure, and the weighting terms reflect the percentages illustrated in Figure 2.2. The parameters which influence the empirical estimation are listed across the top. Reference 2.2 contains a detailed description of the parameters listed. Relationship weighting terms were inserted in the matrix to reflect the importance of the parameter on the particular DOC estimate. A quadratic weighting scheme was selected for this matrix build. A weighting of 9 reflects a *strong positive* affect on the estimate, a weighting of 3 reflects a *positive* affect on the estimate, and a

weighting of 1 reflects a *moderate* effect on the estimate. No negative weighting terms are used in this matrix build. Finally, the DOC weighting estimates are multiplied across the matrix by the relationship weighting terms, and then summed vertically. The results of this relationship matrix are attained by normalizing the vertical summations by the maximum value, and then grouping the technical parameters. The technical parameters obtained thus represent the implicit customer needs, and the resultant normalized prioritization will serve as the implicit customer needs weighting terms. Table 2.2 illustrates the implicit customer needs and the weighting terms that were obtained from the DOC relationship matrix.

<b>Table 2.2 DOC Relationship Matrix Results</b>	
Priority Weighting	Implicit Customer Needs
10	Minimize Aircraft Weight
6	Minimize Aircraft Purchase Price
6	Minimize Block Fuel Consumption
6	Minimize Number of Engines
5	Minimize Maintenance Man Hours
5	Minimize Depreciation



9	Quadratic Weights
3	Strong Positive
1	Positive
1	Week

	Other Cost	Depreciation Cost	Maintenance Cost	Flying Cost					
	Minimize Fuel and Oil Cost				31	9			Minimize Block Fuel Consumption
	Minimize Crew Cost				7	3			Minimize Fuel Price
	Minimize Airframe Cost				4	1			Maximize Fuel Density
	Minimize Airframe/Systems Labor MC				5				Minimize Weight of Oils and Lubricants
	Minimize Engine Labor MC				5				Minimize Number of Engines
	Minimize Airframe/Systems Materials MC				5		9	3	Minimize Annual Block Time
	Minimize Engine Materials MC				5			3	Maximize Oil/Lubricant Density
	Minimize Applied Materials MC				5			3	Minimize Oil/Lubricant Price
	Minimize DC of Airplane without Engines				5			3	Minimize Number of Pilots/Crew
	Minimize DC of Engine				5			9	Minimize Aircraft Purchase Price
	Minimize DC of Avionics Systems				5			9	Maximize Annual Block Time
	Minimize DC Airplane Spare Parts				5			9	Maximize Block Speed
	Minimize DC Engine Spare Parts				5			3	Minimize Flight Delays
	Minimize Landing Fees				1			3	Minimize Maintenance Man Hours
	Minimize Registry Taxes				1			9	Minimize Labor Rate
	Minimize Financing Cost				7			9	Minimize Aircraft Weight
6	279								Minimize Takeoff Thrust
2	93								Minimize Engine Purchase Price
1	31								Maximize Time Between Engine Overhaul
1	31								Minimize Depreciation Rate
6	258	3	9	3	3	3	9	9	Maximize Number of Engines
2	76								Maximize Engine Price
1	31								Maximize Price Of Avionics
1	31								Maximize Depreciation Period
1	63								Maximize Block Time
6	284	9	3	3	9	9	9	9	
0	12								
3	110		3	3	3	3	3	3	
1	25								
5	225								
1	45								
10	437	9	9	9	9	9	9	9	
0	20								
1	60								
1	60								
5	225								
0	10								
0	10								
0	5								
5	225								
2	78								

Figure 2.3 DOC Relationship Matrix

## 2.5 Requirements QFD Build

At this point in the requirements analysis, the explicit and implicit customer needs have been identified. The customer needs include both performance and cost considerations, and these results are summarized in Table 2.3. It is seen from this table that the customer needs are conveniently categorized to cost, performance, and operational drivers. The weighting terms of the combined customers needs reflect the weighting terms illustrated in each of the explicit and implicit builds. However, there is one exception; the minimized aircraft purchase price from a DOC perspective had a weighting of 6, but because of the importance of purchase price in military procurement, the purchase price weighting was increased to a 10.

**Table 2.3 Explicit and Implicit Customer Needs**

<b>Cost Drivers:</b>		<b>Performance Drivers:</b>	
10	Minimize Aircraft Takeoff Weight	10	Large Payload Capacity
10	Minimize Aircraft Purchase Price	10	Long Range
7	Minimize Block Fuel Consumption	4	High Speed
7	Minimize Number of Engines	4	High Altitude
6	Minimize Maintenance Man Hours	4	Long Endurance
6	Minimize Depreciation		
<b>Operational Drivers:</b>			
10	Reliability, Maintainability, and Supportability (R, M,& S)		
7	Advanced Avionics		
7	Survivability		

The final step of the requirements analysis is to perform a Quality Function Deployment (QFD) analysis on the prescribed customer needs. This was accomplished by using the guidelines specified in Reference 2.4. The relationship between the technical requirements and the customer needs is expressed in the matrix via relationship weighting parameters. Finally, a prioritized list of technical

requirements is produced by vertically summing the columns of the relationship matrix. Furthermore, conflicts between technical requirements are identified in the correlation matrix.

Given the customer needs illustrated above, a QFD matrix was constructed for the NSA, and it is illustrated in Figure 2.4. The customer needs along with their weightings are represented in the left vertical columns. The technical requirements are represented across the top of the matrix, and the technical requirements are grouped into the following categories:

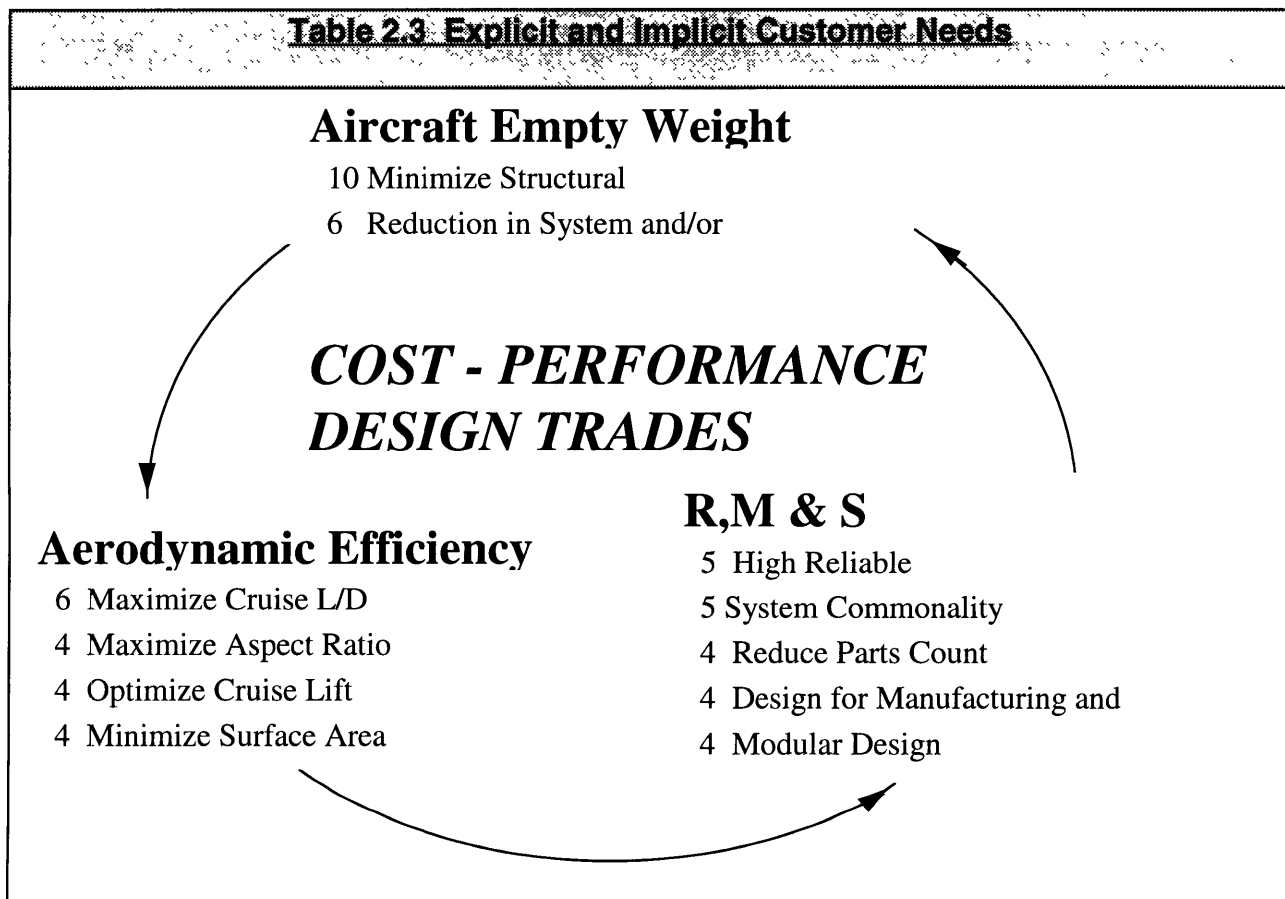
- Aircraft Empty Weight,
- Aerodynamic Efficiency,
- Engine Efficiency,
- Engine Sizing,
- Manufacturing,
- Technology, and
- Support.

The categorization of technical requirements was assumed by the author based on previous airplane design heritage. The intent of the list is to represent some of the primary design drivers which affect the customer needs. The list is not intended to be all inclusive.

As with the DOC relationship matrix, the QFD relationship matrix reflects the importance of the technical requirements for a particular customer need. Again, a quadratic weighting scheme was selected for this matrix build. A weighting of 9 reflects a *strong positive* affect on the customer need, a weighting of 3 reflects a *positive* affect on the customer need, a weighting of 1 reflects a moderate effect on the customer's need, and a blank reflects no effect. Additionally, negative weighting terms were included in this matrix. Note, negative weighting terms are not traditionally included in QFD matrix builds. The author decided to include them for the purpose of highlighting the conflicts between customer's needs and technical requirements, and a -3 weighting reflects a *negative* affect on the customer's need. The -3 was selected versus -1 or -9 because it was an intermediate value.



Finally, the customer's needs weighting terms are multiplied across the matrix by the relationship weighting terms, and then summed vertically. Results of this QFD matrix are attained by normalizing the vertical summations by the maximum value, and then grouping the technical requirements. The technical requirements obtained thus represent the derived technical requirements. Table 2.4 illustrates the derived technical requirements and their relative importance (weightings) to the design of the NSA.



## 2.6 Conclusions

The requirements analysis was performed for the New Strategic Airlifter. Explicit customer's needs were identified from a requirements hierarchy build. Implicit (derived) customer's needs were identified based on Life-Cycle Cost. Customer needs were prioritized, and a QFD analysis was

performed. Finally, prioritized technical requirements were extracted from the QFD. The results of the technical prioritization are illustrated in Table 2.3. Additionally, three primary technical requirements categories were identified: aircraft empty weight, aerodynamic efficiency, and reliability, maintainability, and supportability (R,M&S).

The purpose of the requirements analysis was to translate customer's words into technical requirements for which to initiate the physical design process. Given the requirements analysis for the entire aircraft, the categorization of derived technical requirements were applied to the AFW assessment study. The questions this study should answer in relation to the derived technical requirements are as follows:

1. Wing Structural Weight

*What are the potential weight savings with an AFW for high aspect ratio configuration?*

*What are the potential penalties for system integration and complexity?*

2. Aerodynamic Efficiency

*What are the potential aerodynamic efficiency benefits/drawbacks?*

- *Induced Drag*
- *Control Surface Reversal*
- *Load Alleviation*
- *Elastic Mode Control*

3. Reliability, Maintainability, and Supportability

*What are the reliability, maintainability, and supportability issues that may affect the implementation of AFW technology?*

Numerous design trade studies are needed to completely and to properly evaluate the derived technical requirements. However, as outlined in Section 1.2, only a small fraction of the design trades is addressed in this project. This AFW assessment study focused on the potential weight savings, and the resultant effect of AFW on the aerodynamic efficiency. Reliability, maintainability, and supportability issues were not addressed.

## Chapter 3 Baseline Configuration and Mission

This chapter outlines the baseline configuration and mission for the AFW assessment study. In particular, this chapter contains a general discussion of the baseline configuration of the New Strategic Airlifter. Additionally, the baseline wing parameters, wing structural arrangement, and material selection is presented. A flight envelope point is presented along with a V-n diagram. Finally, the Military Specification for roll performance is reviewed. The objective of the chapter is to outline the assumptions, constraints, and specifications for the AFW assessment.

### 3.1 NSA Baseline Configuration

The proposed role of the NSA is to provide a replacement for the aging C-141 Starlifter fleet. The primary military role of the NSA will be that of deploying U.S. strategic forces throughout the world in both times of crisis and times of peace. The NSA will also have airdrop and tanker capabilities so as to provide multiple functionality. Additionally, due to the rapidly expanding commercial airfreight market, the airlifter will have commercial applications ranging from overnight package services to high priority oversized shipping.

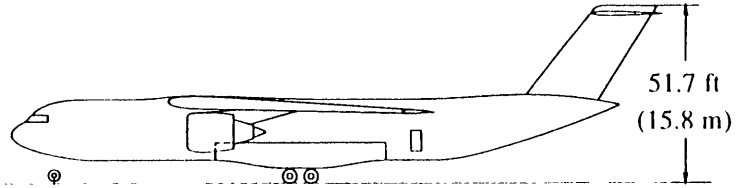
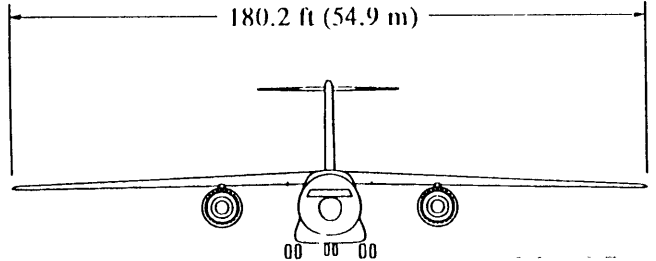
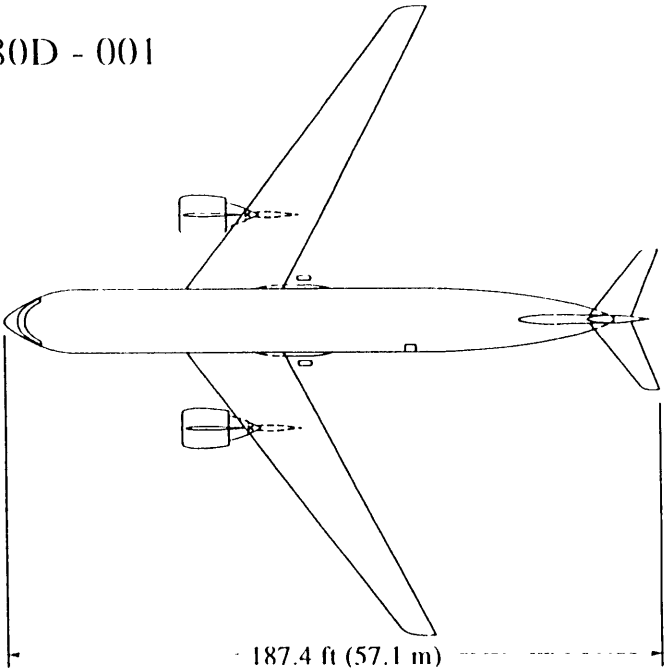
Several NSA configurations were provided by Lockheed Martin Aeronautical Systems. [Ref. 3.1 through 3.6] These included variants with two engines and four engine with various cargo capabilities. The particular NSA configuration selected for this assessment study is the LGA180D, which is a single stick — accommodation for only a single row of 463L pallets — twin engine concept. A three-view of the geometric configuration is provided in Figure 3.1. The attributes of the LGA180D configuration are as follows:

**TYPE:** Twin Engine, Long Range Military Airlifter

**STRUCTURE:** Nominal B777 material technology levels are assumed.

LGA180D - 001

Wing Area	3425.8 ft**2	318.2 m**2
Wing Sweep	35.0 deg	35.0 deg
Aspect Ratio	9.5	9.5
Cargo Box Width	13 ft	4.0 m
Range	3,300 nm	6,112 km
Payload	120,000 lb	54,432 kg
Cruise Speed	0.82 M	0.82 M
MTOW	399,330 lb	181,136 kg
OWE	165,984 lb	75,290 kg
2 CF6 - 80C2 Engines	61,500 lb ea.	27,896 kgf



**Figure 3.1 NSA LGA180D Configuration Three-View**  
 (Copied from Reference 3.1)



**LANDING GEAR:** The landing gear is an underfloor storage pod configuration similar to that used for the C-5.

**POWERPLANT:** Two CF6-80C2 ( each 61,500 lb. static, uninstalled ) high-bypass turbo-fan engines. This engine is a major redesign of the CF6-80A1 for higher thrust and improved specific fuel consumption. The fan diameter is 93 inches, and it has a four-stage compressor and 5.5 stage turbine.

**ACCOMMODATIONS:** Flight crew requires two pilots and the cargo crew requires 1 loadmaster. Up to 6 flight crew can be accommodated for extended missions. The airlifter can transport both palletized bulk and oversized cargo.

### **DIMENSIONS, EXTERNAL**

Wing Span	180.2 ft
Wing Chord: at root	29.3 ft
at tip	8.8 ft
Wing Aspect Ratio	9.5
Wing Sweep (quarter chord)	35.0°
Length Overall	187.4 ft
Fuselage: Length	174.5 ft
Max Diameter	17.58 ft
Height Overall	51.7 ft
Tailplane Span	38.5 ft

### **DIMENSIONS, INTERNAL**

Floor Length	55.8 ft
Floor Width	13.0 ft

### **AREAS**

Wing, gross	3426. ft <sup>2</sup>
Fin	496.2 ft <sup>2</sup>
Tailplane	336.0 ft <sup>2</sup>

### **WEIGHTS AND LOADINGS**

Basic Operating Empty Weight	165,984 lb.
Max Usable Fuel	114,931 lb.
Max Payload	120,000 lb.

Gross T-O Weight	399,330 lb.
Max Wing Loading	113.8 psf

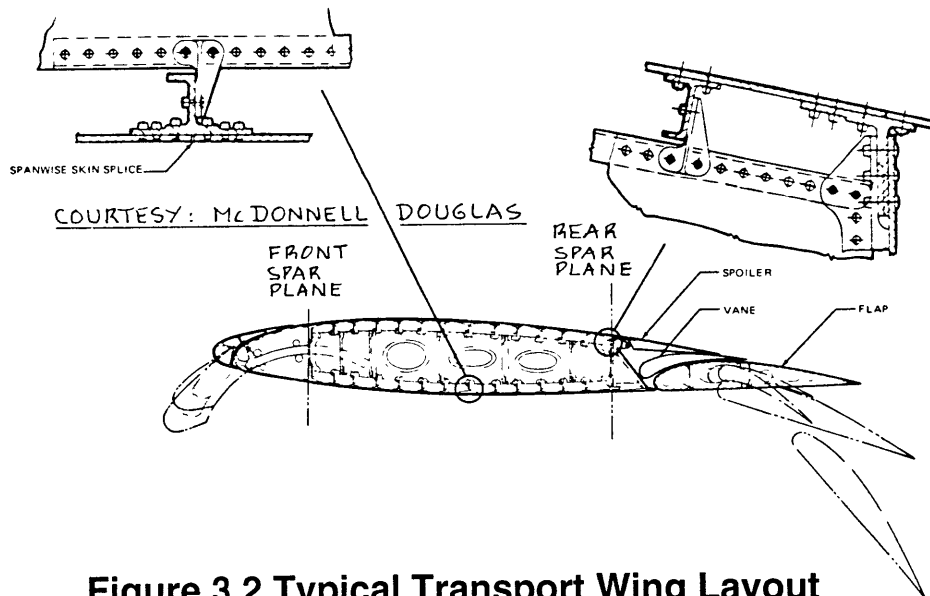
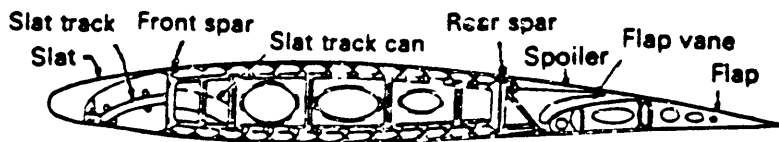
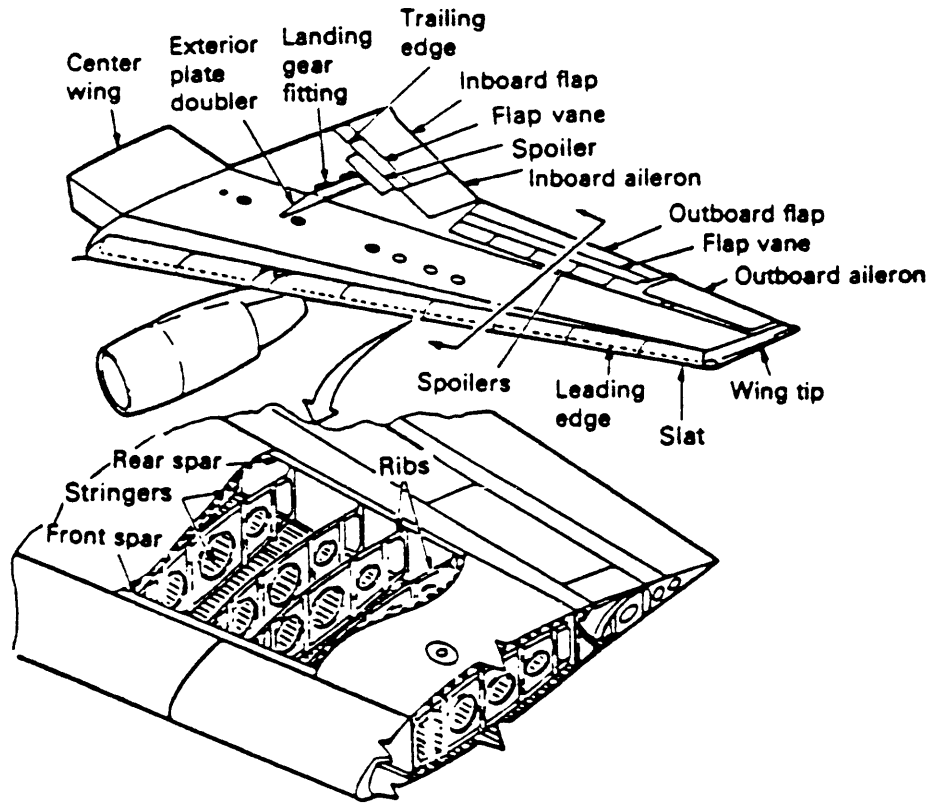
## PERFORMANCE

Max Cruise Speed	502 knots
Range	3,300 NM
Critical Field Length	7,488 ft

### 3.2 Wing Structural Layout

The primary function of a wing is to produce lift, and in doing so, the wing must transmit the lift forces to the fuselage. The aerodynamic functionality is provided by the airfoil, and the load transfer is accomplished by the wing's torque box.

Wing structural design is based on a semimonocoque structure where the strength is derived from the skin and the skeleton structure inside the wing. The primary spanwise members of the structural skeleton are the spars, stringers, and shear webs, and the primary chordwise member is the rib. A typical transport wing is illustrated in Figure 3.2. Of particular interest in Figure 3.2 is the primary structural elements that are identified in the figure. Spar caps, which define the corners of the wing's torque box, are structural members whose primary function is to provide bending stiffness both in-plane and out-of-plane. In-plane bending is produced primarily from lift, and out-of-plane bending is generated from the drag, the engine thrust, and the lift in high angle of attack conditions. Shear webs, which bridge the gap between the upper and lower spar caps, are structural members that transmit shear loads generated by the in-plane bending loads to the fuselage.



**Figure 3.2 Typical Transport Wing Layout**

(Copied from References 3.7 and 3.8)

The skin of the aircraft provides dual functionality. The primary function of the skin is to provide torsional stiffness. Furthermore, the skin provides bending stiffness in both directions. Like the spar caps, the skin is located the greatest distance from the centroid of the torque box, and this results in a significant contribution to the bending stiffness. Due to the dual functionality, the skin transmits both bending and torsional loads to the fuselage. Another structural member illustrated in Figure 3.2 is the stringer. Stringers are attached to the upper and lower skins, and serve the primary function of transmitting in-plane bending moments to the fuselage; thus, relieving the skin of its bending stiffness functionality. Additionally, stringers prevent local buckling of the skin. Nui, Reference 3.7, suggests that a stringer area to skin area ratio of about 1.7. Thus, for a skin-stringer panel, the stringers provide most of the bending stiffness and the skin provides most of the torsional stiffness. The net effect of this combination is a lighter weight structure.

Finally, the primary function of the ribs is to maintain the airfoil external shape along the chord of the wing without appreciable distortions. Ribs also transmit the sectional chordwise loads to the spar caps and shear webs.

Considering the structural functionality prescribed above, a baseline structural arrangement was selected for the assessment study. The NSA wing planform parameters were provided by Lockheed Martin Aeronautical Systems, Ref. 3.1 through 3.6, which serve as a basis for the structural layout. The NSA wing planform parameters are as follows:

#### **WING PLANFORM DATA**

Span	180.2 ft
Taper	0.3
$\Lambda_{.25C_{bar}}$	35°
Root Chord	29.3 ft
Tip Chord	8.80 ft
MAC	20.9 ft
Area	3,425.8 ft <sup>2</sup>
AR	9.5
Anhedral	2°
Twist	-3° @ tip

t/c: @ wing/body	16.3%
t/c: @ .95 $b_{bar}/2$	12.0%

### OUTBOARD AILERON DATA

Chord:	75%-100% $C_{bar}$
Span:	70%-90% $b_{bar}/2$

### FLAP DATA

Type:	Single-Slotted Fowler
Chord:	70%-100% $C_{bar}$
Span:	Wing/Body-65% $b_{bar}/2$
High-Lift Chord	70%-110% $C_{bar}$
High-Lift Deflection	45°

### SPOILER DATA

Chord:	70%-80% $C_{bar}$
Span:	Wing/Body-65% $b_{bar}/2$

In addition to the wing planform illustrated above, an inboard aileron was added to this configuration. The need for the inboard aileron came about because of the inability to model the spoilers for the analysis presented in Chapter 4. The primary functionality of spoilers is to provide roll control power at high speeds; thus, considering that the objective is roll performance at high speeds, the inboard aileron was substituted for this assessment study. It is important to note that inboard ailerons, also known as high speed ailerons, are common for transports. Typically, when the high-lift system becomes a dominant design driver and limits the available space for the inboard aileron, a designer resorts to the use of spoilers for high speed roll control power.

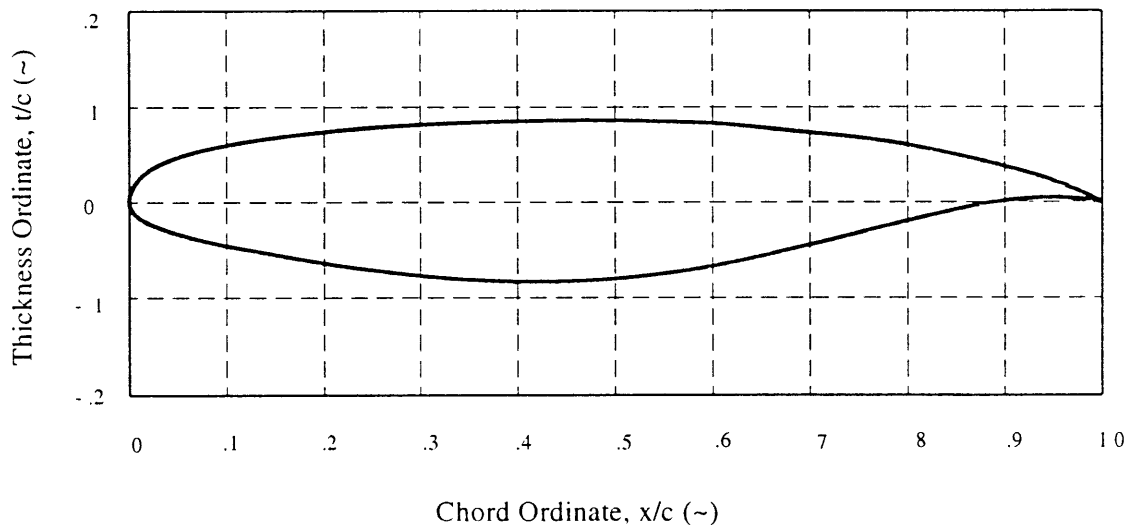
The inboard aileron was sized such that the rigid wing aileron control power derivative of the inboard aileron was equal to that of the outboard aileron. Based on this sizing, the planform parameters for the inboard aileron are as follows:

### INBOARD AILERON DATA

Chord:	75%-100% $C_{bar}$
Span:	52%-70% $b_{bar}/2$

The structural arrangement of the wing was assumed based on conventional standards presented in References 3.7 and 3.8. There are two spars with the front spar located at 15% of the chord and the rear spar located at 65% of the chord. As specified by Reference 3.5, the wing is a root-root attachment. The wing's configuration is a straight tapered wing versus a cranked wing due to the fact that the concept is a high wing configuration and that the landing gear is fuselage mounted. Rib spacing was assumed to be 24 inches. The rib spacing was altered at various spanwise stations to account for the engine integration and flight control surface attachment points. No leading edge devices were included. The stringer spacing was assumed to be 12 inches. In accordance with design for manufacturing and assembly considerations, the stringers and the ribs are oriented parallel and perpendicular to the rear spar respectively.

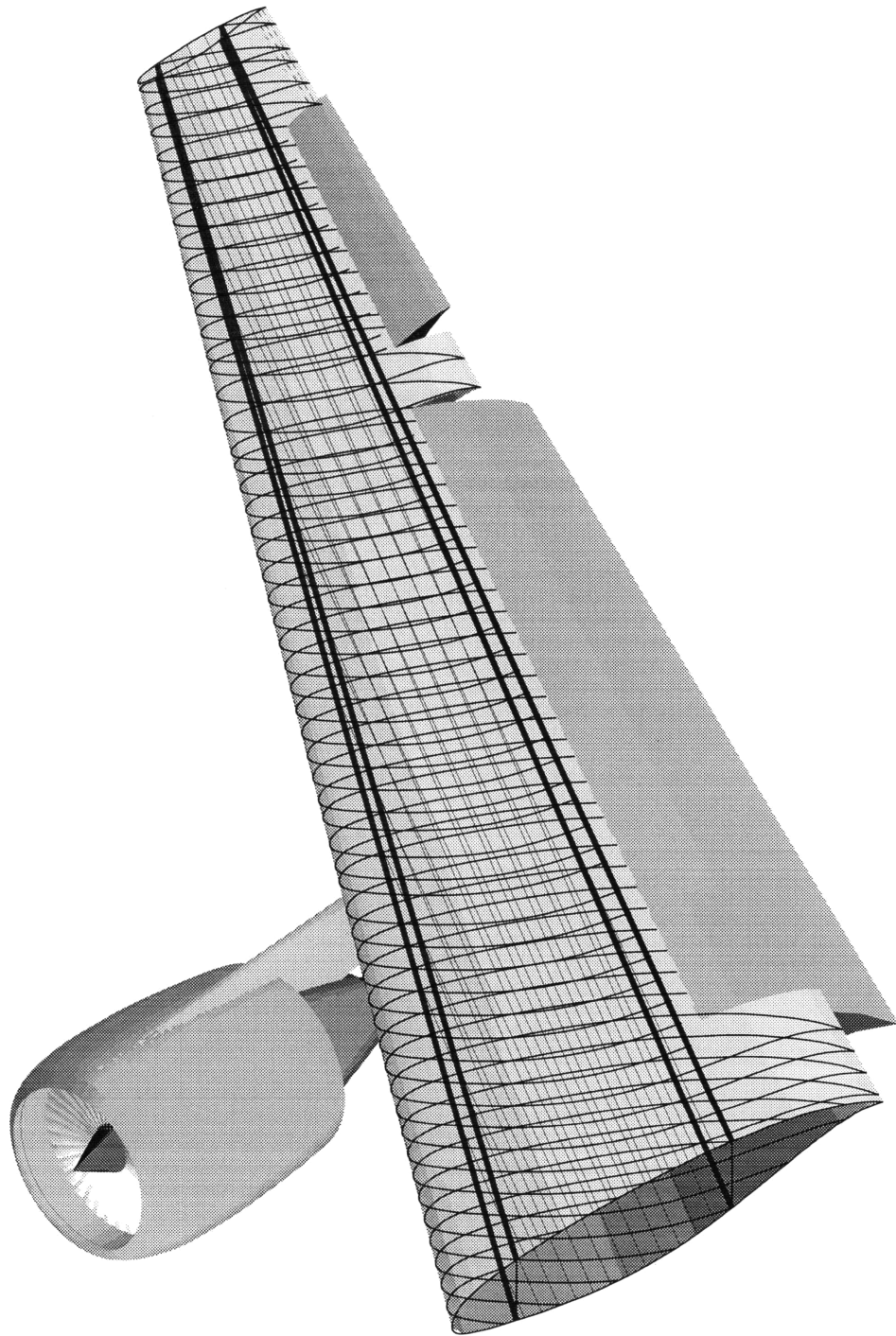
To finalize the structural arrangement, a generic supercritical airfoil was used for the baseline wing configuration. The airfoil is representative of the airfoil used on the Boeing 777, Reference 3.9, and it is illustrated in Figure 3.3.



**Figure 3.3 Supercritical Airfoil Ordinates**

Considering the selected structural disposition and airfoil, a 3-dimensional schematic of the structural arrangement was generated, and the half-span layout is illustrated in Figure 3.4. The four lines that traverse the span of the wing illustrate spar caps, and the shear webs are symbolically represented as the structural sheets between the top and bottom spar caps. The non-highlighted lines that transverse the span between the front and rear spars illustrate the stiffeners. The ribs are illustrated by the sectional airfoil shapes that transverse the span. Finally, the shaded surface represents the top and bottom skin.

In addition to the basic structural layout, the aileron, flap, engine pylon, and the engine were included in this layout representation. The utility of this model will become evident with the analysis model builds in Chapter 4 which are variants of the structural layout presented in Figure 3.4.



**Figure 3.4 Selected Wing Structural Arrangement for the NSA**



### 3.3 Wing Material Selection

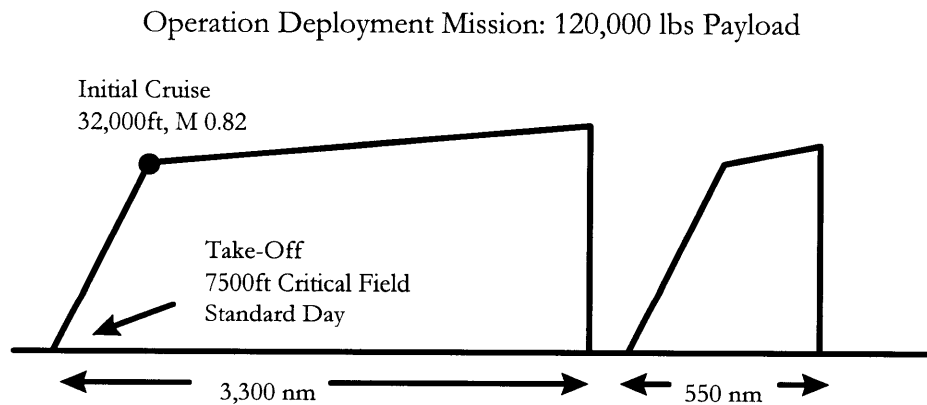
The material selection for the wing is based on typical transport wing data presented in References 3.7 and 3.8. An all metallic wing is assumed for this assessment study. Trade studies should be performed to assess the impact of metallic and non-metallic wing structure on the AFW concept, and this is recommended for future investigations.

The wing's upper skin and stringers are designated to be AL-7075-T6 which has desirable compression characteristics. The wing's lower surface, stringers, spar caps, and shear webs are assumed to be AL-2024-T3 due to its desirable strength characteristics and corrosion resistance. The material properties, illustrated in Table 3.1, were obtained from the military handbook, MIL-HDBK-5E.

Material/Form	AL-7075-T6 Sheet	AL-2024-T3 Sheet	AL-2024-T3 Bar
Specification	QQ-A-250/12	QQ-A-250/4	QQ-A-200/3
Thickness/Areas	.040-.125 in	.010-.128 in	.750-1.50 in <sup>2</sup>
F <sub>tu</sub> , ksi	78	64	65
F <sub>ty</sub> , ksi	70	47	46
F <sub>cy</sub> , ksi	69	39	41
F <sub>su</sub> , ksi	47	39	33
E, 10 <sup>3</sup> ksi	10.3	10.5	10.8
E <sub>c</sub> , 10 <sup>3</sup> ksi	10.5	10.7	11.0
G, 10 <sup>3</sup> ksi	3.9	4.0	4.1
η	.33	.33	.33
ω, lb. in <sup>3</sup>	.101	.101	.101
Note, all properties correspond to the A Basis and L direction were applicable.			

### 3.4 Baseline Missions and Design Point Selection

The NSA ORD specifies two baseline missions in terms of range and payload. The operational mission consists of a 3300 NM range and a payload of 120,000 lb. The maximum mission consists of a 6000 NM range with no payload. For both missions, the range is specified as the distance from departure to the intended landing field with no refueling and no wind. Both missions are to take-off from a 7500 x 86 foot, level, dry paved runway, standard day, at sea level with no obstacles. The initial cruise is specified to be 32,000 ft at 0.82 Mach, and the maximum cruise altitude is 39,000 ft. Additionally, the maximum airspeed is either 350 KEAS or 0.86 Mach. This breakpoint in maximum airspeed occurs at approximately 24,000 ft in a standard atmosphere. Finally, both missions must have enough fuel reserves to fly an additional 550 NM to an alternative landing field. The baseline mission profile is illustrated in Figure 3.5.



**Figure 3.5 NSA Baseline Operation Mission**

*The initial cruise point in the operational mission is selected for the AFW assessment study because the point represents the heaviest weight and highest dynamic pressure combination. Recall that*

- aeroelastic effects are more prominent at high dynamic pressures;
- heavy weight translates to larger wing loading; and

- heavy weight translates to a larger rolling moment of inertia (unburned fuel is in the wing) which inhibits rolling performance.

Ideally, the assessment study would investigate the entire flight envelope including take-off and landing load cycles.

### 3.5 V-n Diagram for Selected Design Point

Given the design point selection, a V-n diagram was constructed. The V-n diagram build was based on MIL-A-8861(ASG), and the parameters that were used for this build are contained in Table 3.2.

<b>Table 3.2 V-n Diagram Parameters for Initial Cruise Point</b>	
Altitude	32,000 ft
Initial Cruise Weight	380,000 lb.
Wing Area	3426 ft <sup>2</sup>
Positive $CL_{MAX}$	1.5
CD @ Positive $CL_{MAX}$	0.1123
Negative $CL_{MAX}$	-1.125
CD @ Negative $CL_{MAX}$	0.0710
Positive Load Factor, $n_{LIMIT}$	2.5
Negative Load Factor, $n_{LIMIT}$	-1.0
Mean Geometric Chord	20.83 ft
$CL_{\alpha}$	6.20 rad <sup>-1</sup>
Maximum Speed	239.1 KEAS

The initial cruise weight of 380,000 lb. was determined by assuming a 5% mass credit for the taxi, take-off, and climb segments of the mission profile. The gross take-off for the operational mission is 399,330 lb.. The  $CL_{MAX}$  for cruise was provided by Lockheed, Reference 3.10. The CD at the

$CL_{MAX}$  was calculated based on empirical methods based in Reference 3.11, and the drag polar was determined to be:

$$CD = 0.0180 + 0.0419 CL^2$$

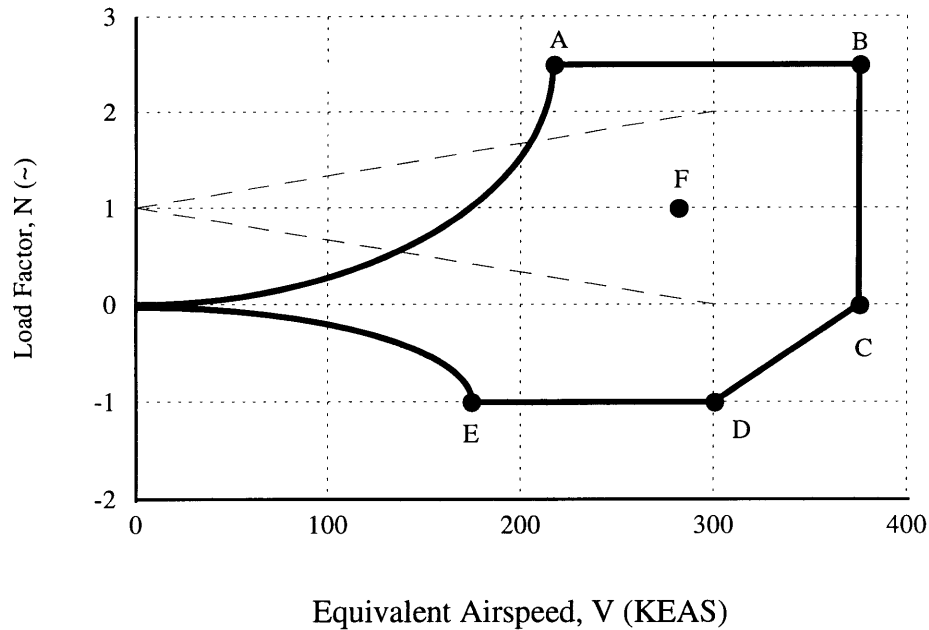
The negative  $CL_{MAX}$  was assumed to be 75% of the positive  $CL_{MAX}$ . The  $CL_{\alpha}$  was determined through empirical estimates contained in Reference 3.11. The load factors were based on specifications for a medium cargo/transport in MIL-A-8861(ASG). Finally, the maximum cruise speed corresponding to M 0.86 at 32,000 ft was determined to be 239.1 KEAS based on standard atmosphere.

The results of the V-n diagram build are as follows:

- 2.5 g Stall Speed: 239.1 KEAS
- 2.5 g - 0.0 g Dive Speed: 370.1 KEAS
- -1.0 g Max. Speed: 296.1 KEAS
- -1.0 g Stall Speed: 174.6 KEAS

Additionally, it was determined that the initial operational cruise point is not gust critical. Figure 3.5 illustrates the V-n diagram.

It is important to note that corners of the V-n diagram represent the worst case scenarios for the wing structural design for the given design point in the flight envelope. Imagine an aircraft at an initial altitude of 32,000 ft. in a straight level flight, and the pilot pushes the yoke forward to perform a push-over maneuver. The push-over maneuver is performed at a constant -1.0 g load factor; thus, the pilot initiates the maneuver by commanding maximum negative  $Cl_{max}$ , and then trades negative angle of attack for speed to maintain the desired load factor. In doing so, the aircraft transitions into a dive, and eventually reaches a terminal velocity (steady state dive speed). As the aircraft plunges towards the ground, the pilot pulls back the yoke at about 20,000 ft to perform a pull-up maneuver. The pull-up is performed at a constant 2.5 g; thus, the pilot trades speed for angle of attack, or as the speed decreases, the angle of attack increases to maintain 2.5 g's. After the pull-up maneuver, the pilot proceeds with a straight and level flight at an altitude below 20,000 ft and



**Figure 3.5 V-n Diagram for Initial Operational Cruise Point**  
 (h=32,000 ft, M=0.82, W=380,000 lb.)

hopefully above the ground. The maneuver just described is illustrated in Figure 3.8 through the boundary points from points E through A. Points E to D represent the push-over maneuver, and Points D to C represent the transition from horizontal flight to a steady state vertical flight trajectory. Points C through B represent the steady state dive from 32,000 ft to 20,000 ft. Points B to A represent the pull-up maneuver.

It is important to note that the maneuver prescribed above is a longitudinal maneuver only, and lateral maneuvers should be considered in the wing structural design. The lateral directional maneuver is performed about point F in the flight envelope. Ideally, the wing design should be performed with coupled longitudinal and lateral maneuver such as a rolling pullout; however, the computational analysis presented in Chapter 4 can only perform uncoupled maneuvers. The details of the lateral maneuver will be detailed in the next section.

Considering the longitudinal and lateral maneuvers described above, the six design points were obtained from the V-n diagram, and these points are detailed in Table 3.3. A further tutorial of a V-

n diagram and the relationship of the maneuvers to the structural characteristics are contained in Section 2.7 of Reference 3.12.

<b>Table 3.3 Design Points for Initial Operational Cruise Condition</b>			
Point	Longitudinal Maneuver Description	Load Factor	Velocity
A	Positive Lift, Stall Boundary	2.5	239 KEAS (0.69 M)
B	Positive Lift, Maximum Speed	2.5	370 KEAS (1.07 M)
C	Zero Lift, Maximum Speed	0.0	370 KEAS (1.07 M)
D	Negative Lift, Maximum Speed	-1.0	296 KEAS (0.86 M)
E	Negative Lift, Stall Boundary	-1.0	174 KEAS (0.50 M)
Point	Lateral Maneuver Description	Load Factor	Velocity
F	Level I Roll Performance	1.0	282 KEAS (0.82 M)

### 3.6 Roll Performance for Selected Design Point

Recall that the objective of the AFW assessment is to determine whether or not the torsional stiffness of the wing is a design driver based on the required roll performance. The metric for evaluating the roll performance is provide by the Military Specification MIL-F-8785C. As specified in MIL-F-8785C, for a Class III Aircraft and a Category B Flight Phase, the Level I roll performance requires that the:

- Aircraft must be able to bank  $30^\circ$  in 2.0 seconds, and
- Maximum roll-mode time constant,  $\tau_r$ , must be less than or equal to 1.4 seconds.

A Class III Aircraft is defined as a large, heavy, low-to-medium maneuverability airplane [Ref. 3.13]. Furthermore, a Category B Flight Phase is defined as a non-terminal flight phase which consists of gradual maneuvers without precision tracking although accurate flight-path control may be required [Ref. 3.13]. Finally, Level I is defined as flying qualities that are clearly adequate for the mission [Ref. 3.13].

To translate roll performance requirement into physical design constraints, the *rolling approximation* is used. [Ref. 3.13] The rolling approximation is based on the lateral-directional small perturbation equations of motion where only the rolling degree-of-freedom is considered. Based on this approximation, the time domain roll response for a given aileron step input is:

$$\phi(t) = -\frac{L_{\delta A} \delta_A}{L_P} t + \frac{L_{\delta A} \delta_A}{L_P^2} (e^{-L_P t} - 1)$$

where:  $\phi(t)$  is the aircraft bank angle,

$L_{\delta A}$  is the dimensional aileron control power derivative,

$L_P$  is the dimensional roll damping derivative, and

$\delta_A$  is the aileron deflection.

From this rolling approximation, the roll mode time constant is identified and its relationship to the Level I Roll Performance specification is:

$$\tau_R \cong \frac{-1}{L_P} \leq 1.4 \text{ sec.}$$

Additionally, the time domain specification results in the following constraint:

$$\phi(2.0 \text{ sec.}) \geq 30^\circ$$

These two constraints are used for the analysis in Chapter 4.

### 3.6 Conclusions

This chapter discussed the baseline configuration and mission for the AFW assessment study. The baseline aircraft configuration is the New Strategic Airlifter, NSA. The particular NSA configuration selected for this assessment study is the LGA180D, which is a single stick twin engine concept.

One modification was made to LGA180D for this assessment study. An inboard aileron control surface was used instead of the specified spoiler layout. The need for the inboard aileron came about because of the inability to model the spoilers for the analysis presented in Chapter 4. The primary functionality of spoilers is to provide roll control power at high speeds; thus, considering that the objective is roll performance at high speeds, the inboard aileron was substituted for this assessment study. The inboard aileron was sized such that the rigid wing aileron control power derivative of the inboard aileron was equal to that of the outboard aileron.

Using the NSA concept as a template, the structural arrangement of the wing is assumed based on conventional standards presented in References 3.7 and 3.8. There are two spars with the front spar located at 15% of the chord and the rear spar located at 65% of the chord. Rib spacing was assumed to be 24 inches. The stringer spacing was assumed to be 12 inches. In accordance with design for manufacturing and assembling considerations, the stiffeners and the ribs are oriented parallel and perpendicular to the rear spar respectively. To finalize the structural arrangement, a generic supercritical airfoil was used for the baseline wing configuration.

The material selection for the wing is based on typical transport wing data presented in References 3.7 and 3.8. An all metallic wing is assumed for this assessment study. The wing's upper skin and stringers were designated to be AL-7075-T6, and the wing's lower surface, stringers, spar caps, and shear webs were assumed to be AL-2024-T3.

The NSA ORD specifies two baseline missions, an operational and maximum mission, and a single point in the operational mission flight envelope was selected for the assessment study. *The initial cruise point in the operational mission is selected for the AFW assessment study because the point represents the heaviest weight and highest dynamic pressure combination.* Recall that:

- Aeroelastic effects are more prominent at high dynamic pressures;
- Heavy weight translates to larger wing loading; and



- Heavy weight translates to a larger rolling moment of inertia (unburned fuel is in the wing) which inhibits rolling performance.

The initial cruise is specified to be 32,000 ft at 0.82 Mach, and the operation baseline mission is defined as a 3300 NM range with a payload of 120,000 pounds.

Given the design point selection, a V-n diagram is presented. The V-n diagram build is based on MIL-A-8861(ASG), and it represents the worst case scenario for the wing structural design for the given design point in the flight envelope. Based on the V-n diagram build, five longitudinal maneuver design points are obtained. The design maneuver points are listed in Table 3.3.

Lateral maneuvers are also considered in the wing structural design. This is accomplished by performing a Military Specification MIL-F-8875B Level I roll maneuver. As specified in MIL-F-8785C, for a Class III Aircraft and a Category B Flight Phase, the Level I roll performance requires that the

- Aircraft must be able to bank 30° in 2.0 seconds, and
- Maximum roll-mode time constant,  $\tau_r$ , must be less than or equal to 1.4 seconds.

Based on the lateral-directional small perturbation rolling approximation, the Level I roll performance requirements were translated into the following design constraints:

$$\tau_R \cong \frac{-1}{L_P} \leq 1.4 \text{ sec.}$$

$$\phi(2.0 \text{ sec.}) \geq 30^\circ$$

Only one point in the one flight envelope was considered, for which only 6 wing loading scenarios were considered out of 38 possible scenarios listed in Reference 3.7. There are typically thousands of different loading and flight envelope combination that must be evaluated in a wing design; this assessment study will evaluate only one.

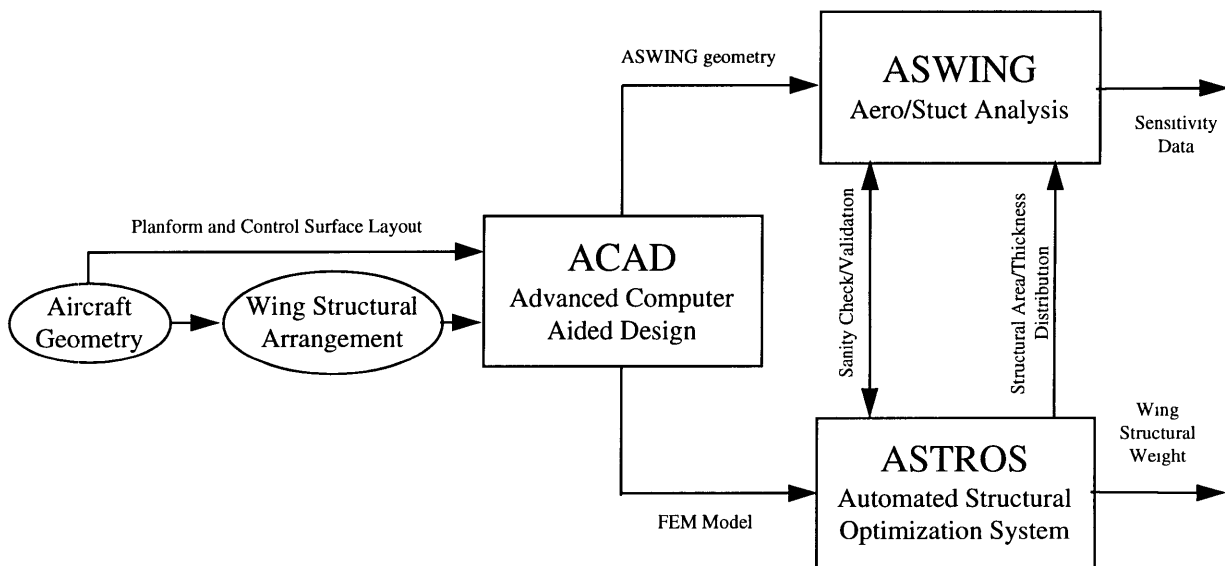


# Chapter 4 NSA Wing Design and Sensitivity Analysis

This chapter details the design of the NSA wing for the AFW assessment study. Section 4.1 provides a discussion of the design process that is used for this assessment study. Section 4.2 provides a description of the multidisciplinary design of the NSA wing, and Section 4.3 presents sensitivity analysis. Finally, Section 4.4 presents the conclusions of the design and sensitivity analysis.

## 4.1 NSA Wing Design Process Overview

This section details the design process that is used for this assessment study. The design process is illustrated in Figure 4.1.



**Figure 4.1 NSA Wing Design Process**

The first step of the design process was to obtain the baseline NSA configuration. Given the baseline geometry, a wing structural arrangement was assumed. The wing structural arrangement is

detailed in Section 3.2. With the baseline configuration and the structural arrangement, a three-dimensional wing model was constructed in Lockheed's Advanced Computer Aided Design (ACAD) program. The ACAD program is currently the primary tool used by Lockheed for geometric synthesis. It also allows the geometric definitions to be translated directly into structural analysis models. Lockheed was able to provide the team with a digital file of the NSA concept chosen for this assessment study.

The next step of the design process is to generate a finite element model of the baseline structural arrangement. This was performed by using a multidisciplinary optimization tool called Automated Structural Optimization System (ASTROS) program [Ref. 4.1-4.2]. ASTROS was selected for this assessment study because of its multidisciplinary applicability which allows simultaneous aerodynamic and structural analysis. Furthermore, ASTROS has an optimization tool that given the aerodynamic and structural analysis, will determine the minimum weight structure based on the to-be-specified design constraints. The aerodynamic loads analysis is provided by USSAERO-C which is an advanced panel modeling method. Structural analysis, which forms the core of ASTROS, is provided by finite element modeling methods. For the optimization aspect, ASTROS uses the Automated Design Synthesis (ADS) procedure and optimality criteria methods to carry out the optimization. Constraints on strength, deflections, flexible stability derivatives, and aileron effectiveness can be included in the optimization.

The multidisciplinary analysis is performed by first calculating the aerodynamic loads which are based on the input planform, airfoil parameters, and flight condition. Then, the aerodynamic loads are translated to the structural grid points by surface spline techniques. With the applied loads, the structural analysis is performed and the resultant deflections and stresses for each member are calculated. The deflections are then used to update the aerodynamic model and new aerodynamic loads are calculated, and the process is repeated until the aerodynamic loads and the structural deflections converge. Additionally, the deflections and stresses for each member are calculated for all of the maneuvers that are specified. At this point, the optimization routine computes a gradient of the structural weight such that constraints are not violated, and an optimization step is performed. Design variables are the thickness or area of the structural elements. At the conclusion

of this step, an updated structural arrangement is determined, and the aerodynamic and structural analyses are repeated. The global optimization routine continues to update the structural model until an optimum solution is found that minimizes structural weight while not violating the prescribed design constraints. The resultant output from ASTROS is the structural weight of the torque box, area and thickness distributions for the modeled structural members, structural node deflections of the wing, flexible and rigid stability derivatives, trim conditions, and aileron control effectiveness.

The other major computer tool used in this assessment study is Aerodynamic and Structural Wing (ASWING) program. Like ASTROS, ASWING is a multidisciplinary analysis tool which is used for the sensitivity analysis for the assessment study. ASWING couples a lifting line aerodynamic model to that of a non-linear beam model [Ref. 4.3]. This code was chosen for this project because of the ease of use and simplicity when compared with ASTROS. The program is an excellent tool for performing sensitivity studies because structural parameters can be varied easily. In order to perform the sensitivity analysis, ASTROS derived area and thickness sizing are input into the program. The program is used to generate sensitivity results for the effect of torsional stiffness on reversal speed, aerodynamic span efficiency, and maximum principal strains. Additionally, the program is used to cross-check the ASTROS results.

## **4.2 NSA Wing Design**

This section outlines the generation of the ASTROS model which includes a structural and an aerodynamic model. Furthermore, the optimization problem is formalized, and results of the optimization are presented. The aerodynamic and structural model along with the material and performance constraints are based on the information that is presented in Chapter 3.

### **4.2.1 ASTROS Structural Modeling**

The static structural analysis is based on a finite element representation of the wing. The static analyses compute response to statically applied aerodynamic, mechanical, and gravity loads. Static deformation and their resultant stresses are among the computed responses. A detail description of the structural static analysis is provided in Reference 4.1 and 4.2.

Considering the structural arrangement presented in Section 3.2, a finite element model was constructed for the ASTROS program. The ASTROS input file was partially generated by using ACAD as a preprocessor. The actual finite element model is a simplified version of the baseline structural arrangement, and it is illustrated in Figure 4.2. It is seen from this figure that the stringers and most of the ribs are not modeled. This was done in order to reduce the complexity of the model. Only 13 of the 57 ribs in the original structural layout are included in the model. Flap attachment points, engine pylon attachment points, and aircraft center of gravity attachment points were included. Additionally, leading and trailing edge trusses are added to this model though not illustrated. The trusses are necessary for the aerodynamic modeling which is outlined in the next section. From the wing structural viewpoint, the truss layout is modeled as structural elements that add stiffness in the chordwise direction and add negligible stiffness in the spanwise direction. Validation tests were performed to ensure that the trusses did not have a significant effect on the design structural stiffness.

An assumption in the modeling of the wing is that the skin and stringers were modeled as a uniform skin-stringer panel; thus, the stringers are simulated in the model without the complexity usually associated with their inclusion. However, this style of modeling will result in a stringer which contributes to the modulus of rigidity. The torsional rigidity,  $GJ$ , is defined as the modulus of rigidity,  $G$ , times the torsional moment of inertia,  $J$ . Knowing that the torsional moment of inertia,  $J$  is too large due the stringer contribution, the modulus of rigidity,  $G$ , must be reduced in order to cancel the stringer contribution. Considering design practices presented in Reference 3.7, a stringer area to skin area ratio should be approximately 1.7. For the purpose of this design, 63% of the



**Figure 4.2 ASTROS Design Model Schematic**

design uniform panel area is modeled as stringers, and 37% of the design uniform panel area is modeled as skin. Thus, to compensate for excessive torsional rigidity, the modulus of rigidity was scaled down to 37% of the original value, accounting for the stringer's contribution to the torsional stiffness. Note, this reduction only applies to the skin.

Dead weight is added to the model to provide inertial relief. The initial wing weight is estimated to be 41,212 pounds, Reference 3.2, and it is assumed that 5% of the estimate wing weight is in the leading edge and that 35% of the wing weight is in the trailing edge. The total half span leading edge weight added to the model is 1030 pounds, and this weight is distributed along the leading edge grid points proportionally according to the average spanwise leading edge volume. The total half span trailing edge weight added is 7212 pounds, and this was distributed based on the spanwise volume of the trailing edge. Fuel is also included in the finite element model. The fuel weight was estimated to be 114,931 pounds, Reference 3.2, and all of the fuel is to be contained in the wing with a 15% surge tank at the tip. Based on a 5% mass fraction reduction in gross take-off weight due to taxi, takeoff, and cruise, the initial cruise fuel weight is 95,600 lb. Thus, a total fuel weight of 47,800 pounds is distributed from the wing's root to 85% of the half span according to the spanwise volume of the torque box. Note, that all fuel is contained in the torque box.

The engine weight and thrust effects are also included in the ASTROS model. The engine weight is 15,000 lb. and the cruise thrust is 11,333 pounds, Reference 4.4. The center of gravity of the engine is located at 35 % of the half span, and 14 feet in front of the leading edge at 35% half span. The engine pylon is assumed to be rigidly attached to the center of gravity of the engine and to the front and rear spars at the 35% half span.

The rest of the aircraft, excluding the wing, is integrated into the ASTROS model through a fictitious fuselage point. The wing connection with the fuselage was performed by rigidly connecting the four spar caps at the root to the center of gravity of the aircraft. The aircraft center of gravity is illustrated in Figure 4.2. The center of gravity was assumed to be located 5% of the mean geometric chord behind the airplane's aerodynamic center. Finally, a half-span dead weight of 106,594 LB was added at the center of gravity of the aircraft so as to bring the nonstructural weight



of the model up to design point weight of 380,000 pounds excluding 60% of the estimated wing weight.

To provide some statistics on the structural model, there are 88 nodes in the structure for which a variety of structural elements are attached to:

Rod Elements:	220
Shear Panel Elements:	39
Quadrilateral Membrane Elements:	28
Rigid Bar Elements:	6
Concentrated Mass Elements	<u>82</u>
Total Elements:	375

Additionally, there are 528 degrees of freedom of which 263 degrees of freedom are constrained, 24 are dependent multipoint constrained, and 1 degree of freedom is support at the aircraft center of gravity. Thus, the resulting structural model contains 240 design degrees of freedom.

#### **4.2.2 Aerodynamic Modeling**

The aerodynamic analysis in ASTROS includes both steady and unsteady formulation though only the steady aerodynamics were used for this assessment. The steady aerodynamics analysis provides the loads on the free flying aircraft for the specified longitudinal flight conditions and provides estimates of the rolling effectiveness of control surfaces in antisymmetric maneuvers. All the design conditions that can be applied to the static analysis can also be imposed on the symmetric flight condition. In addition, limits on the aircraft's lift effectiveness and the rolling effectiveness can be imposed.

Considering the planform arrangement presented in Chapter 3, an aerodynamic model was constructed for the ASTROS program. The aerodynamic panel model was generated by specifying

sectional airfoil characteristics in the input file. The airfoil camber and thickness at 15 chord stations were input for the root and the tip. From this information, the ASTROS program linearly interpolated between the root and the tip to define the wing. The aerodynamic surface is then discretized into a panel model. The panel model consists of 8 panels in the chord direction and 21 panels in the span direction; thus, there are 168 panels on the wing. Both an inboard and an outboard aileron are accounted for in the aerodynamic model. Each of the control surfaces has 16 panels with a cosine distribution in both the chordwise and spanwise directions. Additionally, the panel distribution around the control surfaces is a cosine distribution.

The steady aerodynamic quantities are computed at the panels, which do not coincide with the structural grid points. Thus, a surface spline is performed. The transfer of aerodynamic loads to the structure is historically a troublesome area. As a result, ASTROS has three surface spline techniques with the primary interconnection algorithms being the surface spline and beam spline. [Ref. 4.1-4.2] A spline sanity check is provided by ASTROS by inspecting the panel and the spline aerodynamic stability derivatives in the output file. For a proper spline, there should not be any significant discrepancy between the two. The leading and trailing edge trusses mentioned in the previous section are a result of this sanity check. The trusses add structural grid points at the aerodynamic leading and trailing edges; thus, matching the aerodynamic panel model platform.

To finalize the aerodynamic model, the trim parameters are specified in the bulk data input file. Recall that the trim parameters are the boundaries of the V-N diagram plus the additional point to evaluate the roll performance. The longitudinal trim parameters are Mach, dynamic pressure, free stream velocity, type of trim required, the value to trim, and the free symmetric control parameter to perform the trim. For example, consider the longitudinal pull-up at  $C_{l_{max}}$  —design point A, Figure 3.5 and Table 3.3 — :

Mach Number:	$M=0.69$
Dynamic Pressure:	$Q_{bar}=1.34$ psi (193 psf)
Free Stream Velocity:	$V_{\infty}=8214$ in/sec (239 KEAS)
Type of Trim:	Lift Acceleration

Value to Trim: NZ=2.5  
Free Trim Parameter:  $\alpha$ , angle of attack

Thus, to perform the longitudinal trim for the given conditions, the angle of attack of the free flying aircraft is changed until the wing produces a vertical acceleration of 2.5 g's. For the lateral directional maneuver, the trim parameters are again Mach, dynamic pressure, free stream velocity, type of trim required, the value to trim, and the free symmetric control parameter to perform the trim. However, the type of trim is roll acceleration, the type of trim required is roll rate, and the free control parameter is the deflection of either the inboard or outboard aileron.

### 4.2.3 Multidisciplinary Optimization

The general optimization problem stated simply is to find a set of design variables that will minimize an objective function given a set of constraints. Clearly, the objective is the minimization of the wing structural weight. The design variables are the area or thickness of the structural elements, and the constraints are material properties and performance specifications related to the five design point maneuvers.

The optimization task is separated into four phases [Ref. 4.1-4.2]. The first phase is the analysis of the specified design points. In other words, the structure is analyzed for strength for the various maneuvers. In the second phase, the sensitivities of the constraints to the design variables are calculated. The third phase is the optimization step where the information on the objective function and the active constraints are assimilated to find iteration step size and direction. Finally, the fourth phase is a convergence test for termination, and if the solution has not converged, the optimization task is repeated.

For the NSA evaluation model, the design variables are the thickness or area of an individual element of the wing's torque box. The statistics of the design variables are as follows:

Skin Thickness Design Variables:	28
Spar Cap Area Design Variables:	52
Shear Web Thickness Design Variables:	26
Rib Web Thickness Design Variables:	13
Rib Caps Area Design Variables:	30
<u>Rib Post Area Design Variables:</u>	<u>3</u>
TOTAL Design Variables	152

Constraints are added to the optimization in terms of material properties, minimum material thickness or area, and flexible aileron control power derivative. The material property constraints are expressed in terms of maximum principal strain allowable before the onset of yield. A common characteristic of aluminum is that the yield failure criteria are more critical than the ultimate design load failure criteria; thus, limit loads material data is used for the design. Note, limit load is defined as the maximum anticipated loads, and these limit loads correspond to yield, Reference 4.5. The maximum principal strains for tension, compression, and shear are determined by dividing the yield stress for tension, compression, and shear outlined in Table 3.1 by their appropriate moduli.

The minimum area and thickness constraints for the structural elements are assumed. The minimum spar cap area is assumed to be 0.5 in<sup>2</sup>, and the minimum skin thickness is assumed to be 0.050 inches for the bottom skin and 0.032 inches for the top skin. Finally, the minimum shear web and rib thickness are assumed to be 0.050 inches.

Given the material constraints, the roll performance constraint is required to perform the assessment study. Recall that the roll performance requirements were outlined in Section 3.6 in terms of the time to roll through a specified bank angle in a specified time and the minimum allowable roll mode time constant. Incorporation of these constraints within the framework of the ASTROS input data deck is straightforward. It is assumed that the minimum allowable roll mode time constant is inversely proportional to the nondimensional roll damping derivative, and ASTROS has stability the necessary derivative constraints. The time domain specification is more involved. Within the framework of ASTROS, the designer can specify a steady state roll rate or an aileron deflection

within the aerodynamic trim parameter. Additionally, as already mentioned, stability derivative constraints along with aileron control effectiveness constraints, which is a ratio of the nondimensional aileron control power derivative to the nondimensional roll damping derivative, can be specified. Thus, there are four data deck parameters that can be used to enforce the roll performance constraint.

The approach used for this assessment study is to determine the steady state roll rate that the aircraft must produce in order to meet the Level I Roll Performance. The idea here is that regardless of the flexibility of the wing, in order to roll through 30° in 2.0 seconds, the aircraft must be capable of producing the same minimum steady state roll rate. The key assumption here is that the dimensional roll damping derivative does not change much. This assumption was verified, and the maximum change in the flexible roll damping derivative is less than 5.0 %. Additionally, the conservative value of the roll damping derivative was used for the derivation of the steady state roll rate required for Level I roll performance.

To determine the required steady state roll rate, the lateral-directional small perturbation rolling approximation is used

$$\phi(t) = -\frac{L_{\delta A} \delta_A}{L_P} t + \frac{L_{\delta A} \delta_A}{L_P^2} (e^{-L_P t} - 1)$$

$$\dot{\phi}(t) = -\frac{L_{\delta A} \delta_A}{L_P} (1 - e^{-L_P t})$$

and:  $\phi(t)$  is the aircraft bank angle,

$L_{\delta A}$  is the dimensional aileron control power derivative,

$L_P$  is the dimensional roll damping derivative, and

$\delta_A$  is the aileron deflection.

Some additional definitions are useful:

$$L_{\delta A} = \frac{\bar{q} S b}{I_{xx}} Cl_{\delta A} \quad L_P = \frac{\bar{q} S b^2}{2 I_{xx} V_{\infty}} Cl_P$$

where:  $\bar{q}$  is the dynamic pressure,  
 $S$  is the reference wing area,  
 $b$  is the reference wing span,  
 $I_{xx}$  is the rolling moment of inertia,  
 $V_{\infty}$  is the free stream velocity,  
 $Cl_{\delta A}$  is the nondimensional aileron control power derivative, and  
 $Cl_P$  is the nondimensional roll damping derivative.

It is important to note that the dimensional derivatives are dependent of the flight point — Mach and altitude — and rolling moment of inertia of the aircraft. The flight point for the evaluation is 32,000 feet at a speed of 0.82 Mach, and the rolling moment of inertia for this class of aircraft at 380,000 pounds is estimated to be  $8.60 \times 10^6$  slug ft<sup>2</sup>. The rolling moment of inertia was estimated using the non-dimensional radius of gyration method presented in Reference 4.6.

The rigid wing roll damping derivative was estimated to be:

$$Cl_P = -0.5508$$

This was obtained from the rigid trim output from ASTROS and it was verified by another aerodynamic paneling algorithm. Using this value, the dimensional roll damping derivative is determined to be:

$$L_P = -1.1888 \text{ sec}^{-1}$$

Note, the roll mode time constant requirement is easily satisfied. With this dimensional derivative, the bank angle rolling approximation can be solved to produce the following result:

$$Cl_{\delta A} \delta A = 0.5032 \text{ sec}^{-2}$$

Finally, the steady state roll rate to achieve Level I roll performance is obtained from the rolling rate approximation equation above:

$$\dot{\phi}(t) = 24.25^\circ/\text{sec}$$

To recap the progress towards implementing the roll performance constraint, the steady state roll rate has been identified above, and its utility is that regardless the wing's flexibility, the aircraft must be capable of obtaining the minimum value of the steady state roll rate in order to satisfy the time domain constraint. Additionally, it was shown that the roll mode time constant requirement is satisfied for this wing configuration.

With the steady state roll rate identified for the lateral maneuver parameter, a nondimensional aileron control power constraint is added to the optimization, and the resultant solution determines the required aileron deflection to produce the steady state roll rate to satisfy the Level I roll performance. The value of the constraint is determined by obtaining the unconstrained aileron control power derivative and then increasing its value from there. The effect of increasing the aileron control power constraint above that of the inherent value is that the optimized wing structural weight will increase while the aileron deflection required to produce the roll will decrease.

With the design variables and constraints identified, the optimization problem is mathematically formulated as follows:

Objective Function:

$$f(\mathbf{x}) = f(\chi_1, \chi_2, \dots, \chi_{152}) \equiv \text{weight of wing's torque box}$$

Constraints:

$$g_i(\mathbf{x}) \equiv g_i(\chi_1, \chi_2, \dots, \chi_{152}) \leq 0; \quad i=1 \text{ to } 1575, \text{ or:}$$

top skin maximum principal strains constraint:

$$\epsilon_1 - 0.0067 < 0 \quad \epsilon_2 + 0.0067 < 0 \quad \gamma_{12} - 0.0327 < 0$$

bottom skin maximum principal strains constraint:

$$\epsilon_1 - 0.0045 < 0 \quad \epsilon_2 + 0.0037 < 0 \quad \gamma_{12} - 0.0264 < 0$$

spar caps maximum principal strains constraint:

$$\epsilon_1 - 0.0042 < 0 \quad \epsilon_2 + 0.0037 < 0 \quad \gamma_{12} - 0.0080 < 0$$

shear webs and ribs maximum principal strains constraint:

$$\epsilon_1 - 0.0045 < 0 \quad \epsilon_2 + 0.0036 < 0 \quad \gamma_{12} - 0.0098 < 0$$

top skin minimum thickness constraint:

$$-t_{ts} + 0.050 \leq 0 \text{ in}$$

bottom skin minimum thickness constraint:

$$-t_{ts} + 0.032 \leq 0 \text{ in}$$

spar cap minimum area constraint:

$$-A_{sc} + 0.5 \leq 0 \text{ in}^2$$

shear webs and ribs minimum thickness constraint:

$$-t_{w,r} + 0.032 \leq 0 \text{ in}$$

minimum aileron control power derivative constraint:

$$-Cl_{\delta a} + 0.1744 * N \leq 0 \text{ where } N \text{ is a scaling factor above } 1.0$$

As a final note, both buckling and flutter constraints are absent from the model. The buckling constraints were not added because the ASTROS version for which the assessment was performed did not have a mature buckling constraint.

#### 4.2.4 NSA Design Results

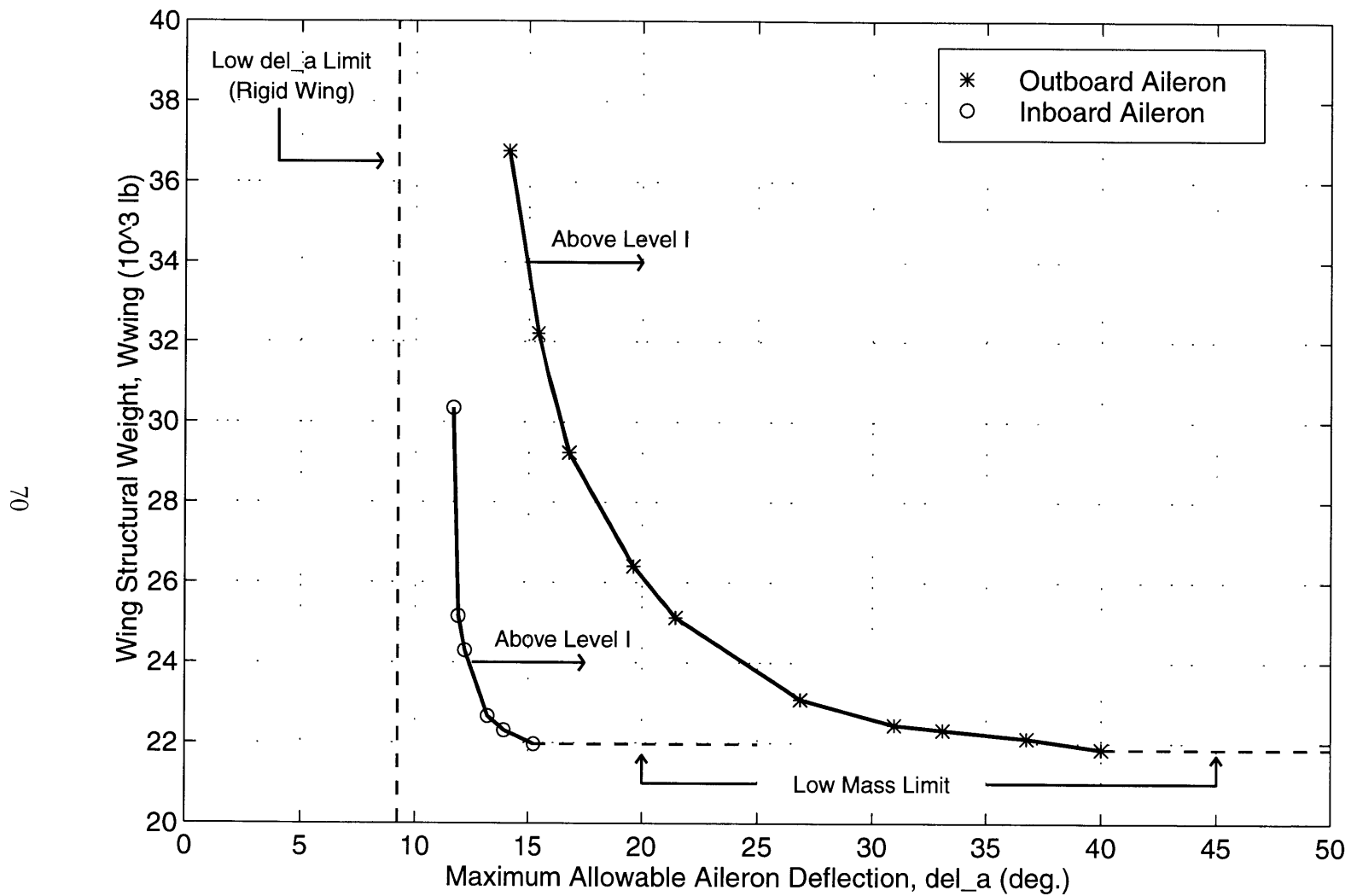
Based on the prescribed optimization problem and the generated wing structural and aerodynamic model, an optimization of the wing's torque box weight was conducted. Figures 4.4 through 4.12 present the results. Figure 4.4 illustrates the maximum allowable aileron deflection versus the



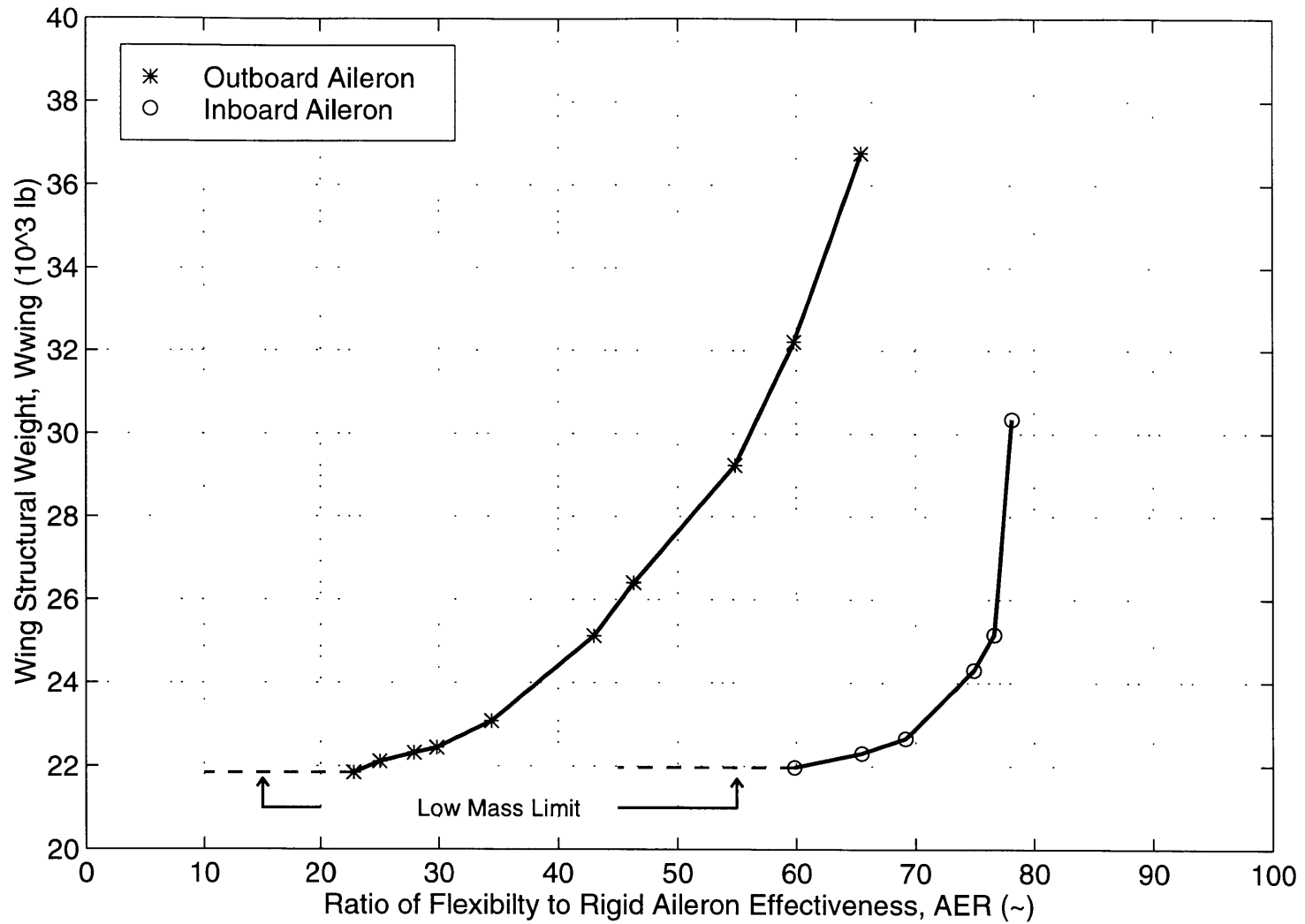
required wing structural weight for Level I roll performance. Recall the discussion in Section 1.2. The first important observation from this figure is that the ailerons are non-reversed. Additionally, the low wing mass limits for the ailerons are 21,847 pounds for the outboard aileron and 21,970 pounds for the inboard aileron. Again, these values represent the wing structural weight for no torsional constraints. The aileron deflections required for Level I roll at the minimum structural weight are  $40.0^\circ$  for the outboard aileron and  $15.2^\circ$  for the inboard aileron. In both cases, as the torsional constraint is increased, the structural weight increases. As the maximum allowable aileron deflection approaches the rigid wing value of  $9.2^\circ$ , the wing structural weight approaches infinity. Figure 4.4 also illustrates significant differences between the inboard and outboard ailerons. For an allowable aileron deflection of  $15.0^\circ$ , the required structural weight for the outboard aileron is approximately 33,700 pounds where the required structural weight for the inboard aileron is approximately 22,000 pounds which is a 35% reduction in weight.

The next illustration is Figure 4.5 which presents the Aileron Effectiveness Ratio (AER) versus required wing structural weight for Level I roll performance. As in the previous figure, the low mass limit is illustrated. Additionally, at the low mass limit, the AERs for the ailerons are 22.8% for the outboard aileron and 59.8% for the inboard aileron. As the AER approaches 100%, the required structural weight approaches infinity. This figure is also useful for comparing the performance of the inboard and outboard ailerons. For an AER of 60%, the required wing structural weight for Level I roll performance is approximately 32,000 pounds for the outboard aileron and 22,000 pounds for the inboard aileron which is a 31% reduction in weight.

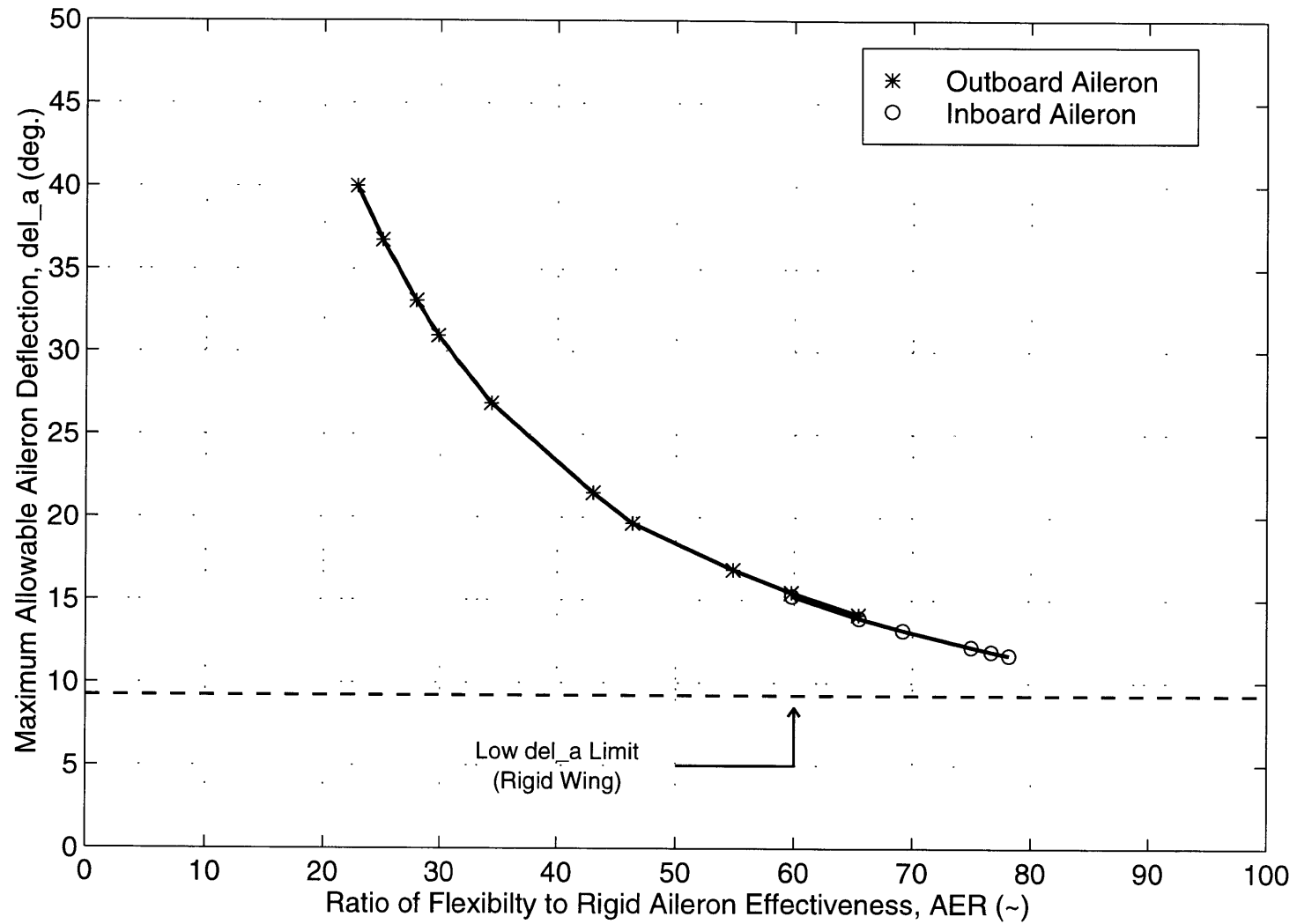
Figure 4.6 illustrates AER required for Level I roll performance versus maximum allowable aileron deflection. This figure illustrates that as the torsional stiffness constraint is increased, the maximum aileron deflection required for the roll performance decreases towards the rigid wing solution.



**Figure 4.4 Maximum Allowable Aileron Deflection Versus Required Wing Structural Weight for Level I Roll Performance**



**Figure 4.5 Aileron Effectiveness Ratio Required Versus Required Wing Structural Weight for Level I Roll Performance**



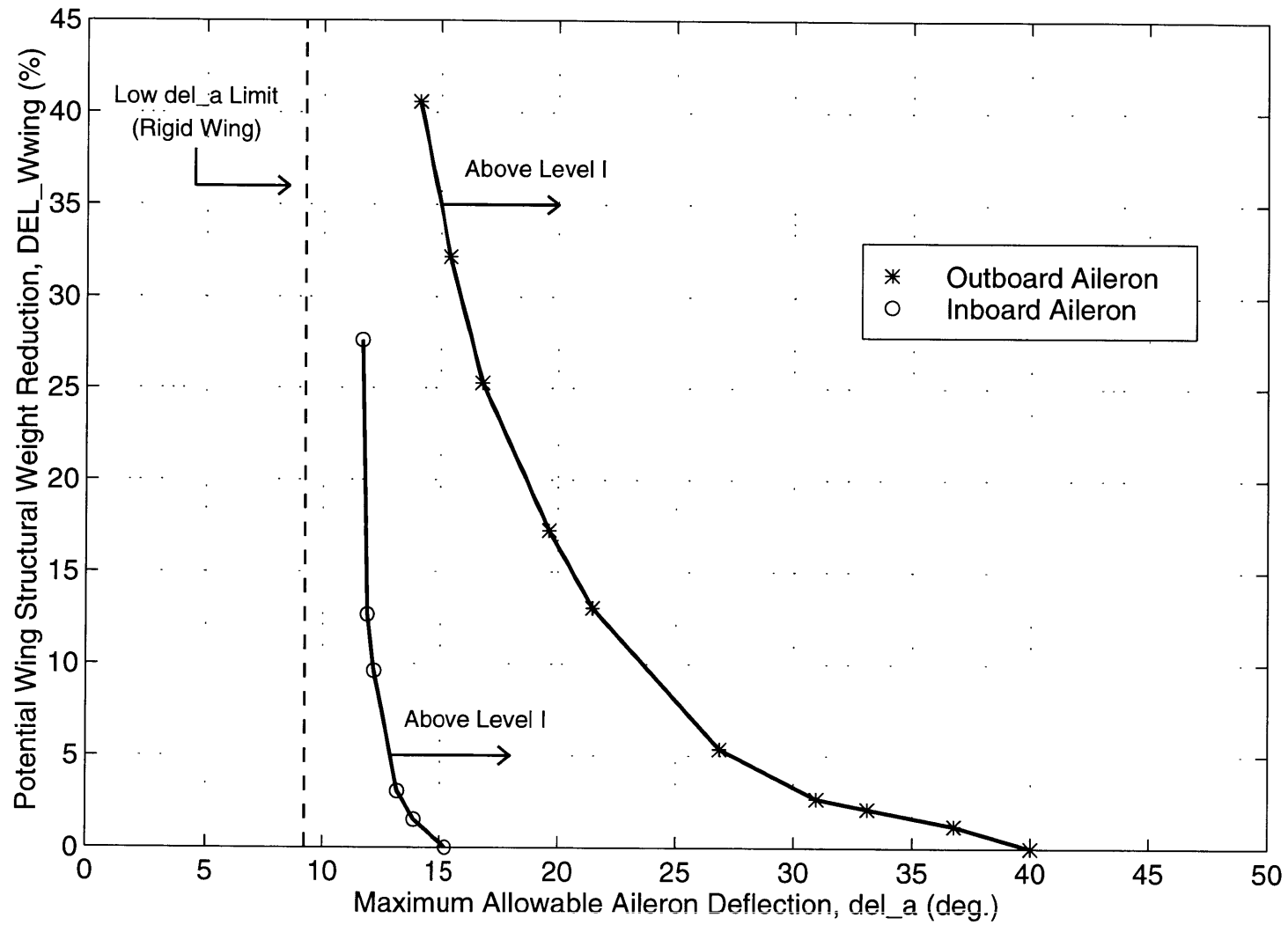
**Figure 4.6 Aileron Effectiveness Ratio Required for Level I Roll Performance Versus Maximum Allowable Aileron Deflection**

This figure also illustrates that the two ailerons at the same AER result in approximately the same required maximum aileron deflection as expected.

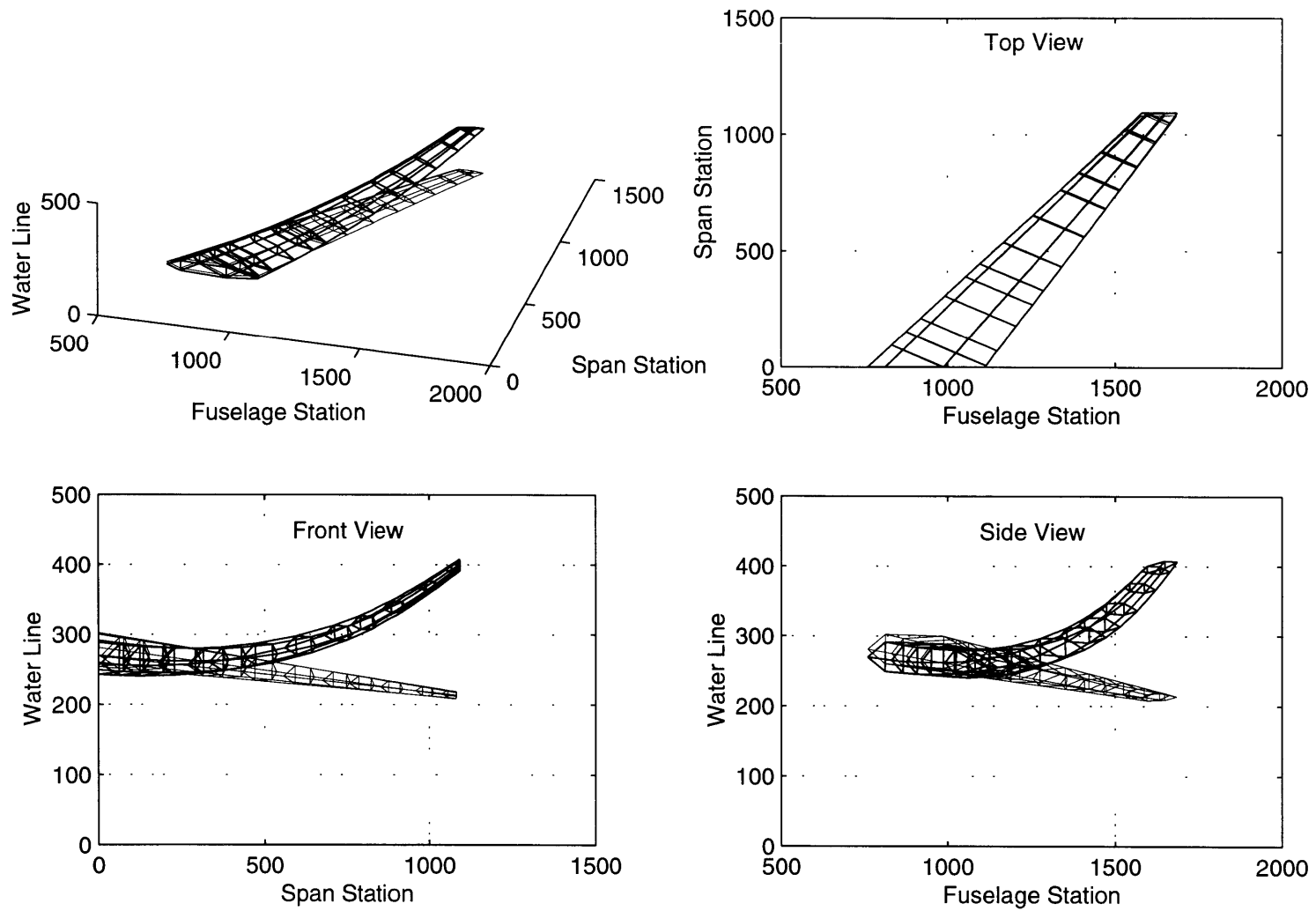
The next presentation, Figure 4.7, illustrates the maximum allowable aileron deflection versus potential wing structural weight reduction. This figure is a reproduction of Figure 4.4 where the potential weight savings is determined by taking the difference between the roll performance curve and the low mass limit curve. The normalization is done with the roll performance curve. Recall, the concept of AFW is a transport or fighter wing that will not fail for the expected design load, but its passive stiffness performance will be inadequate for the desired mission. The roll performance curve represents the design which will not fail for the expected load and will have inherent Level I roll performance. On the contrary, the low mass limit represents a design that will not fail for the expected load but will not have inherent roll performance. Thus, the difference between these designs is the potential weights saving attributed to the AFW concept. As illustrated in the figure, if the maximum allowable aileron deflection is less than  $40.0^\circ$  then the outboard aileron configuration has potential weight savings. Additionally, if the maximum allowable aileron deflection is less than  $15.2^\circ$  then the inboard aileron configuration has potential weight savings.

Acceptable values for the maximum allowable aileron control surface deflection vary from aircraft to aircraft, but typically, lateral control surfaces deflections should not exceed  $25^\circ$  for ailerons [Ref. 4.7]. Based on a  $25^\circ$  maximum allowable aileron deflection, the potential weight savings for the outboard aileron configuration is approximately 8% of the wing structural weight. However, the potential weight reduction for the inboard aileron configuration is negligible.

The final set of illustrations, Figure 4.8 through 4.12 presents the NSA wing deflections for the various design points for the minimum weight wing with an outboard aileron configuration. Figure 4.8 illustrates the wing deflection for the  $M=0.60$ ,  $N_z=2.5$  flight condition. From this figure, it is observed that this flight condition represents the largest deflection. The tip deflection is approximately 15.8 feet. The next three figures illustrate the design points for  $M=1.07$  and  $N_z=2.5$ ,

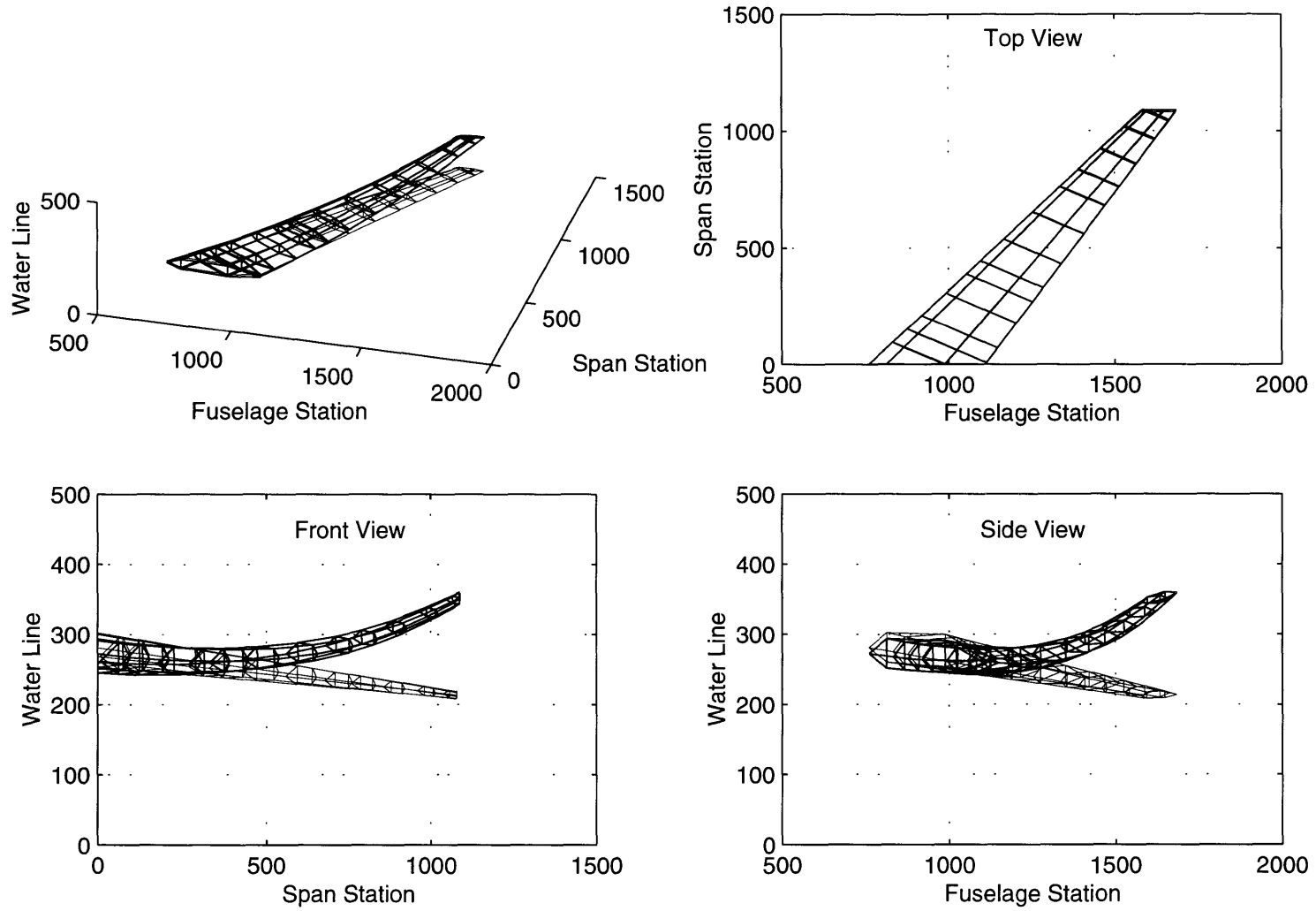


**Figure 4.7 Maximum Allowable Aileron Deflection Versus Potential Wing Structural Weight Reduction**



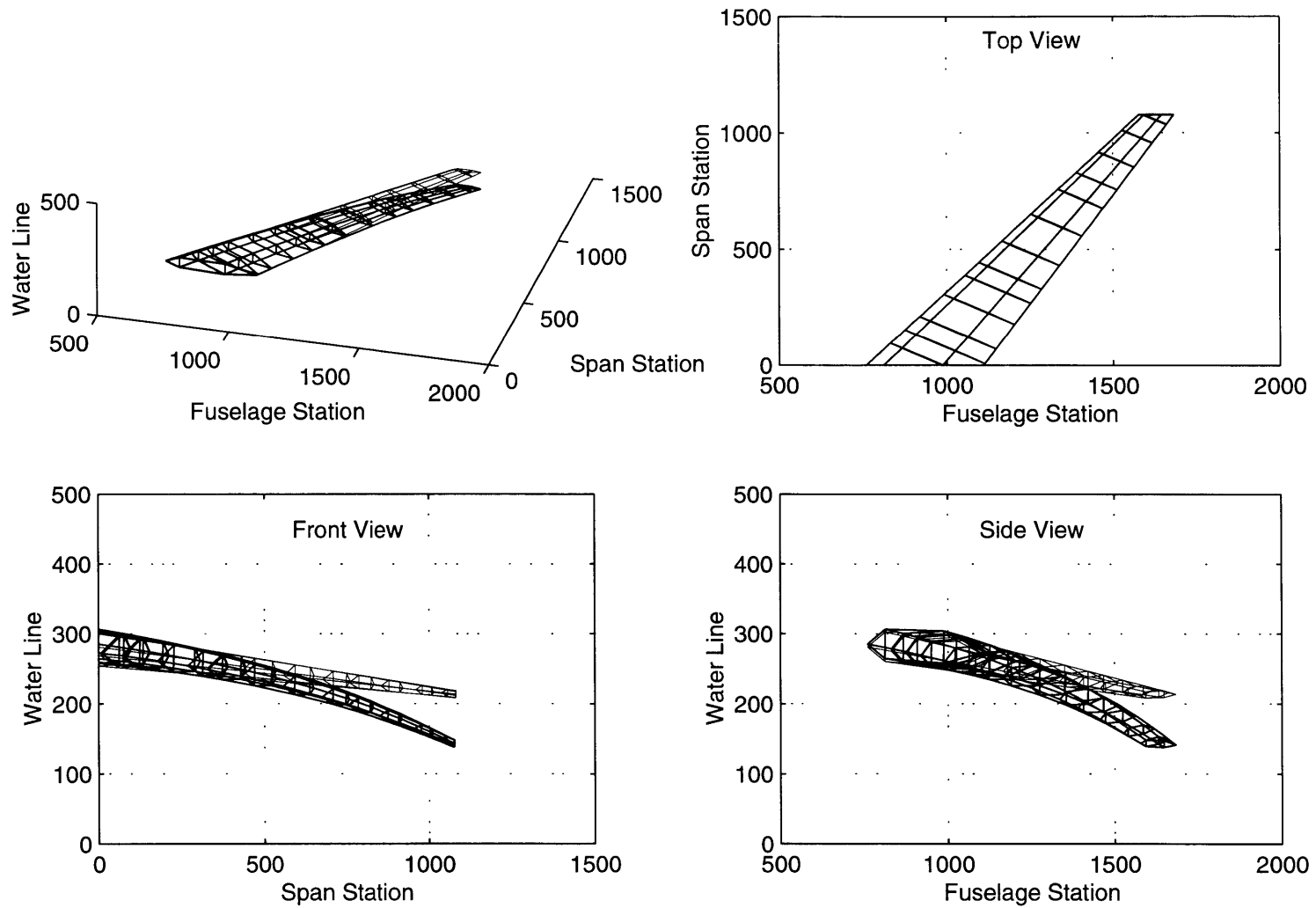
75

**Figure 4.8 NSA Minimum Weight Wing Structural Deflections for the Outboard Aileron Configuration at  $M=0.69$ ,  $N_z=2.5$  g's**

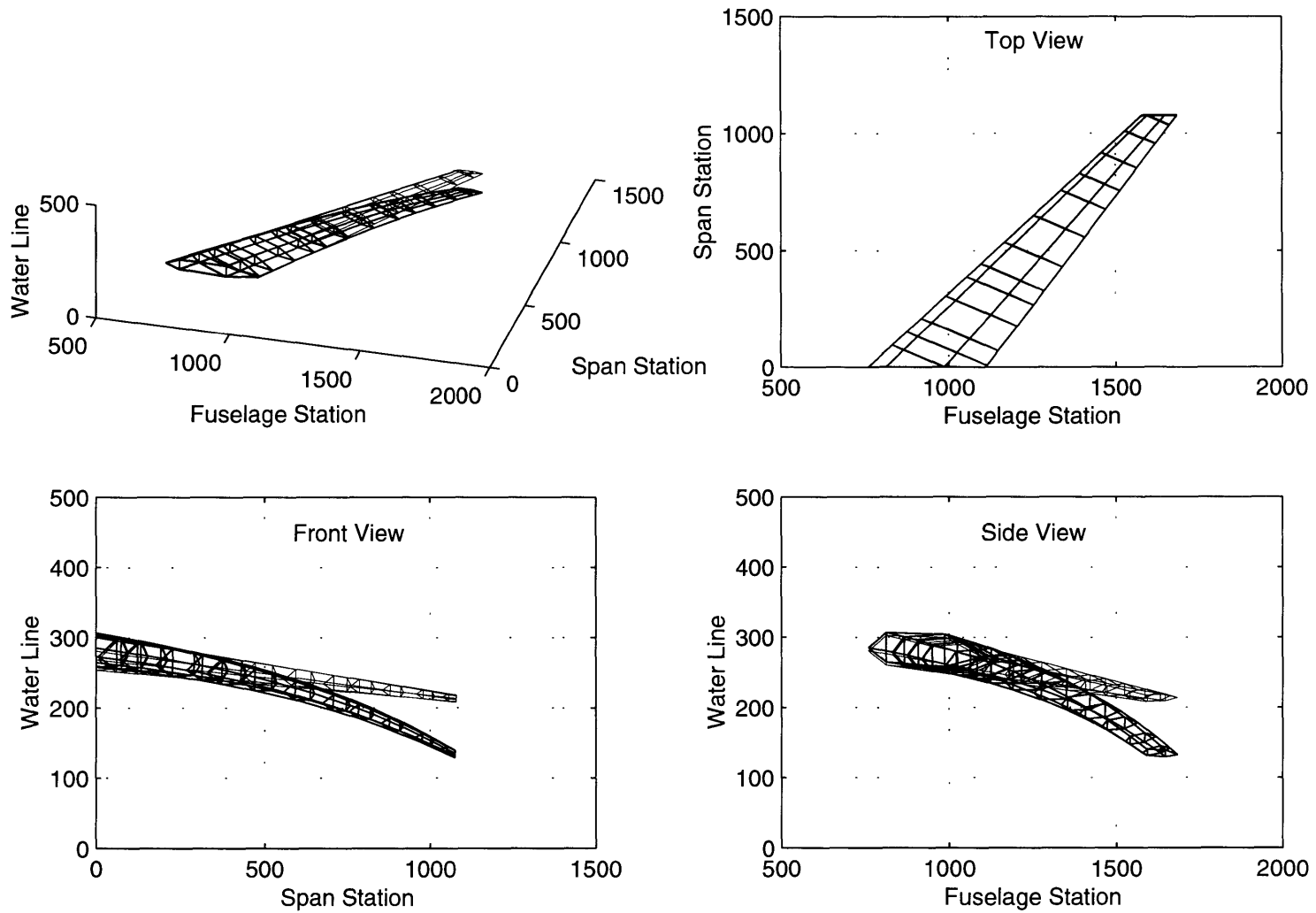


**Figure 4.9 NSA Wing Minimum Weight Structural Deflections for the Outboard Aileron Configuration at M=1.07, Nz=2.5 g's**



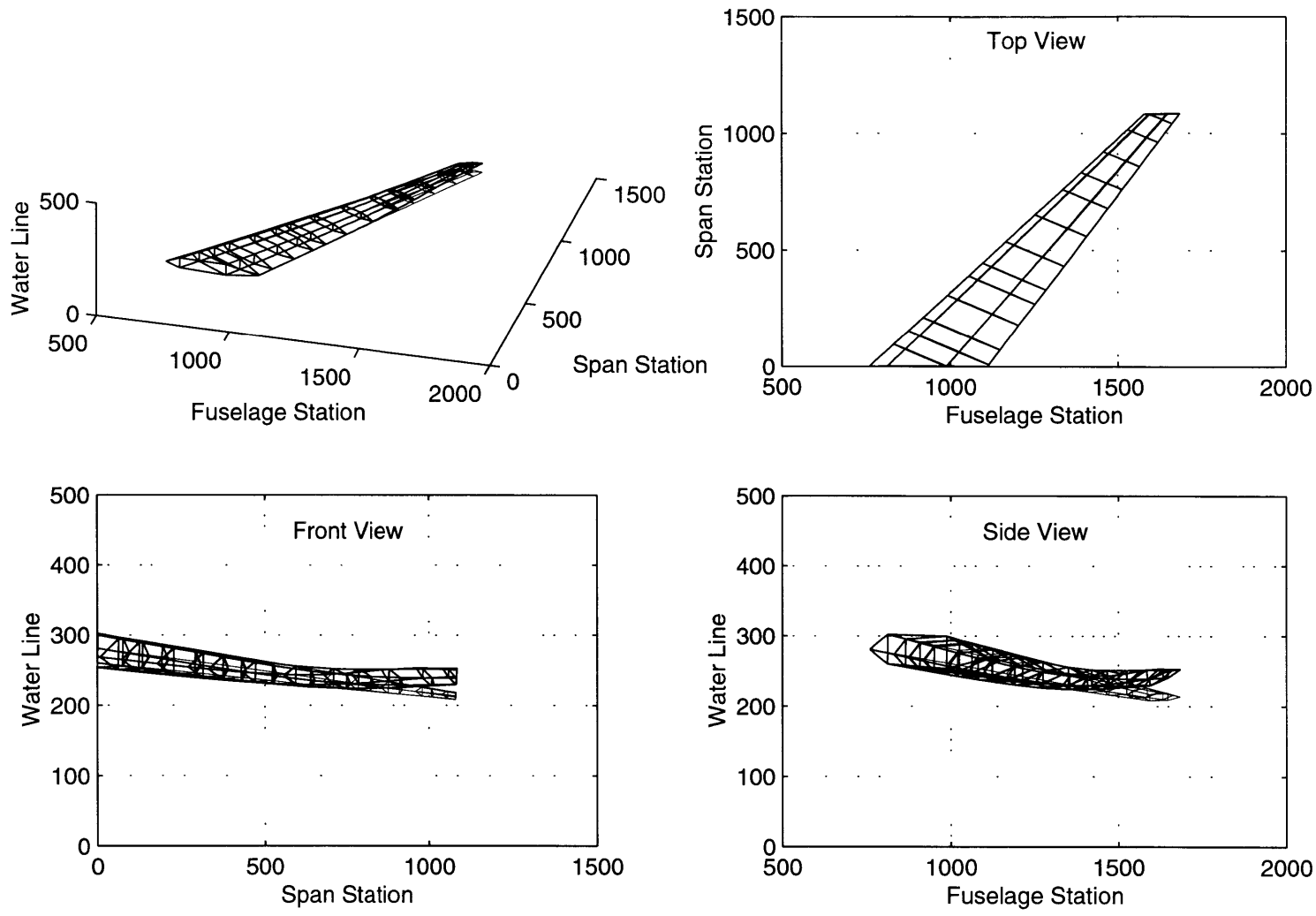


**Figure 4.10 NSA Wing Minimum Weight Structural Deflections for the Outboard Aileron Configuration at M=0.86, Nz=-1.0 g's**



87

**Figure 4.11 NSA Wing Minimum Weight Structural Deflections for the Outboard Aileron Configuration at  $M=0.50$ ,  $N_z=-1.0$  g's**



**Figure 4.12 NSA Wing Minimum Weight Structural Deflections for the Outboard Aileron Configuration at  $M=0.82$ ,  $N_z=1.0$  g's**

$M=0.86$  and  $N_z=-1.0$ , and  $M=0.50$  and  $N_z=-1.0$ . The final illustration, Figure 4.12 presents the resultant wing deflection for a  $40^\circ$  outboard aileron deflection.

The results in this section and their relationship to the assessment study objectives outlined in Section 1.2 are summarized as follows:

- 1) The minimum wing weight designs with no torsional constraints for roll performance are 21,847 pounds for the outboard aileron and 21,970 pounds for the inboard aileron;
- 2) The aileron control is not reversed;
- 3) Based on the maximum allowable aileron deflection of  $25^\circ$ , the potential weight savings are approximately 8% for the outboard aileron configuration and is negligible for the inboard aileron configuration.; and
- 4) The sensitivities of torsional stiffness on reversal speed, span efficiency, and maximum strain will be detailed in the next section.

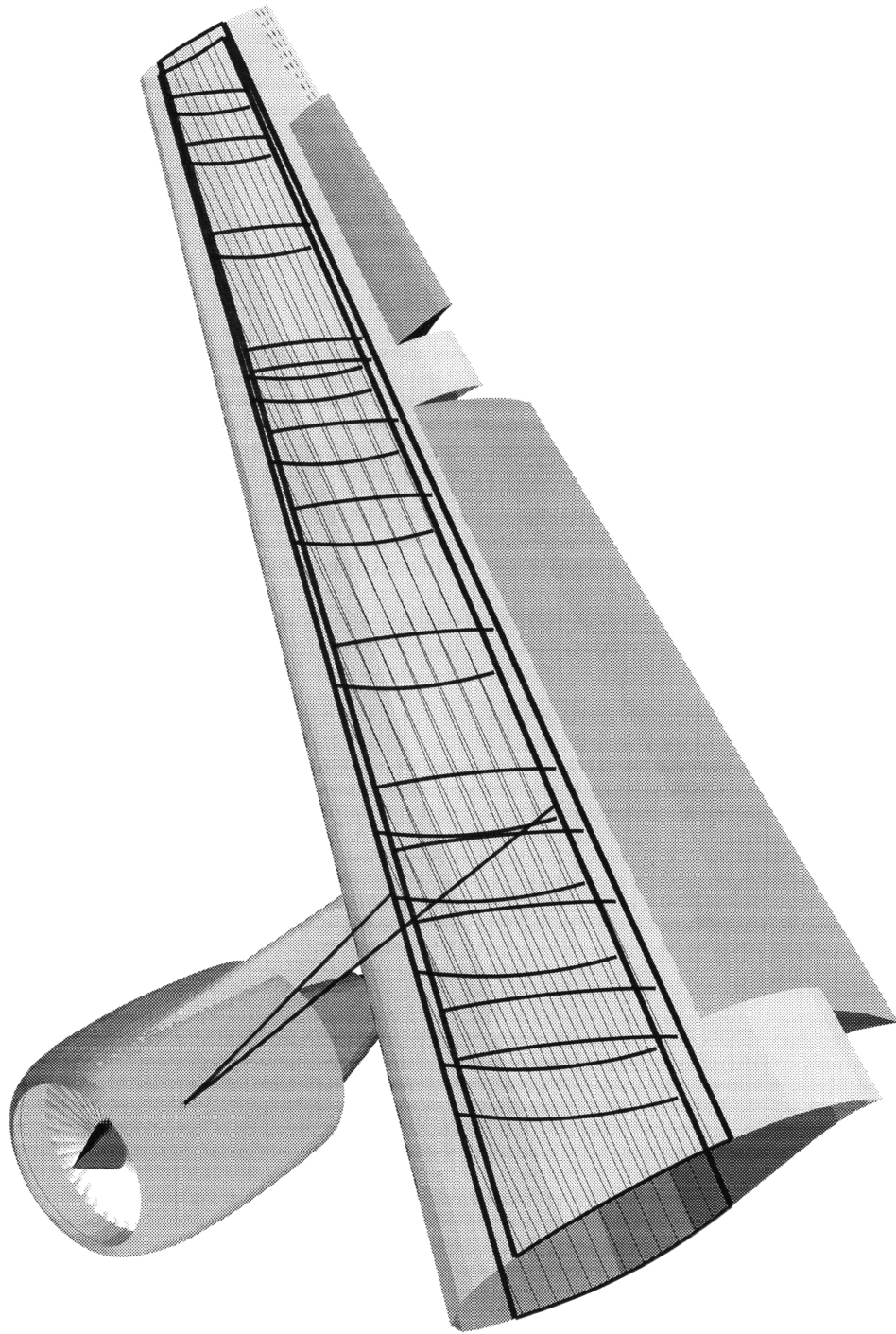
As a final note, these results represent a lower bound to the design problem because additional constraints on the design can only increase the weight of the wing and the resultant performance. In other words, even if additional flight envelope design points and loading scenarios are considered, the performance can not decrease, but rather it can either remain invariant or increase.

### 4.3 NSA Sensitivity Analysis

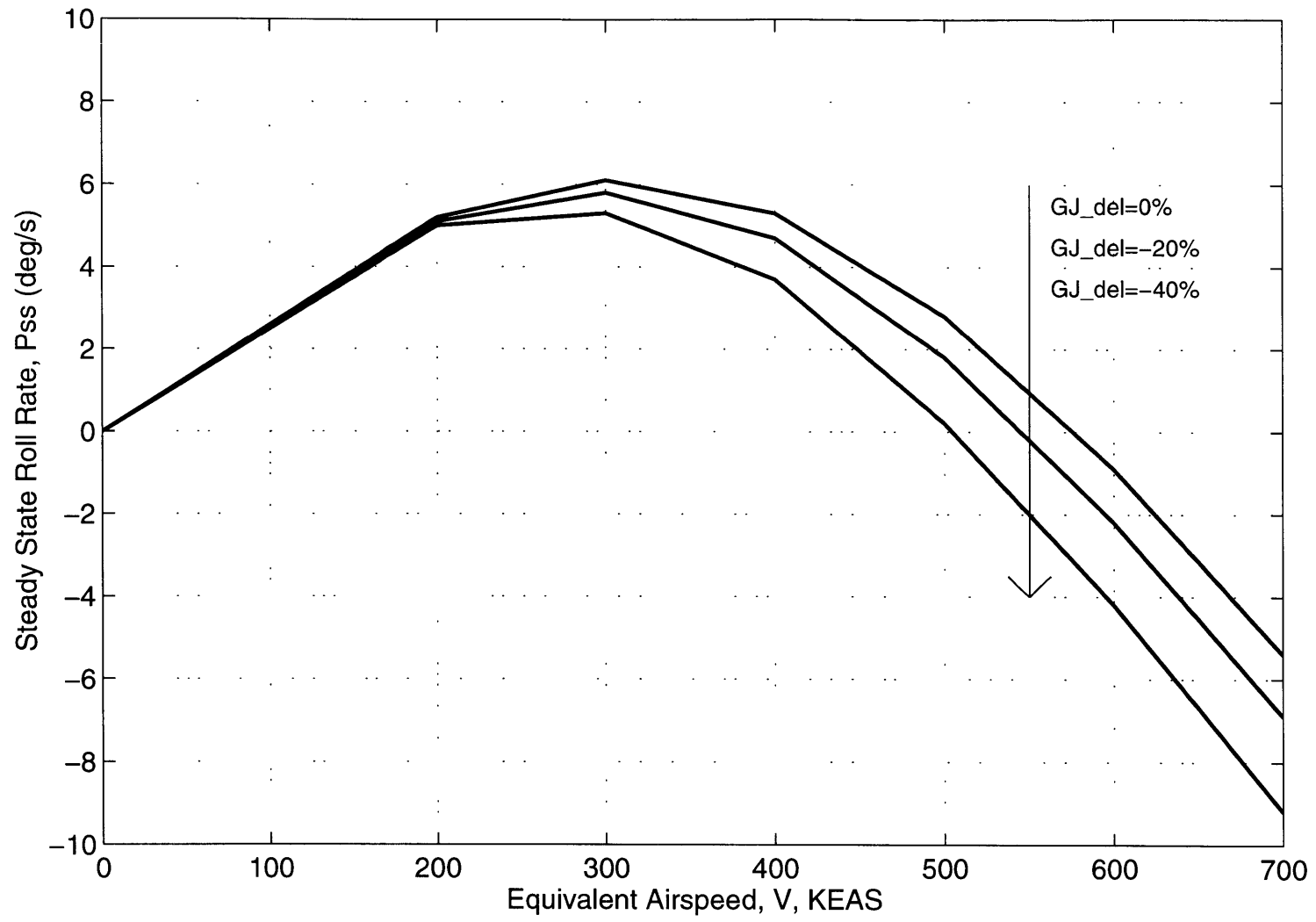
An ASWING model was generated for the purpose of sensitivity analysis. The parameters of the sensitivity are torsional stiffness,  $\Delta GJ$ , and the jig washin angle,  $t$ . The evaluation criteria is roll reversal speed and span efficiency.

The ASWING model build is a simplified version of the baseline structural arrangement, and it is illustrated in Figure 4.13. It is seen from this figure that only 15 of the 57 ribs in the original structural layout were modeled. Furthermore, the stringers were directly included in this model. As mentioned in the process design sequence, ASTROS material distributions were input into the model, and the material properties used for this sensitivity analysis pertain to the minimum mass wing with an outboard aileron configuration. All details of the ASWING model are contained in Reference 4.8.

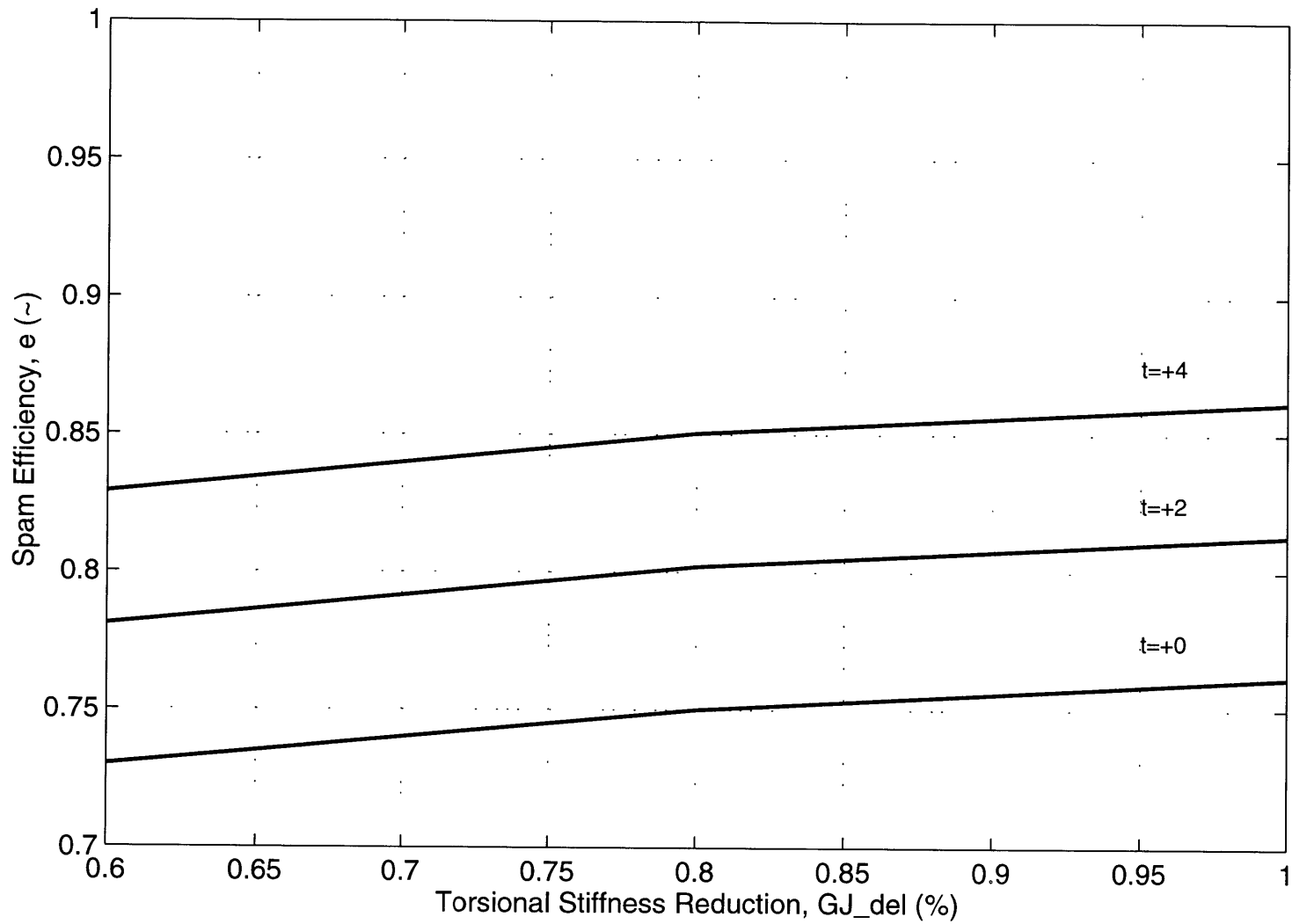
The results of the sensitivity study are illustrated in Figures 4.14 through Figure 4.16. From Figure 4.14, the steady state roll rate is plotted with respect to the equivalent airspeed. This figure illustrates that as the airspeed is increased, a flexible wing will lose its capability to generate roll. The sensitivity analysis shows that reducing the torsional stiffness results in a reduction of the reversal speed. It is also noted from Figure 4.14 that for the baseline, the reversal speed is 570 KEAS which is considerably outside the flight envelope since the high design speed is at 370 KEAS. Furthermore, even with a 40% reduction in torque box  $GJ$ , the reversal speed only approaches 500 KEAS.



**Figure 4.13 ASWING Model Schematic**

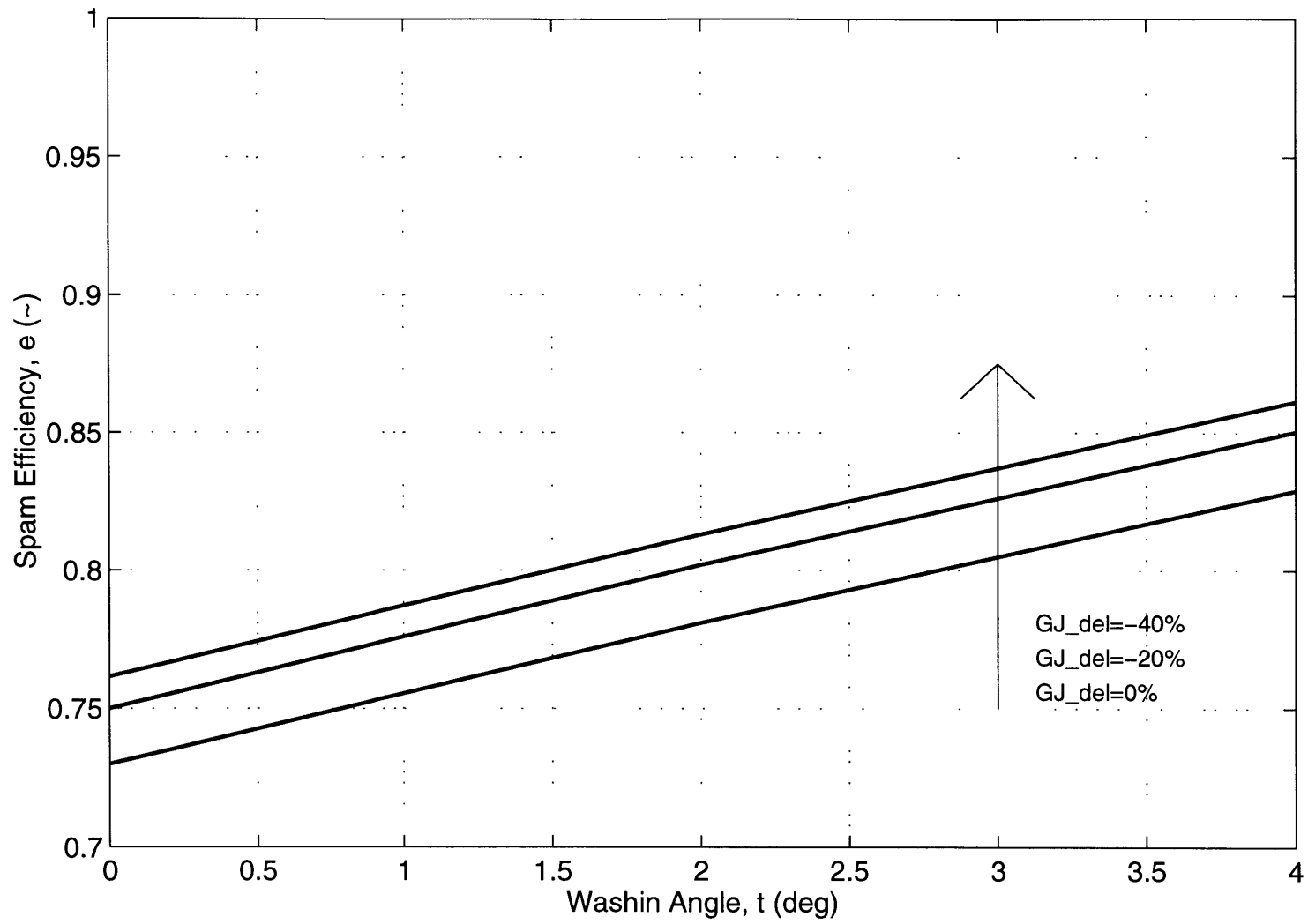


**Figure 4.14 Control Effectiveness Versus Equivalent Airspeed**



**Figure 4.15 Span Efficiency Versus Percentage Change in Torsional Stiffness for  $M=0.82$ ,  $h=32,000$  ft, and  $1.0$  g's.**





**Figure 4.16 Span Efficiency Versus Washin Angle for  $M=0.82$ ,  $H=32,000$  ft, and  $1.0$  g's.**

Figures 4.15 and 4.16 illustrates the span efficiency as a function of torsional stiffness and jig washin angle. The concept here is that as torsional stiffness is reduced, the localized angle of attack at the tips is reduced which is commonly referred to as washing out the tips. The result of this reduced GJ induced washout is that the span efficiency decreases. To compensate for this additional washout, jig washin was added to the tip so as to regain the loss of aerodynamic efficiency. Figure 4.15 illustrates this concept. As the torsional rigidity is reduced, the span efficiency decreases, and as washin angle is added, the span efficiency increases. Thus, assuming that the torsional rigidity was decreased by 40%, then ideally, less than 2° of washin angle would be required to regain the loss in aerodynamic efficiency.

Finally, the effect of torsional rigidity on maximum principal strains was investigated, and it was observed that there was a minor increase in maximum strain and torsional stress associated with an increase in washin at the tip. Furthermore, it was observed that the reduction in torsional stiffness has a negligible effect on the maximum shear stress and tensile strain. Note, this observation is only valid for variations in GJ.

The results in this section and their relationship to the assessment study objectives outlined in Section 1.2 are summarized as follows:

- 1) Outlined in Section 4.2.4;
- 2) Outlined in Section 4.2.4;
- 3) Outlined in Section 4.2.4; and
- 4) The reversal speed for the minimum weight wing with an outboard configuration is 570 KEAS which is considerably outside the flight envelope since the high design speed is at 370 KEAS. Furthermore, even with a 40% reduction in torque box GJ, the reversal speed only approaches 500 KEAS. Additionally, assuming that the torsional rigidity was decreased by 40%, then ideally less than 2° of washin angle would be required to regain the loss in aerodynamic efficiency. Finally, variations of torsional rigidity resulted in a minor increase in maximum strain and

torsional stress associated with an increase in washin at the tip and resulted in a negligible effect on the maximum shear stress and tensile strain.

## 4.4 Conclusions

This chapter presented a general discussion of the design process for the AFW assessment study, the actual design of the wing, and the resulting sensitivity data. The design process consisted on building a three-dimensional wing model in the ACAD program, and then translating this geometry into two structural models: one for ASTROS and one for ASWING. The ASTROS program was used as the primary synthesis tool, and ASWING was used as the primary sensitivity analysis tool.

The simplified ASTROS structural model, which is the basis of these results, included aerodynamic analysis, structural analysis, and optimization. The multidisciplinary optimization was performed for the six loading cases identified in Chapter 3.0. Constraints were added to this model to reflect maximum material yield strains and minimum material thickness or area. Finally, roll performance requirements were added to this model via aileron effectiveness.

The results of this chapter and their relationship to the assessment study objectives are summarized as follows:

- 1) The minimum wing weight designs with no torsional constraints for roll performance are 21,847 pounds for the outboard aileron and 21,970 pounds for the inboard aileron;
- 2) The aileron control configurations are not reversed;
- 3) The potential weight savings based on the maximum allowable aileron deflections of 25° is approximately 8% for the outboard aileron configuration and is negligible for the inboard aileron configuration; and
- 4) The reversal speed for the minimum weight wing with an outboard configuration is 570 KEAS which is considerably outside the flight envelope since the high design speed is at 370 KEAS.

Furthermore, even with a 40% reduction in torque box GJ, the reversal speed only approaches 500 KEAS. Additionally, reducing torsional stiffness results in a reduction in aerodynamic spanwise efficiency. This loss in aerodynamic spanwise efficiency is attributed to tip unloading. However, the addition of washin angle at the tip would be required to recover the spanwise efficiency. Thus, assuming that the torsional rigidity was decreased by 40%, then ideally, less than 2° of washin angle would be required to regain the loss in aerodynamic efficiency. Finally, the results illustrated that the reduction in torsional stiffness and/or the addition of washin angle would increase the maximum tensile strain and shear stress.

Note, the key assumptions of AFW assessment as applied to the NSA are as follows:

- Wing Structural Arrangement
  - Two spars versus multiple cell box
  - Rib and stringer spacing
- Material Selection
- Inboard Aileron Configuration
- No Buckling Constraints

Based on the key assumptions of AFW as applied to the NSA, these results represent a lower bound to the design problem. Additional constraints and/or the evaluation of more design points will result in either an increase in the structural weight and the resulting roll performance or it will remain invariant.

# Chapter 5 Conclusions and Recommendations

## 5.1 Conclusions

An Advanced Flexible Wing (AFW) technology assessment as applied to the New Strategic Airlifter (NSA) is reported in this thesis. The seed for this project originated from an assessment study performed on a generic strike fighter where significant potential weight savings were identified. The AFW concept — also known as Active Aeroelastic Wing (AAW) — is composed of several elements that serve to make aeroelastic deformations an asset rather than a limitation on the wing's design.

The focus of this assessment study is to determine if the roll control element of the AFW concept can be used for the NSA, and what is the potential wing structural weight savings that can be achieved by using the technology. More specifically, the assessment study objectives are to:

1. Identify the minimum wing weight design with no torsional constraints for roll performance,
2. Identify the region of aileron control: non-reversed or reversed,
3. Identify the potential weight savings based on the maximum allowable aileron deflections, and
4. Identify the sensitivities of torsional stiffness on reversal speed, span efficiency, and maximum strain.

The load alleviation, drag reduction, and flutter suppression elements of AFW are not explored nor are the effects of reducing the torsional stiffness on the flutter characteristics.

The objectives of this thesis were met. The results of the analysis and their relationship to the assessment study objectives are summarized as follows:

1. The minimum structural weight designs with no torsional constraints for roll performance are 21,847 pounds for the outboard aileron and 21,970 pounds for the inboard aileron;
2. The aileron control configurations are not reversed;

3. The potential weight savings based on the maximum allowable aileron deflections of  $25^\circ$  is approximately 8% for the outboard aileron configuration and is negligible for the inboard aileron configuration; and
4. The reversal speed for the minimum weight wing with an outboard configuration is 570 KEAS which is considerably outside the flight envelope since the high design speed is at 370 KEAS. Furthermore, even with a 40% reduction in torque box GJ, the reversal speed only approaches 500 KEAS. Additionally, reducing torsional stiffness results in a reduction in aerodynamic spanwise efficiency. This loss in aerodynamic spanwise efficiency is attributed to tip unloading. However, the addition of washin angle at the tip would be required to recover the spanwise efficiency. Thus, assuming that the torsional rigidity was decreased by 40%, then ideally, less than  $2^\circ$  of washin angle would be required to regain the loss in aerodynamic efficiency. Finally, the results illustrate that the reduction in torsional stiffness and/or the addition of washin angle would increase the maximum tensile strain and shear stress.

This design process was conducted by first performing a requirement analysis based on the Lockheed provided Operational Requirements Document (ORD). Then, the baseline NSA configuration and mission profile were identified. From this, a baseline design point was selected. A NSA wing was then synthesized using the ACAD and ASTROS, and sensitivity analysis was obtained from the ASWING.

The requirements analysis was performed for the New Strategic Airlifter. Explicit customer's needs were identified from a requirements hierarchy build. Implicit (derived) customer's needs were identified based on Life-Cycle Cost. Customer needs were prioritized, and a QFD analysis was performed. Finally, prioritized technical requirements were extracted from the QFD. From this analysis, three primary technical requirements categories were identified: aircraft empty weight, aerodynamic efficiency, and reliability, maintainability, and supportability (R,M&S).

The baseline aircraft configuration chosen for this assessment study is the New Strategic Airlifter, NSA. The particular NSA configuration selected for this assessment study is the LGA180D, which

is a single stick twin engine concept. One modification was made to LGA180D for this assessment study; an inboard aileron control surface was used instead of the specified spoiler layout. The need for the inboard aileron came about because of the inability to model the spoilers for the ASTROS analysis. The primary functionality of spoilers is to provide roll control power at high speeds; thus, considering that the objective is roll performance at high speeds, the inboard aileron was substituted for this assessment study. The inboard aileron was sized such that the rigid wing aileron control power derivative of the inboard aileron was equal to that of the outboard aileron.

Using the NSA concept as a template, the structural arrangement of the wing is assumed based on conventional standards. There are two spars with the front spar located at 15% of the chord and the rear spar located at 65% of the chord. Rib spacing was assumed to be 24 inches. The stringer spacing was assumed to be 12 inches. In accordance with design for manufacturing and assembling considerations, the stiffeners and the ribs are oriented parallel and perpendicular to the rear spar respectively. To finalize the structural arrangement, a generic supercritical airfoil was used for the baseline wing configuration.

The material selection for the wing is based on typical transport wing. An all metallic wing is assumed for this assessment study. The wing's upper skin and stringers were designated to be AL-7075-T6, and the wing's lower surface, stringers, spar caps, and shear webs were assumed to be AL-2024-T3.

The NSA ORD specifies two baseline missions, an operational and maximum mission, and a single point in the operational mission flight envelope was selected for the assessment study. *The initial cruise point in the operational mission is selected for the AFW assessment study because the point represents the heaviest weight and highest dynamic pressure combination.* Recall that:

- Aeroelastic effects are more prominent at high dynamic pressures;
- Heavy weight translates to larger wing loading; and
- Heavy weight translates to a larger rolling moment of inertia (unburned fuel is in the wing) which inhibits rolling performance.

The initial cruise is specified to be 32,000 ft at 0.82 Mach, and the operation baseline mission is defined as a 3300 NM range with a payload of 120,000 pounds.

Given the design point selection, a V-n diagram is presented. The V-n diagram build is based on MIL-A-8861(ASG), and it represents the worst case scenarios for the wing structural design for the given design point in the flight envelope. Based on the V-n diagram build, five longitudinal maneuver design points are obtained. The design maneuver points are listed in Table 3.3.

Lateral maneuvers are also considered in the wing structural design. This is accomplished by performing a Military Specification MIL-F-8875B Level I roll maneuver. As specified in MIL-F-8785C, for a Class III Aircraft and a Category B Flight Phase, the Level I roll performance requires that the:

- Aircraft must be able to bank  $30^\circ$  in 2.0 seconds, and
- Maximum roll-mode time constant,  $\tau_r$ , must be less than or equal to 1.4 seconds.

Based on the lateral-directional small perturbation rolling approximation, the Level I roll performance requirements are translated into the following design constraints:

$$\tau_r \cong \frac{-1}{L_p} \leq 1.4 \text{ sec.}$$

$$\phi(2.0\text{sec.}) \geq 30^\circ$$

Note, only one point in the one flight envelope was considered. Furthermore, for that single point, only 6 wing loading scenarios were considered out of 38 possible scenarios listed in Reference 3.7. There are typically thousands of different loading and flight envelope combinations that must be evaluated in a wing design; this assessment study evaluated only a single flight point due to time considerations.



The key assumptions of AFW assessment as applied to the NSA are summarized as follows:

- Wing Structural Arrangement
  - Two spars versus multiple cell box
  - Rib and stringer spacing
- Material Selection
- Inboard Aileron Configuration
- No Buckling Constraints

The design process consisted on building a three-dimensional wing model in the ACAD program, and then translating this geometry into two structural models: one for ASTROS and one for ASWING. The ASTROS program was used as the primary synthesis tool, and ASWING was used as the primary sensitivity analysis tool. The simplified ASTROS structural model, which is the basis of these results, included aerodynamic analysis, structural analysis, and optimization. The multidisciplinary optimization was performed for the six loading cases identified. Constraints were added to this model to reflect maximum material yield strains and minimum material thickness or area. Finally, roll performance requirements were added to this model via aileron effectiveness.

Based on the key assumptions of AFW as applied to the NSA, these results represent a lower bound to the design problem. Additional constraints and/or the evaluation of more design points will result in either an increase in the structural weight and the resulting roll performance, or it will remain invariant.

## **5.2 Recommendations**

The recommendation of this assessment study is that a higher fidelity analysis is required in order to further substantiate the assessment of AFW for the NSA. Further analysis is required to determine the impact of the material selection and the structural arrangement on this assessment with regards to the NSA configuration. Composites could potentially produce different results because of there

tailorability and high strength characteristics. The structural arrangement could also have an impact on the torsional stiffness design driver. Buckling constraints need to be added to this model when the new version of ASTROS is available. An additional recommendation is that the other elements of AFW such as load alleviation, drag reduction, and flutter suppression need to be assessed. Furthermore, the effects of reducing the torsional stiffness on the flutter characteristics need to be determined. Finally, the design integration issues and consequences of AFW need to be evaluated.

### **5.3 Contribution**

To the author's knowledge, this was the first assessment of AFW as applied to a large aspect ratio wing. A minimum weight design with no torsional constraints was identified for inboard and outboard aileron configurations. Additionally, it was determined that the wing does not reverse within the flight envelope. Potential weight savings were also identified for inboard and outboard aileron configurations. Finally, the sensitivity of torsional stiffness on reversal speed, span efficiency, and maximum strain was determined.

## References

- 1.1 Perry, B., and Cole, S., "Summary of an Active Flexible Wing Program," *AIAA Journal of Aircraft*, Vol. 32, No. 1., January-February, 1995.
- 1.2 Walter, S., and R. Bennett, "Application of Transonic Small Disturbance Theory to the Active Flexible Wing Model," *AIAA Journal of Aircraft*, Vol. 32, No. 1., January-February, 1995.
- 1.3 Buttrill, C., Bacon, B., and et al, "Simulation and Model Reduction for the Active Flexible Wing Program," *AIAA Journal of Aircraft*, Vol. 32, No. 1., January-February, 1995.
- 1.4 Hoadley, S. And S. McGraw, "Multiple-Function Digital Controller System for Active Flexible Wing Wing-Tunnel Model," *AIAA Journal of Aircraft*, Vol. 32, No. 1., January-February, 1995.
- 1.5 Wieseman, C., Hoadley, S. And S. McGraw, "On-Line Analysis Capabilities Developed to Support the Active Flexible Wing Wind-Tunnel Tests," *AIAA Journal of Aircraft*, Vol. 32, No. 1., January-February, 1995.
- 1.6 Mukhopadhyay, V., "Flutter Suppression Control Law Design and Testing for the Active Flexible Wing," *AIAA Journal of Aircraft*, Vol. 32, No. 1., January-February, 1995.
- 1.7 Adams, W. And D. Christhilf, "Design and Multifunction Tests of a Frequency Domain-Based Active Flutter Suppression System," *AIAA Journal of Aircraft*, Vol. 32, No. 1., January-February, 1995.
- 1.8 Waszak, M. and S. Srinathkumar, "Flutter Suppression for the Active Flexible Wing: A Classical Design," *AIAA Journal of Aircraft*, Vol. 32, No. 1., January-February, 1995.
- 1.9 Woods-Vedeler, J. Pototzky, A., and S. Hoadley, "Rolling Maneuver Load Alleviation Using Active Controls," *AIAA Journal of Aircraft*, Vol. 32, No. 1., January-February, 1995.
- 1.10 Woods-Vedeler, J. Pototzky, A., and S. Hoadley, "Rolling Maneuver Load Alleviation Using Active Controls," *AIAA Journal of Aircraft*, Vol. 32, No. 1., January-February, 1995.
- 1.11 Norris, M, and J. Miller, "Active Flexible Wing Technology Assessment Study," Lockheed Aeronautical Systems Company, Marietta, Georgia, 1994.
- 1.12 Field, p., "Active Aeroelastic Wing Kickoff Meeting," Presentation, Phantom Works, McDonnell Douglas Aerospace, St. Louis, MO, August, 1996.

- 1.13 Yurkovich, R., "Optimum Wing Shape for an Active Flexible Wing," *36th AIAA Structure, Structural Dynamics, and Materials Conference*, New Orleans, LA, April, 1995.
- 2.1 Boppe, C., "System Requirement Types," Class Lecture Notes, Course 16.870, Massachusetts Institute of Technology, Cambridge, MA, Fall, 1995.
- 2.2 Roskam, J., "Airplane Design: Part VIII: Airplane Cost Estimation: Design, Development, Manufacturing, and Operating," Roskam Aviation and Engineering Corporation, Rt4, Box 274, Ottawa, KS 66067.
- 2.3 Wohletz, J., Hesse, C., and et al, AE 522, Spring 1994, "Preliminary Design of the Avocet: A Low Cost Commercial Transport," University of Kansas, Lawrence, KS, 66045.
- 2.4 Boppe, C., "QFD- Quality Function Deployment ," Class Lecture Notes, Course 16.870, Massachusetts Institute of Technology, Cambridge, MA, Fall, 1995.
- 3.1 Goodrich, H.L., Interdepartmental Communication E7306-459-95, "LGA180C; A Single Stick, Four Engine Concept for NSA," Lockheed Martin Aeronautical Systems, Marietta, Georgia, 8/8/95.
- 3.2 Honrath, J.F., Interdepartmental Communication E7306-425-95(R1),"Comparative Sizing Results for the New Strategic Airlifter (NSA) Single and Double Stick Configurations Using Alternative CF6-80 Engines," Lockheed Martin Aeronautical Systems, Marietta, Georgia, 6/14/95.
- 3.3 Honrath, J.F., Interdepartmental Communication E7306-387-95,"Sizing Results for the New Strategic Airlifter (NSA) Single and Double Stick Configurations Using Four CFM56-5B1 or -5C3 Engines or Two CF6-80C2A2 Engines," Lockheed Martin Aeronautical Systems, Marietta, Georgia, 4/27/95.
- 3.4 Honrath, J.F., Interdepartmental Communication E7306-426-95,"Sensitivity Sizing Results for the New Strategic Airlifter (NSA) Single Stick Configuration Using Four CFM56-5B1 Engines," Lockheed Martin Aeronautical Systems, Marietta, Georgia, 6/14/95.
- 3.5 Goodrich, H.L., and R.S. Justice, Interdepartmental Communication E7306-461-95," "LGA180C; A Single Stick, Four Engine Concept for NSA," Lockheed Martin Aeronautical Systems, Marietta, Georgia, 8/8/95.
- 3.6 Justice, R.S., Telephone Conversation, Lockheed Martin Aeronautical Systems, Marietta, Georgia, 4/4/95.
- 3.7 Nui, "Aircraft Structural Design," Unknown Publisher.

- 3.8 Roskam, J., "Airplane Design: Part III: Layout Design of Cockpit, Fuselage, Wing and Empennage: Cutaways and Inboard Profiles," Roskam Aviation and Engineering Corporation, Rt4, Box 274, Ottawa, KS 66067.
- 3.9 Drela, M., Personal Communication, Massachusetts Institute of Technology, Cambridge, Massachusetts, 3/15/96.
- 3.10 Goodrich, H.L., Telephone Conversation, Lockheed Martin Aeronautical Systems, Marietta, Georgia, 4/24/95.
- 3.11 Roskam, J., "Airplane Design: Part VI: Preliminary Calculation of Aerodynamic, Thrust and Power Characteristics," Roskam Aviation and Engineering Corporation, Rt4, Box 274, Ottawa, KS 66067.
- 3.12 Roskam, J., "Airplane Flight Dynamics and Automatic Flight Controls: Part I," Roskam Aviation and Engineering Corporation, Rt4, Box 274, Ottawa, KS 66067.
- 3.13 Perry, D.J., and J.J. Azar, "Aircraft Structures," Second Edition, McGraw-Hill Publishing Company, New York, 1982.
- 4.1 Neill, D., Herendeen, D., and V. Venkayye, "ASTROS Enhancements: Volume III - ASTROS Theoretical Manual," Final Contractor Report WL-TR-95-3006, Wright Laboratory, March 1993.
- 4.2 Neill, D., Herendeen, D., and V. Venkayye, "ASTROS Enhancements: Volume I - ASTROS User Manual," Interim Contractor Report WL-TR-93-3025, Wright Laboratory, May 1995.
- 4.3 Drela, M., "Method for Simultaneous Wing Aerodynamic and Structural Load Prediction," AIAA Journal of Aircraft, August, 1990.
- 4.4 Taylor, J.W.R., "Jane's All the World Aircraft," Published Annually by: Janes's Publishing Company, 238 City Road, London EC1V 2PU, England, 1995/1996.
- 4.5 Ewing, M., "Aerospace Structures," Class Lecture Notes, Aerospace Engineering 507, University of Kansas, Lawrence, KS, Fall, 1992.
- 4.6 Roskam, J., "Airplane Design: Part V: Component Weight Estimation," Roskam Aviation and Engineering Corporation, Rt4, Box 274, Ottawa, KS 66067.
- 4.7 Roskam, J., "Airplane Design: Part VII: Determination of Stability, Control, and Performance Characteristics: FAR and Military Requirements," Roskam Aviation and Engineering Corporation, Rt4, Box 274, Ottawa, KS 66067.
- 4.8 Hanegan, S.J., "Advanced Flexible Wing Technology Assessment for Transport Applications," Massachusetts Institute of Technology Master of Engineering Thesis, Cambridge, MA, Spring 1996.



# Appendix A Operational Requirements Document

# OPERATIONAL REQUIREMENTS DOCUMENT

## New Strategic Airlifter

### 1. GENERAL DESCRIPTION OF OPERATIONAL CAPABILITY:

#### A. Mission Area:

Provide a new strategic airlifter (NSA) which fills the void created by the retirement of the C-141 fleet. US military strategy is increasingly dependent upon strategic airlift as forces are withdrawn from forward positioning and a central reserve is maintained within the US to be deployed in time of crisis. Mobility/transport aircraft will continue to play an important role in the future from large-scale conventional war to humanitarian aid and peacekeeping efforts. The new airlifter will also have airdrop and tanker capabilities. Additionally, commercial air cargo transport growth will outpace passenger growth for the foreseeable future. The new airlifter will therefore have commercial business applications ranging from overnight package services to high priority oversize shipping.

#### B. Type of Proposed System:

(1) This requirement can be broken down into two main markets:

1. Military (USAF / European Union / Rest of World)

- Deployment
- Airdrop
- Tanker

2. Commercial (Domestic / International)

- Overnight
- Intermodal

(2) This ORD will concentrate on the "primary" military market. The aircraft design will be based on deployment since it possesses the dominate requirement parameters. The specific requirements for commercial and other operations will be outlined in Table 1.



### **C. Anticipated Operational and Support Concepts:**

The NSA shall be FAA-certified. It shall have roll-on/roll-off capability and carry palletized bulk and oversize cargo. It will meet minimum Army requirements for personnel, containerized delivery system (CDS), and low velocity airdrop (LVAD) operations. Previously developed manuals (operations, maintenance, and performance) will be used to meet military requirements and restrictions.

### **2. THREAT:**

The NSA will routinely operate in the same threat environment currently experienced by the C-141, C-5, and C-17 (in its non-tactical role).

### **3. SHORTCOMINGS OF EXISTING SYSTEMS.**

The early retirement of the C-141 fleet combined with a possible reduction in C-17 procurement creates a shortfall in airlift capability. The shortfall could be alleviated to some extent with a NDAA procurement, however, the million ton mile per day requirements will still not be satisfied. Force delivery times required to meet strategic and tactical objectives could be jeopardized. There will also be a shortage in available tankers due to the aging KC-135 aircraft fleet which constitutes 82% of the tanker fleet. Additionally, the aging fleet of DC-8/707 freighters combined with the continued expansion in commercial air cargo requirements will create a gap that must be filled.

### **4. CAPABILITIES REQUIRED: (USAF Military)**

- A. Basic Performance.** Operate in the organized track systems, comply with minimum navigation performance standards for worldwide operations, meet reduced vertical separation minima (RVSM) requirements, and be transoceanic capable. Flight performance must be compatible with commercial aircraft. Must meet FAA Stage 3 noise and ICAO pollution standards.
- B. Range/Payload.** Fly 3300 NM unrefueled, no wind, from a point of departure to first point of intended landing, with a 120,000 US pound payload and arrive with enough reserve fuel to go an additional 500 NM (per MACR 55-2). The maximum range will be 6000 NM with zero payload. The unit payload weight is 69,460 lb (based on the DV-43 forklift). The maximum dimensions per unit are height - 149 in (crane), width - 149 in (CH-47C helicopter), and length - 509 in (CH-47C helicopter). The aircraft should be able to carry 14 to 20 463L pallets or up to 200 troops.

- C. **Minimum Runway/Turning.** Take off under the above range/payload conditions from a 7500 x 86 foot, level, dry, paved runway, standard day, at sea level with no obstacle, using USAF performance criteria. Required landing length under the same conditions is 5000 feet. Aircraft LCN  $\geq$  60. Turn requirements are 180 degrees on a 90 foot wide taxiway.
- D. **Cruise Speed/Altitude.** Initial cruise altitude is 32,000 feet at a speed of .82 Mach. Max cruise altitude is 39,000 feet. Max cruise air speed of 350 KEAS or 0.86 Mach.
- E. **Crew.** Flight crew requires 2 pilots and cargo crew requires 1 loadmaster. Up to 6 flight crew required for relief.
- F. **Weight and Balance Information.** Onboard automated weight and balance computation system required. Integration with the flight management system (FMS) is desired.
- G. **Mission Planning.** Automated capability to do aircraft performance analysis such as takeoff and landing data (TOLD), airfield analysis, flight planning, and essential information contained in DD Form 365-4 computation is required. This capability integrated with the FMS is desired.
- H. **Flight Station.** Crew positions must be kept to a minimum. The desired objective is a two-pilot cockpit. A station for a loadmaster must be provided with oxygen/radio/interphone capability. An FMS is desired. System redundancy should be optimized to allow safe operation of the aircraft from pilot or copilot crew positions. The cockpit shall contain required emergency/survival equipment and devices to accommodate all crew positions.
- I. **Cargo Capability.** Must carry palletized bulk and oversize cargo. Must be roll-on, roll-off rolling stock capable. The cargo floor height is 60 to 70 in above ground. Must have a 463L-compatible powered roller loading system and a 12 degree max ramp angle. Crew door dimensions are forward port 32 x 48 in.
- J. **Reliability/Maintainability.** Design life of 45,000 flight hours with a maintenance man-hour per flight hour of 12.0.
- K. **Environmental Conditions.** Operate from military and civilian airports worldwide and in all climatic conditions. The equipment shall be protected from and/or resistant to the effects of sand, dust, snow, ice, turbulence, salt-laden air, moisture, and temperature extremes. Aircraft must be able to operate in moderate icing conditions and be tolerant of moderate turbulence conditions. It must be capable of operating in instrument meteorological conditions (IMC) during day and night. Instrument flight rules (IFR)

capability is required to include Category (CAT) II instrument landing system (ILS) approaches. The aircraft must allow the crew to don chemical suits while in flight, land the aircraft, and egress safely.

- L. **Propulsion.** Self-contained start capability. Aircraft operation shall accommodate a safe and routine capability of totally self-contained mission preparation/launch activity including shutdown and engine start from any operating location. Must be able to start with a ground and air power cart and have engine cross starting capability.
- M. **Fuel System.** Control and monitoring should be a "set and forget" system with warnings. Failures should default to a fail-safe, flexible fuel sourcing backup mode. The aircraft/fuel system shall be compatible with JP-8 as the primary fuel and JP-4, -5 and commercial grades of Jet A, A-1, and B as alternate fuels. The system should be serviceable through a single-point receptacle, pressure/closed circuit refuel, and alternate gravity-feed refueling points to completely fill all tanks. Aerial refueling receiver capability is required.
- N. **Airdrop Operations.** The airdrop of heavy equipment, personnel, or CDS will be used to secure key ground objectives or resupply friendly forces. Delivery airspeeds will be 130-135 KIAS for personnel, 150 KIAS for equipment/CDS and 130-150 KIAS for the door bundle. Minimum delivery altitudes will be 500-800 ft. for personnel, 600 ft. for CDS, 1000 ft. for heavy equipment and 300 ft. for the door bundle.
- O. **Avionics Architecture.** The avionics system shall be certified for overwater operation in accordance with all military and civil qualifications. An avionics architecture providing an integrated solution for the following functions is desired: control and display of pilot/flight information, communications, navigation/identification, autopilot/flight director, and integrated diagnostics. The integrated avionics should employ state-of-the-art technologies to the max extent possible including such things as electronic color displays, graphics processor, and BIT. External interfaces should be provided between the avionics and other subsystems for integrating control/displays and diagnostics.
- P. **Communications.** All crewmembers shall have the capability of transmitting and receiving on all command radios.
- Q. **Survivability.** Make maximum use of current infrared (IR) technologies to minimize the proliferated IR missile threat. Shall be equipped with a standard airlift defensive system.

# NEW STRATEGIC AIRLIFTER

	MILITARY (USAF / EUROPEAN UNION / REST OF WORLD)			COMMERCIAL (DOMESTIC / INTERNATIONAL)	
	DEPLOYMENT	AIRDROP	TANKER	OVERNIGHT	INTERMODAL
DESIGN PAYLOAD (TOTAL) KLBS	120	90 EQUIP, 56 7 PERS	180 FUEL OFFL (AD)	82-140	82-140
DESIGN PAYLOAD (ITEM) KLBS	69 46	60	30	15	45
MAX HEIGHT (ITEM) IN	149	126	96	96	96
MAX WIDTH (ITEM) IN	149		125	96	96
MAX LENGTH (ITEM) IN	609		120	125	480
PALLETS	14-20 463L		2 M1 CONTAINERS	18-24	18-24
PASSENGERS	200 TROOPS	150-162 PARATR			
RANGE AT DESIGN PAYLOAD NM	3300 + 500	? + 500	1500 RADIALS	1800-3200	1800-3200
MAX RANGE NM	6000	6000	6000 MIN	6000 MIN	6000 MIN
INITIAL CRUISE ALT FT/MACH	32,000/0 82	32,000/0 82	32,000/0 82	32,000/0 80	32,000/0 80
MAX CRUISE ALTITUDE FT	39,000	39,000	39,000	39,000	39,000
Vc KEAS/Mc	350/0 86	350/0 86	350/0 86	350/0 86	350/0 86
CRITICAL FIELD/TO LENGTH FT	7500 x 86	7500 x 86	7500	8000	8000
LANDING LENGTH FT	5000	5000	5000	5500	5500
LCN	60	60	60	60	60
TURNING DEGREE	180 ON 90 FT	180 ON 90 FT		90 ON 75 FT FILLET	90 ON 75 FT FILLET
SUPPORT EQUIPMENT	SELF LAUNCH/CS	SELF LAUNCH/CS	SELF LAUNCH/CS	SELF LAUNCH/CS	SELF LAUNCH/CS
FLIGHT CREW	2 PILOTS	2 PILOTS	2 PILOTS	2 PIL+JUMPSEAT	2 PIL+JUMPSEAT
CARGO CREW	1 LM	2 LM OR JUMPMAS	2 REFUEL OP STAT	2 LM	2 LM
AVIONICS	INT. FMS, NAV, DATAB	INT. FMS, NAV, DATAB	INT. FMS, NAV, DATAB	INT. FMS, NAV, DATAB	INT. FMS, NAV, DATAB
REST/RELIEF	UP TO 6 FLT CREW	UP TO 6 FLT CREW	UP TO 6 FLT CREW		
CARGO FLOOR HEIGHT IN	60-70	60-70	60-70		
PALLET ROLLERS	463L SYS. INTEGRAL	463L SYS. INTEGRAL	463L SYS. INTEGRAL		
RAMP ANGLE DEG MAX	12	12			
CREW DOORS IN	FWD PORT 32x48	FWD PORT 32x48	FWD PORT 32x48		
PARATROOP DOORS IN		2 36x72 FWD OF RMP			
AIRDROP-PERS. KIAS, FT(MIN)		130-135, 500-800			
AIRDROP-EQUIP. KIAS, FT(MIN)		150, 1000			
AIRDROP-CDS KIAS, FT(MIN)		150, 600			
AIRDROP-DR BUND KIAS, FT(MIN)		130-150, 300			
FUELING			SINGLE PT, PRESS.		
MAINT. MAN HR/FLIGHT HR	12	12	12		
DISPATCH RELIABILITY					
DESIGN LIFE FH	45,000	45,000	45,000		

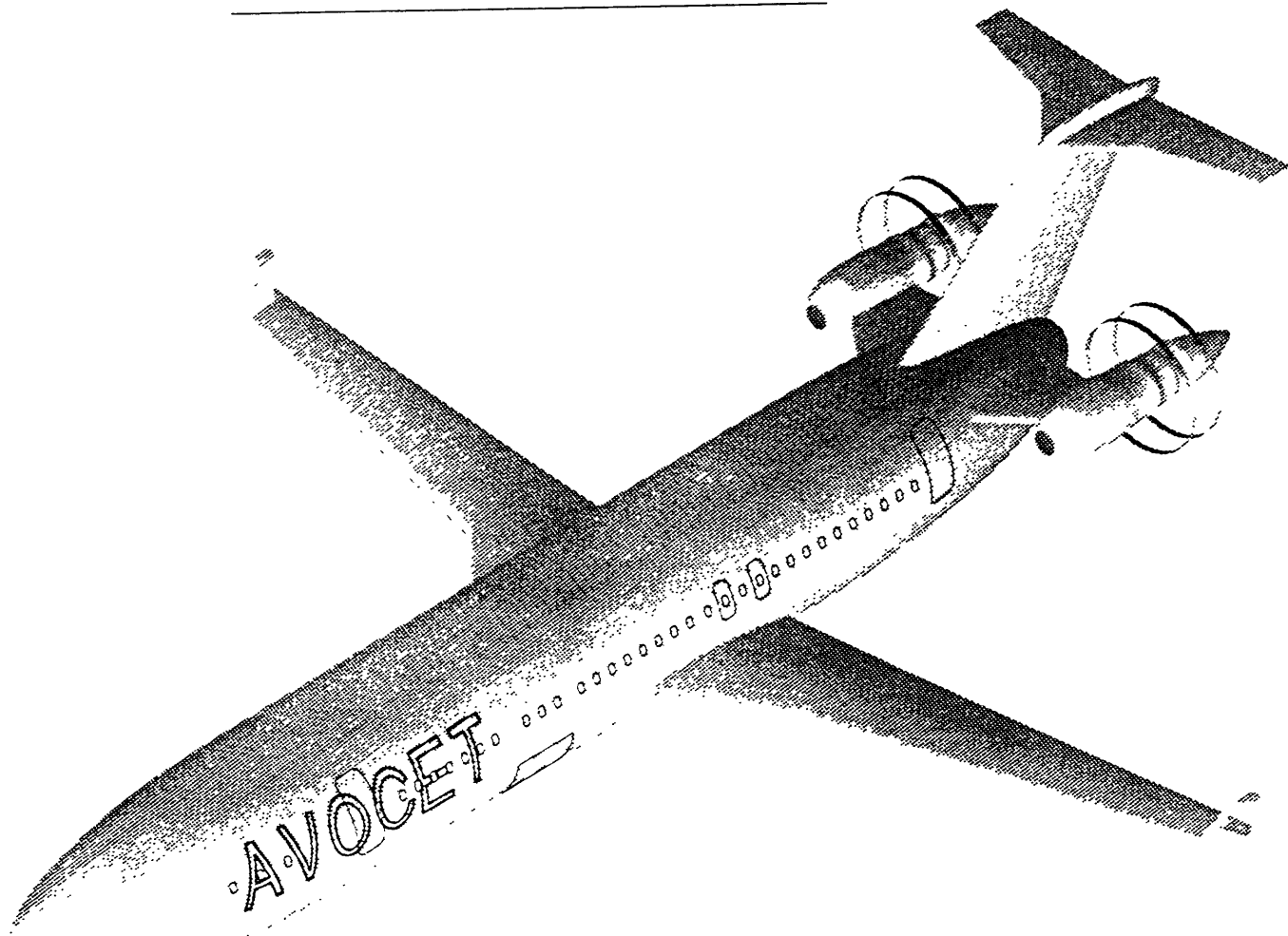
TABLE 1

## **Appendix B DOC Assessment Study for Narrow-Body Commercial Transport**

- 2.1 Hagerott, S., Wohletz, J., and et al, AE 522, Spring 1994, "Preliminary Design of the Avocet: A Low Cost Commercial Transport," University of Kansas, Lawrence, KS, 66045.

# AVOCET

---



PRELIMINARY DESIGN

---

A LOW COST COMMERCIAL TRANSPORT

AIAA / LOCKHEED CORPORATION  
UNDERGRADUATE TEAM AIRCRAFT  
DESIGN COMPETITION 1994

UNIVERSITY OF KANSAS  
AEROSPACE ENGINEERING  
THE RED TEAM



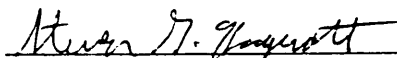
# University of Kansas School of Aerospace Engineering




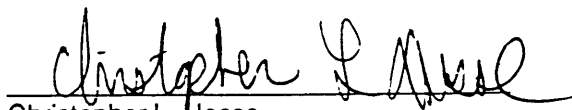
## Preliminary Design of the Avocet: A Low Cost Commercial Transport

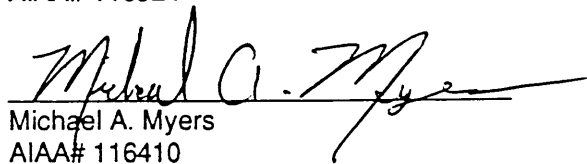
AIAA/Lockheed Corporation Undergraduate Team Aircraft Design Competition 1994

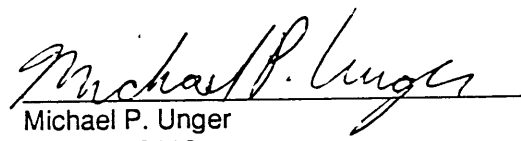
### REDTEAM:

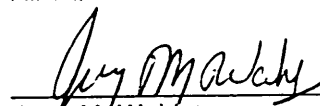
  
\_\_\_\_\_  
Steven G. Hagerott, Team Leader  
AIAA# 077035


  
\_\_\_\_\_  
Richard P. Gaulke  
AIAA# 116790

  
\_\_\_\_\_  
Christopher L. Hesse  
AIAA# 116924

  
\_\_\_\_\_  
Michael A. Myers  
AIAA# 116410

  
\_\_\_\_\_  
Michael P. Unger  
AIAA# 103112

  
\_\_\_\_\_  
Jerry M. Wohletz  
AIAA# 099978

  
\_\_\_\_\_  
Dr. Jan Roskam, Ackers Distinguished  
Professor of Aerospace Engineering  
Project Faculty Advisor

## Chapter 4 Estimation of Current Fleet DOC and Identification of DOC Drivers

---

In this chapter an estimation of the current airline fleet is presented and the major DOC drivers of a commercial transport are identified. Reference 2 was used to define the DOC of transport aircraft. A DOC breakdown tree is presented. DOC is defined, and a quantitative breakdown of the DOC components is presented. The major DOC cost drivers and possible technologies to address these technologies are identified in this tree.

### 4.1 Designer Impact on DOC

The DOC breakdown tree illustrated in Figure 4.1 was constructed according to methods outlined in Reference 2. This tree shows the DOC components and which components are affected by design decisions. Technologies which could possibly reduce DOC follow these components, as shown in Figure 4.1.

The DOC for the fleet average and the Avocet was estimated using methods from Reference 2. As shown in Figure 4.1, DOC is broken into five parts:

1. Flying DOC
2. Maintenance DOC
3. Depreciation DOC
4. Fee and Tax DOC
5. Finance DOC

It is shown in Figure 4.1 that items 1-3 are affected by design decisions. From the DOC tree the direct operating cost of flying, ( $DOC_{\text{tr}}$ ) is shown to consist of:

- Crew cost
- Fuel and oil cost
- Insurance cost

The designer has control over the DOC due to fuel used because the Breguet range equation illustrates that the fuel used is dependent upon three parameters:

- L/D
- s.f.c.
- Airframe weight

It is shown in Figure 4.1 that these parameters are controllable in preliminary design.

It is also shown in Figure 4.1 that the crew and insurance costs cannot be controlled in preliminary design. The crew salary is determined by the airline, but the number of crew is controlled by the designer. The Avocet incorporates the modern aircraft standard of two crew members.

From Figure 4.1 the cost of maintenance ( $DOC_{\text{maint}}$ ) is shown to consist of:

- Labor cost of airframe, systems, and engine maintenance
- Cost of maintenance materials for the airframe, systems, and engines



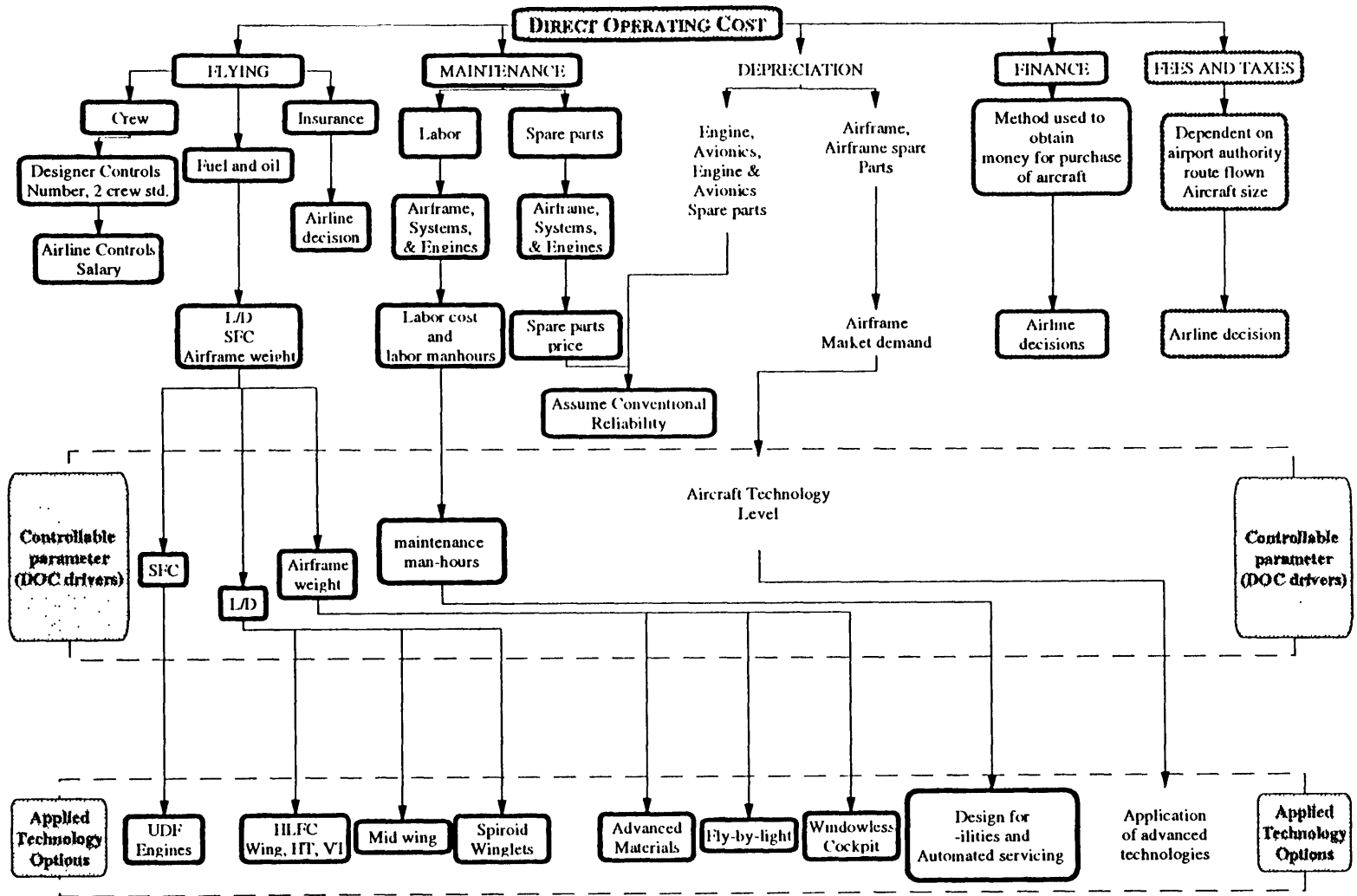


Figure 4.1 DOC Breakdown Tree

The labor cost of maintenance for the airframe, systems, and engines is controlled by the amount of man-hours per block hour of aircraft service. In Figure 4.1 it is shown that the maintenance man hours per block hour can be reduced by designing for maintainability while the cost of maintenance materials for the airframe, systems, and engines is difficult to control by the designer.

From Figure 4.1 the direct operating cost of depreciation ( $DOC_{dpr}$ ) is shown to consist of:

- Airframe depreciation
- Depreciation of avionics systems
- Depreciation of engine spare parts
- Engine depreciation
- Depreciation of airplane spare parts

The depreciation DOC is affected by the current market demand for the aircraft. It is assumed that the more advanced the aircraft airframe, engine, and avionics, the less depreciation will take place for these components. Figure 4.1 indicates that incorporating advanced technologies will keep the demand for an aircraft high and will reduce the cost of depreciation. However, this will increase the acquisition cost.

Items 4 and 5 of the previously mentioned list are not affected in preliminary design. The cost of financing ( $DOC_{fm}$ ) consists of the method of obtaining money to purchase the aircraft. It is illustrated in Figure 4.1 that this is a decision which each individual airline will make. It cannot be affected by the designer.

The direct operating cost of fees and taxes ( $DOC_{lnt}$ ) shown in Figure 4.1 consists of:

- Landing fees
- Registry taxes
- Navigation fees

The landing and navigation costs depend on the airports flown to and the routes flown. The registry taxes are dependent on aircraft size. It will be shown that these components are not major cost drivers.

## 4.2 Estimation of Current Fleet DOC

The RFP requires the estimation of the current airline fleet DOC and the identification of the major cost drivers of commercial transports. The RFP also calls for a comparison of the DOC of the Avocet design to the DOC of the current fleet average. Although the current fleet average could be estimated from publications, the tools used to arrive at the DOC of the fleet are not given. Also, the assumptions and data used to estimate the DOC are not given. To ensure an accurate comparison, the AAA program based on methods in Reference 2 was used as the common DOC estimation tool for each airplane.

The current fleet is represented by three airplanes with ranges and payloads similar to those of the Avocet. The ranges and payloads [Ref. 3] of the fleet airplanes are shown in Table 4.1.

<b>Table 4.1 Range and Payload Capabilities of Fleet Aircraft</b>			
	MD-90-50	B737-300	A320-200
Range (nm)	3,024	2,850	2,800
Payload (lbs)	33,500	29,400	31,400

The DOC of the four ranges listed below was computed and averaged to estimate the fleet average:

- 1,000 nm
- 1,500 nm
- 2,000 nm
- 3,000 nm

This diversity of ranges is used because the Avocet will not exclusively fly a 3,000 nm mission.

The entire methodology used to estimate the DOC is discussed thoroughly in Chapter 14. The MD-90-50 aircraft DOC and the Avocet design DOC is also compared to demonstrate the effectiveness of the design. The main assumptions held constant for each aircraft in the fleet, as well as for the Avocet, are in Table 4.2.

<b>Table 4.2 DOC Estimation Input Data</b>	
Number of cockpit crew members	2
Captain salary	100,000 USD/year
First officer salary	50,000 USD/year
Crew flight time	800 hrs/year
Annual utilization	3200 hrs/year
Fuel price	1.00 USD/year (1992 price, per the RFP)

Each airplane chosen to represent the fleet DOC, including the Avocet, has two cockpit crew members. The salaries of the captain and first officer, crew flight time, and annual utilization are all held constant to standardize the comparison, because these are decided by the airline, not the designer. The fuel price is also variable and is an estimate of the 1992 fuel price, per the RFP. A fuel price obtained from AAA is used. These assumptions standardize the flight DOC calculations. Similar methods for standardizing the maintenance, depreciation, landing, and financing fees are discussed in Chapter 14.

The DOC estimates of each aircraft for each of the four ranges are shown in Figure 4.2. The average DOC for each mission length is also shown in Figure 4.2. The average airline DOC is estimated by averaging the DOC for the missions specified. The average DOC is 9.98 USD/nm.

Figure 4.3 presents a breakdown of the fleet average total DOC. From Figure 4.3, it can be seen that flying, maintenance, and depreciation costs are the primary components of total DOC. It is shown in Figure 4.3 that although the cost of registry taxes can be influenced by the design of the aircraft, these taxes only represent a portion of two percent of the total DOC. It is also shown in Figure 4.3 that the finance cost, identified in Figure 4.1 as a parameter uncontrolled by design, represents only seven percent of the total DOC.

### **4.3 Identification of DOC Drivers**

By correlating the major contributors to DOC shown in Figures 4.3 with Figure 4.1, the design drivers for a transport aircraft can be determined. It can be seen that the flying, maintenance, and depreciation costs are the major contributors to DOC and, therefore, represent the design drivers of a commercial transport. The objective of the RFP is to design a low direct operating cost commercial transport. Technologies are incorporated to reduce the DOC of the Avocet and specifically address the flying, maintenance, and depreciation costs.

The fuel and oil cost is shown in Figure 4.4 to be a major contributor to the flying and total DOC.



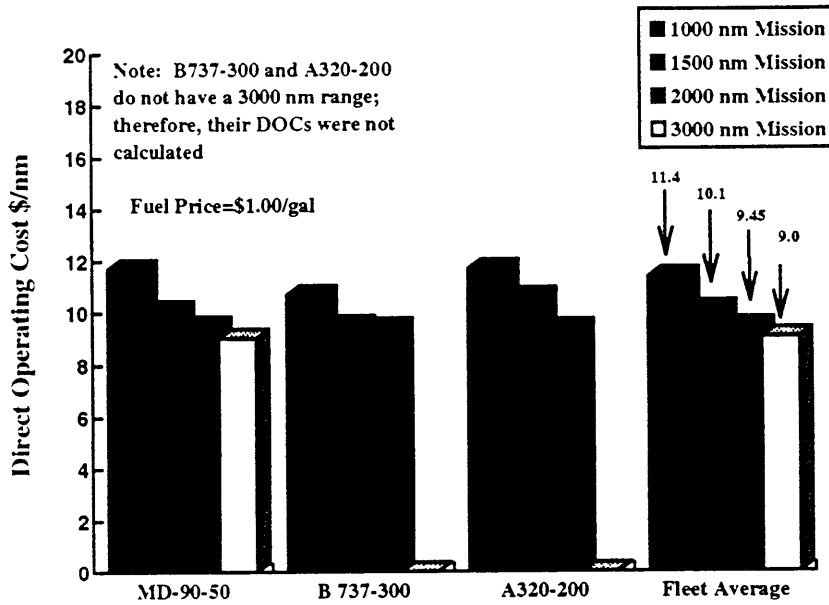
Room 14-0551  
77 Massachusetts Avenue  
Cambridge, MA 02139  
Ph: 617.253.5668 Fax: 617.253.1690  
Email: docs@mit.edu  
<http://libraries.mit.edu/docs>

## **DISCLAIMER OF QUALITY**

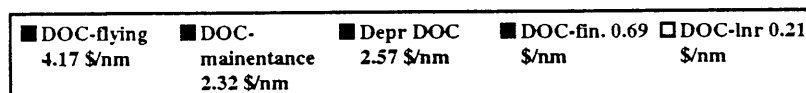
Due to the condition of the original material, there are unavoidable flaws in this reproduction. We have made every effort possible to provide you with the best copy available. If you are dissatisfied with this product and find it unusable, please contact Document Services as soon as possible.

Thank you.

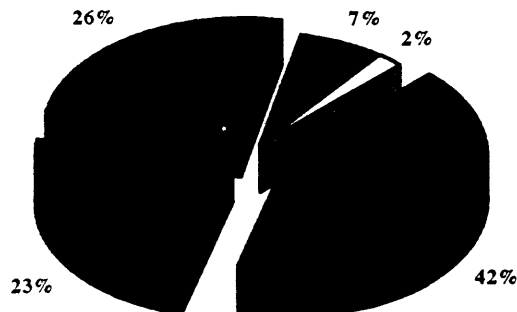
*Pages 112 + 113* in the original document contain .  
pictures or graphics that will not scan or reproduce well.



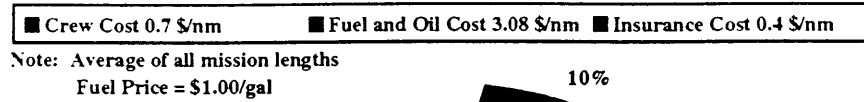
**Figure 4.2 Estimate of Fleet DOC**



Note: Average of all mission lengths  
Fuel Price = \$1.00/gal



**Figure 4.3 Total DOC Breakdown**



**Figure 4.4 Flying DOC Breakdown**

Flying DOC is shown to be approximately 42 percent of the total DOC in Figure 4.3. Fuel and oil costs are shown to be approximately 73 percent of the flying DOC in Figure 4.4. Therefore, the fuel and oil have a 30 percent impact on total DOC. In Figure 4.1 the fuel and oil costs are shown to be controlled through the following parameters:

- L/D
- s.f.c.
- Aircraft weight

Crew and insurance costs make up 27 percent of the flying DOC. Unfortunately, as illustrated in Figure 4.1, these are not controllable in preliminary design.

The DOC of depreciation is shown to be approximately 26 percent of the total DOC in Figure 4.3. Aircraft technology level is the one parameter of depreciation controllable by design decisions. The Avocet incorporates many advanced technologies which will keep the demand for the aircraft high, thus reducing the depreciation cost of the airframe and the spare parts.

In Figure 4.3 it is shown that the maintenance DOC is approximately 23 percent of the total DOC. It is shown in Figure 4.1 that the controllable parameter within maintenance DOC is maintenance man hours. The maintenance man hours can be affected by designing the aircraft for maintainability. This is discussed in detail in Chapter 5.

These parameters are affected by simultaneously incorporating the following technology and design concepts which reduces the flying DOC:

- |              |                    |                              |
|--------------|--------------------|------------------------------|
| UDF engine   | Spiroid winglets   | Fly-by-light flight controls |
| HLFC systems | Advanced materials | Windowless cockpit           |
| Mid wing     |                    |                              |

These technology options will be discussed thoroughly in Section 5.3.